ISSN 2478-057X

SLJOM

SRI LANKA JOURNAL OF METEOROLOGY

Volume:3
September 2018

Published By:
Department of Meteorology
Colombo 07, Sri Lanka

Sri Lanka
Journal of Meteorology

කාලගුණ විද්‍යා දෙපාර්තමේන්තුව
வளிமண்டலவியல் திணைக்களம்
DEPARTMENT OF METEOROLOGY
ශ්‍රී ලංකාව இலங்கை SRI LANKA

Volume 3 **September 2018**

Published by
Department of Meteorology
Colombo 07
Sri Lanka

EDITORIAL

Sri Lanka Journal of Meteorology (SLJoM) is a publication that is dedicated to the developments in climate, weather and atmospheric sciences in Sri Lanka. The journal entertains contributions in the form of research notes, research papers and review articles, case reports etc. in the area of Climate, Climatic Change, extreme weather events and weather forecasting. Aiming to promote the exchange of knowledge about meteorology from across a range of scientific sub-disciplines, the journal serves community of researchers, policy-makers, managers, media and the general public.

SLJoM publishes the latest achievements and developments in the field of atmospheric sciences. With this SLJoM volume 3, research activities carried out in the department of meteorology is now primed for a step forward.

Volume 3 of Sri Lanka Journal of Meteorology is consists of 8 research articles in aspects of meteorological and Climatological science, including applications of meteorological, climatological, analytical and forecasting data, future climate change projections for Sri Lanka, potential forecast of thunderstorms in Sri Lanka , impact analysis to improve long range forecasting and agro meteorology.

The Journal can be accessed on-line to view and download the abstracts full text of the articles published in current volume free of charge by visiting the Department of Meteorology website (http//meteo.gov.lk). Currently the journal is published annually. SLJoM is edited and published by the Department of Meteorology, Sri Lanka.

K. H. M. S. Premalal
Chief Editor,
Sri Lanka Journal of Meteorology, Vol 3
September 2018

Members of Editorial Board

SRI LANKA JOURNAL OF METEOROLOGY

Contents
Vol. 3, September 2018

ARTICLES	Page Nos
Comparison of NEX NASA Statistical Downscaling Data and CORDEX Dynamical Downscaling Data For Sri Lanka ..... H.M.R.C. Herath, I. M. S. P. Jayawardene	3-18
Multi Model Ensemble Climate Change Projections for Annual and Seasonal Rainfall in Sri Lanka ..... D. W. T. T. Darshika, I. M. S. P. Jayawardana, D. M. S. C. Dissanayake	19-27
Modulation of Monthly Rainfall in Sri Lanka by ENSO and ENSO Modoki Extremes ..... H. A. S. U. Hapuarachchi, I. M. S. P. Jayawardene	28-42
Influence of ENSO to the Following Year Southwest Monsoon Dry/Wet Conditions in Sri Lanka .....A. M. A. H. D. Alagiyawanna, I. M. S. P. Jayawardene, D. M. S. C. Dissanayake	43-52
Assessment of the Behaviour of K-Index, Lifted Index and Convective Availability Potential Energy (CAPE) in Development of Thunderstorms in Sri Lanka ..... M. Fernando and M. Millangoda, K. H. M. S. Premalal	53-63
Investigation of Combine Effects of El Nino, Positive IOD and MJO on Second Inter-Monsoon Rainfall 2015 in Sri Lanka ..... K. A. K. T. W. Weerasinghe and I. M. S. P. Jayawardena, P. A. A. Priyantha	64-85
Develop an Equation Between Pan Evaporation and Meteorological Parameters in Sri Lanka Using Regression Method ..... M.R.C.Silva, K. H. M. S. Premalal	86-99
Two-Dimensional Sea Breeze & Land Breeze Model with Application to Sri Lanka ..... H. A. G. Dharmappriya	100-116

Comparison of NEX NASA Statistical Downscaling Data and CORDEX Dynamical Downscaling Data For Sri Lanka

H.M.R.C. Herath
I. M. S. P. Jayawardena
Department of Meteorology
Colombo 07

ABSTRACT

There is an increasing demand for climate information at the national to local scale in order to address the risk posed by projected climate changes and their anticipated impacts. Readily, available climate change projections are provided at coarse spatial scales for the end of the 21st century. These projections, however, do not fit the needs of national adaptation planning that requires regional and local projections. In order to derive climate projections at scales that decision makers' desire, a process termed downscaling has been developed. Downscaling is widely used to improve spatial and/or temporal distributions of meteorological variables from regional and global climate models. This downscaling is important because climate models are spatially coarse (100–200 km) and often misrepresent extremes in important meteorological variables, such as temperature and precipitation. NASA Earth Exchange Global Daily Downscaled Projections data with 25km grid spacing and Coordinated Regional Climate Downscaling Experiment (CORDEX) data with 50km grid spacing of 6 GCM models were used to evaluate models suitability for Sri Lanka. Annual mean precipitation and seasonal mean precipitation for four climatic seasons namely Southwest Monsoon, Northeast Monsoon, First Inter-Monsoon and Second Inter-Monsoon, of model historical runs (1975-2005) were compared with observed climatological average of precipitation to evaluate the models' performance.

Keywords: downscaling, temperature, precipitation, seasonal, monsoon, annual, NEX-GDDP, CORDEX

1 **Introduction**

1.1 Introduction of General Circulation Models (GCMs)

General or General Circulation Models (GCMs) simulate the Earth's climate via mathematical equations that describe atmospheric, oceanic, and biotic processes, interactions, and feedbacks. GCMs are the primary tool for understanding how the global climate may change in the future but local scale precipitation processes are poorly represented due to the coarse resolution of the GCMs and are used to understand present climate and future climate scenarios under increased greenhouse gas concentrations (Trzaska and Schnarr, 2014). For climate change impact assessments finer scale information is required (Maraun et al, 2010).

Downscaling is widely used to improve spatial and/or temporal distributions of meteorological variables from regional and global climate models and subsequently emerged as a means of bridging the gap between what climate modellers are currently able to provide and what impact assessors

require (Wilby and Wigley, 1997). This downscaling is important because climate models are spatially coarse (100–200 km) and often misrepresent extremes in important meteorological variables, such as temperature and precipitation. The two approaches of downscaling are Dynamical downscaling nests a regional climate model (RCM) into the GCM to represent the atmospheric physics with a higher grid box resolution within a limited area of interest and *Statistical downscaling* establishes statistical links between large-scale weather and observed local-scale weather (Maraun et al, 2010).

Dynamical downscaling relies on the use of a regional climate model (RCM), similar to a GCM in its principles but with high resolution. RCMs take the large-scale atmospheric information supplied by GCM output at the lateral boundaries and incorporate more complex topography, the land-sea contrast, surface heterogeneities, and detailed descriptions of physical processes in order to generate realistic climate information at a spatial resolution of approximately 20–50 kilometres (Trzaska and Schnarr, 2014).

Statistical downscaling involves the establishment of empirical relationships between historical and/or current large-scale atmospheric and local climate variables. Once a relationship has been determined and validated, future atmospheric variables that GCMs project are used to predict future local climate variables (Trzaska and Schnarr, 2014). Statistical downscaling can produce site-specific climate projections, which RCMs cannot provide since they are computationally limited to a 20–50 kilometres spatial resolution. However, this approach relies on the critical assumption that the relationship between present largescale circulation and local climate remains valid under different forcing conditions of possible future climates (Zorita and von Storch, 1999).

1.2 Introduction of general climatology of Sri Lanka

The Climate of Sri Lanka is essentially monsoonal, dominated by the Southwest and Northeast monsoons, on which the life and economy of the island is critically dependent. The variations in air temperature are small except in the mountainous area, where the rainfall variations are large. The significant anomalies in climate are mainly decided by the temporal and spatial variations of rainfall, which have a strong impact on agricultural activities in the Country.

Orography plays an important role in the rainfall distribution of Sri Lanka (Fig 1). The central part of the southern half of the island is mountainous with heights of more than 2500m above the mean sea level.

The two monsoons essentially determine the seasonality of Sri Lanka since the temperature shows significant variation throughout the year. The seasons are distinguished only by means of the timing of the two monsoons and the transitional periods separating them, called inter-monsoon seasons (Chandrapala 1996). The Southwest monsoon is from May to September and the Northeast monsoon from December to February. The inter-monsoon periods are from March to April and from October to November.

Objective of this study is to identify the most suitable downscale method to develop future climate projections to Sri Lanka.

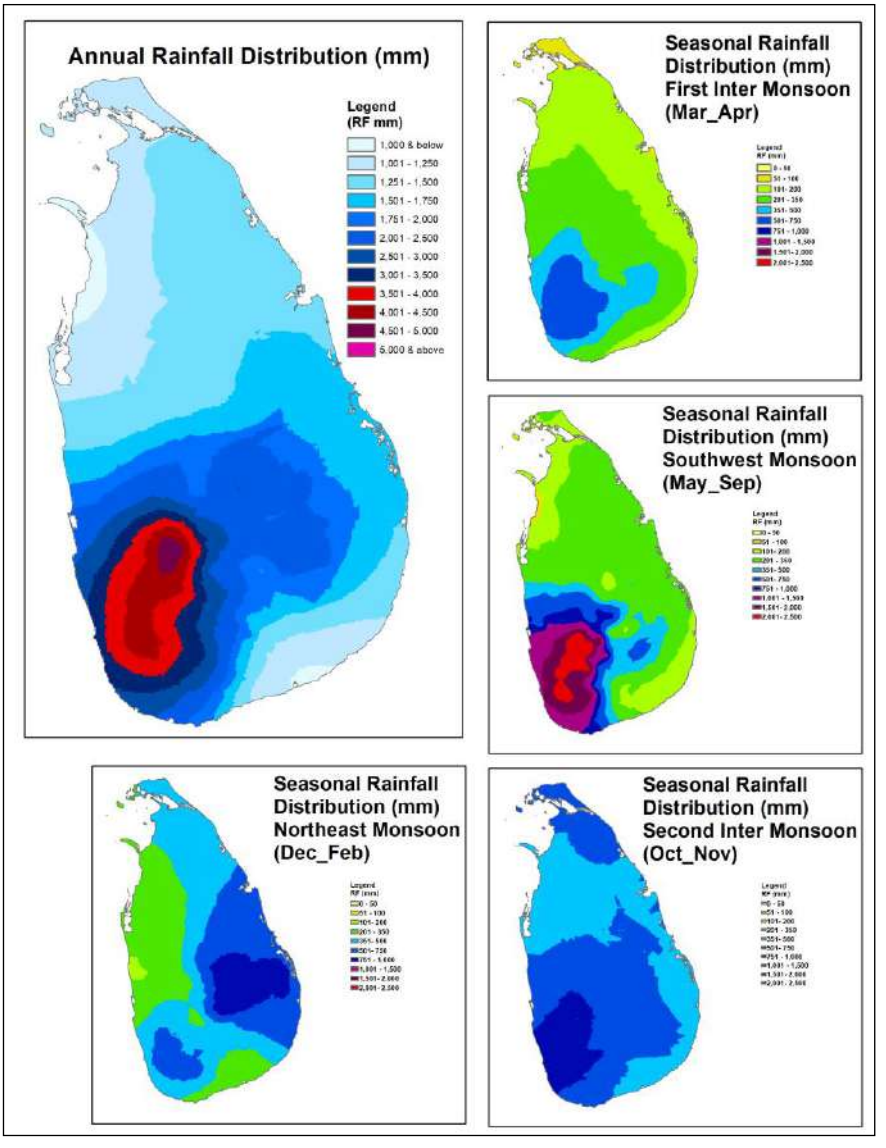

Fig. 1 Rainfall Climatology of Sri Lanka

2 **Data and Methodology**

2.1 GCM and downscaled products from CORDEX and NEX-NASA

Climate Data Sharing and Analysis System (CDAAS) developed and maintained by RIMES, is a simple web based portal to access different Global Climate models and downscaled regional climate model products. CDAAS web portal is used to extract downscaled data from NEX- GDDP and CORDEX for the Sri Lanka region.

NASA Earth Exchange Global Daily Downscaled Projections (NEX-GDDP) dataset is comprised of downscaled climate scenarios for the globe that are derived from the GCM) runs conducted under the CMIP5 (Taylor et al. 2012) and across two of the four greenhouse gas emissions scenarios known as Representative Concentration Pathways (RCPs) (Meinshausen et al. 2011) . The CMIP5 GCM runs were developed in support of the Fifth Assessment Report of the Intergovernmental Panel on Climate Change (IPCC AR5).

The Bias-Correction Spatial Disaggregation (BCSD) method used in generating the NEX-GDDP dataset (Thrasher and Nemani, 2015) is a statistical downscaling algorithm specifically developed to address these current limitations of global GCM outputs [Wood et al. 2002; Wood et al. 2004; Maurer et al. 2008 ; Thrasher et al. 2012].

The dataset compiles 42 climate projections from 21 CMIP5 GCMs and two RCP scenarios (RCP 4.5 and RCP 8.5) for the period from 2006 to 2100 as well as the historical experiment for each model for the period from 1950 - 2005. Each of these climate projections is downscaled at a spatial resolution of 0.25 degrees x 0.25 degrees (Thrasher and Nemani, 2015).

The Coordinated Regional Downscaling Experiment CORDEX aims to foster international collaboration in order to generate an ensemble of high-resolution historical and future climate projections at regional scale, by downscaling different Global Climate Models (GCMs) participating in the Coupled Model Inter-comparison Project Phase 5 (CMIP5) (Taylor et al. 2012).CORDEX produced an ensemble of multiple dynamical downscaling models considering multiple forcing GCMs from the CMIP5 with 50 km grid spacing (Giorgi et al, 2009).

Table 1 Earth System models used to evaluate	
CanESM2	The Second Generation Coupled Global Climate Model Canadian Centre for Climate Modelling and Analysis (2.8*2.8)
CNRM-CM5	National Centre for Meteorological Research/ Meteo-France (1.4 * 1.4)
CSIRO-MK3-6-0	Commonwealth Scientific and Industrial Research Organisation (CSIRO) and the Queensland Climate Change Centre of Excellence (QCCCE). (1.895*1.875)
CSIRO-CCAM-ACCESS-1	Commonwealth Scientific and IndustrialResearch Organisation (CSIRO), Conformal-CubiAtmospheric Model (CCAM; McGregor Dix, 2001)
GFDL-CM3	Geophysical Fluid Dynamic Laboratory NOAA, USA Coupled Climate Model (2 * 2.5)
MRI-CGCM3	Global Climate Model of the Meteorological Research Institute, Japan (1.132*1.125)
NCAR-CCSM4	National Center for Atmospheric Research, USA Coupled Climate Model (0.942 * 1.25)
MPI-ESM-LR& MPI-ESM-MR	Max Planck Institute for Meteorology (MPI-M)
MIROC5	Atmosphere and Ocean Research Institute (The University of Tokyo), National Institute for Environmental Studies, and Japan Agency for Marine-Earth Science and Technology

NASA Earth Exchange Global Daily Downscaled Projections data of 6 GCM models (CanESM2, CNRM-CM5, CSIRO-MK3-6-0, GFDL-CM3, MRI-CGCM3and NCAR-CCSM4) with 25km grid spacing and CORDEX data of 6 GCM models CSIRO-CCAM-ACCESS-1, CSIRO-CCAM-CCSM-4, CSIRO-CCAM-GFDL-CM3,CSIRO-CCAM-MPI-ESM-LR, REMO2009-MPI-ESM-LR, and SMHI-RCA4-ICHEC-EC with 50km grid spacing were used to evaluate models suitable for Sri Lanka.

Annual mean precipitation and seasonal mean precipitation for four climatic seasons namely Southwest Monsoon, Northeast Monsoon, First Inter-Monsoon and Second Inter-Monsoon, of model historical runs (1975-2005) were compared with observed climatological average of precipitation to evaluate the models' performance. Annual cycle of the climatological monthly mean precipitation, Maximum temperature and minimum temperatures of model historical runs (1975-2005) were compared with observed values.

2 Results & Discussion

2.1 CORDEX

Comparison of baseline climatology (rainfall and temperatures) and evaluation using observed data sets (Figure 2) shows Monthly Variation of Model historical Precipitation of dynamical downscaling of CORDEX (1975-2005) (Blue Bars) and Observed Precipitation (Red Line)

Annual cycle of precipitation climatology in Sri Lanka shows bi-model pattern with peaks around May and November (Figure 2, red line).

It shows that the model ACCESS-1 is over estimating the rainfall during the months of July and August with 124% and 183% (Figure 2) with respect to the observed climatology and under estimating during the months of March April and May as well as during the months of October November and December with departures of nearly 30-40%.

Similar results can be observed of the model CCSM_4 with 128% and 172% during the months of July and August and nearly 40% below estimations on April, October and November respectively.

Except July and August first nine months of the GFDL_CM3model goes well with the observations. Difference of model climatology and observed climatology is round 0-40% but the rest of months goes totally away with the observations with significant departures. (Figure 2) Similar results were observed over the model MPI-ESM-LR.

Through the special maps (Figure 4) key seasonal features such as high rainfall amounts (about 3000mm) over the western slopes of central hills during the Southwest monsoon, wide spread rainfall all-over the country during the second inter monsoon, high rainfalls such as 1400mm over the eastern slopes of central hills during the North-east monsoon and more rain over south west quarter of the island during the first inter monsoon were expected through the models.

CORDEX downscaled models were unable to capture the bi-modal pattern of annual cycle of precipitation in Sri Lanka (Figure2& 3) as well as the spatial pattern of precipitation (Figure4).

Temperatures climatology (Figure 3) of all the CORDEX models were able to capture the temporal pattern but showed under estimating (about 10%) in minimum temperature and over estimating ability (about 8%) in the minimum temperature. Spatial features were captured up to some extent but not much acceptable level.

2.2 NEX-GDDP models

All the NEX-GDDP models (Figure 5) were able to capture the temporal pattern mostly within 0-20% departures from the climatology except the months of August and September where the deviations are 50%& 48% respectively.

Capturing abilities of temperature patterns under NEX-GDDP models, especially the minimum temperatures are very good and maximum temperatures showed little bit of under estimating manner during the middle months of the annual cycle (Figure 6).

When ensemble these six models (Figure 10) & (Table 2) results were much better. Six months showed deviations less than 10% from the observed climatology. Only the months of August and September showed higher departures such as 44% and 37% respectively. Though the maximum temperature showed below estimating ability from April to September the departures were about 3%. Other months showed 0% or 1% departures. Minimum temperature is much better than maximum temperature, the deviations are within 1% from the climatology.

All the spatial maps of NEX-GDDP models showed good abilities while capturing key features of our seasonal climatology in rainfall (Figure7) as well as maximum (Figure 8) and minimum (Figure 9) temperatures.

NEX-GDDP downscaled models were captured the bi-modal pattern of annual cycle of precipitation in Sri Lanka (Figure 5 & 6) as well as the spatial pattern of precipitation of annual average as well as seasonal average (Figure 7).

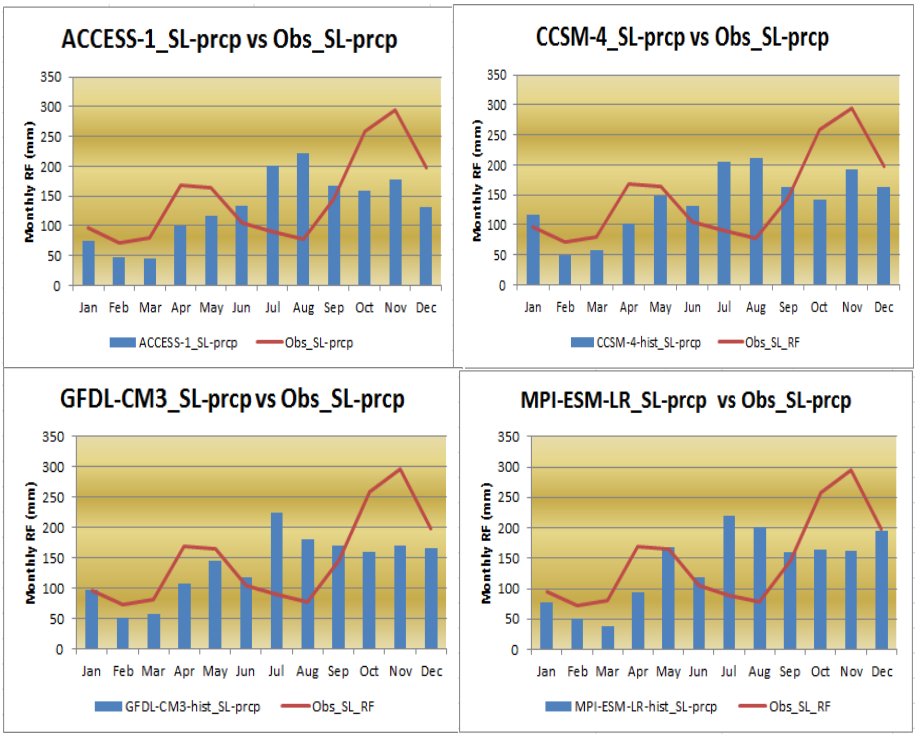

Figure 2 : Monthly Variation of Model historical Precipitation of dynamical downscaling of CORDEX (1975-2005) (bars) Vs Observed Precipitation (Red Line)

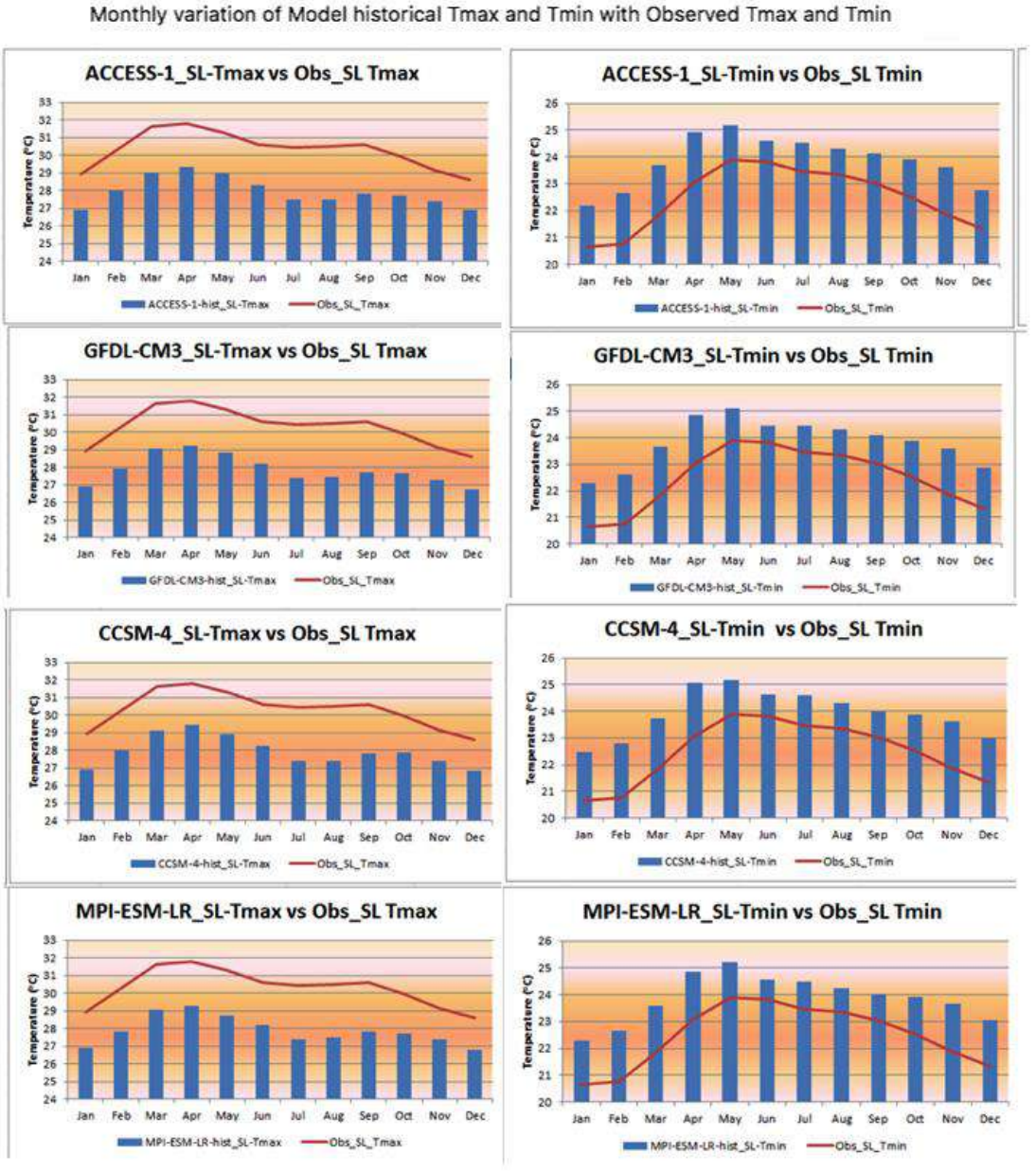

Figure3 : Monthly Variation of Model historical Maximum Temperature (Left) and Minimum Temperature (Right) of dynamical downscaling of CORDEX (1975-2005) (bars) Vs Observed Maximum Temperature (red line, left) and Observed Minimum Temperature (red line, Right)

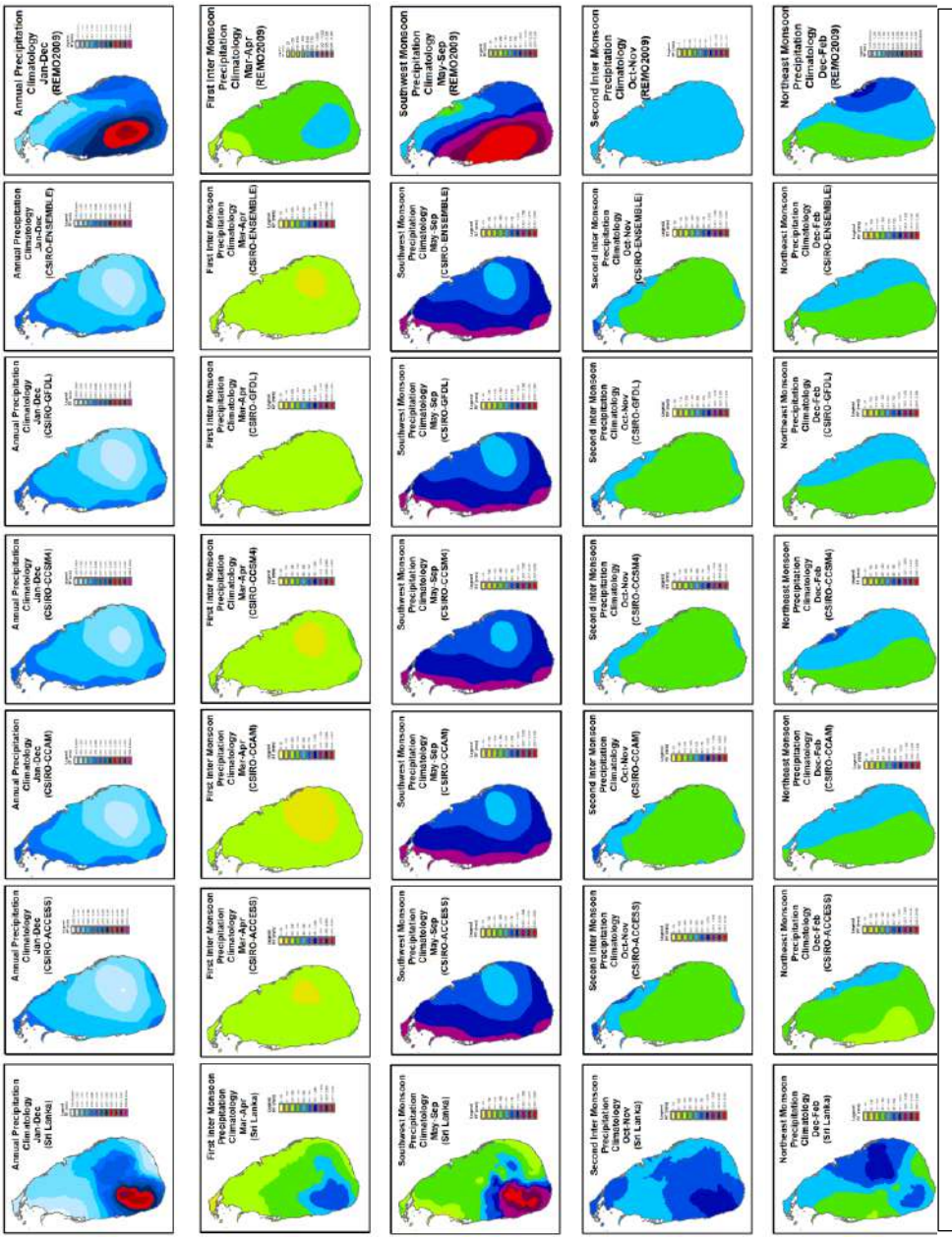

Figure 4 : Spatial variation of Model historical precipitation of dynamical downscaling of CORDEX (1975-2005) Vs Observed precipitation of Annual average (Upper), Southwest Monsoon season (Middle) and Northeast Monsoon Season

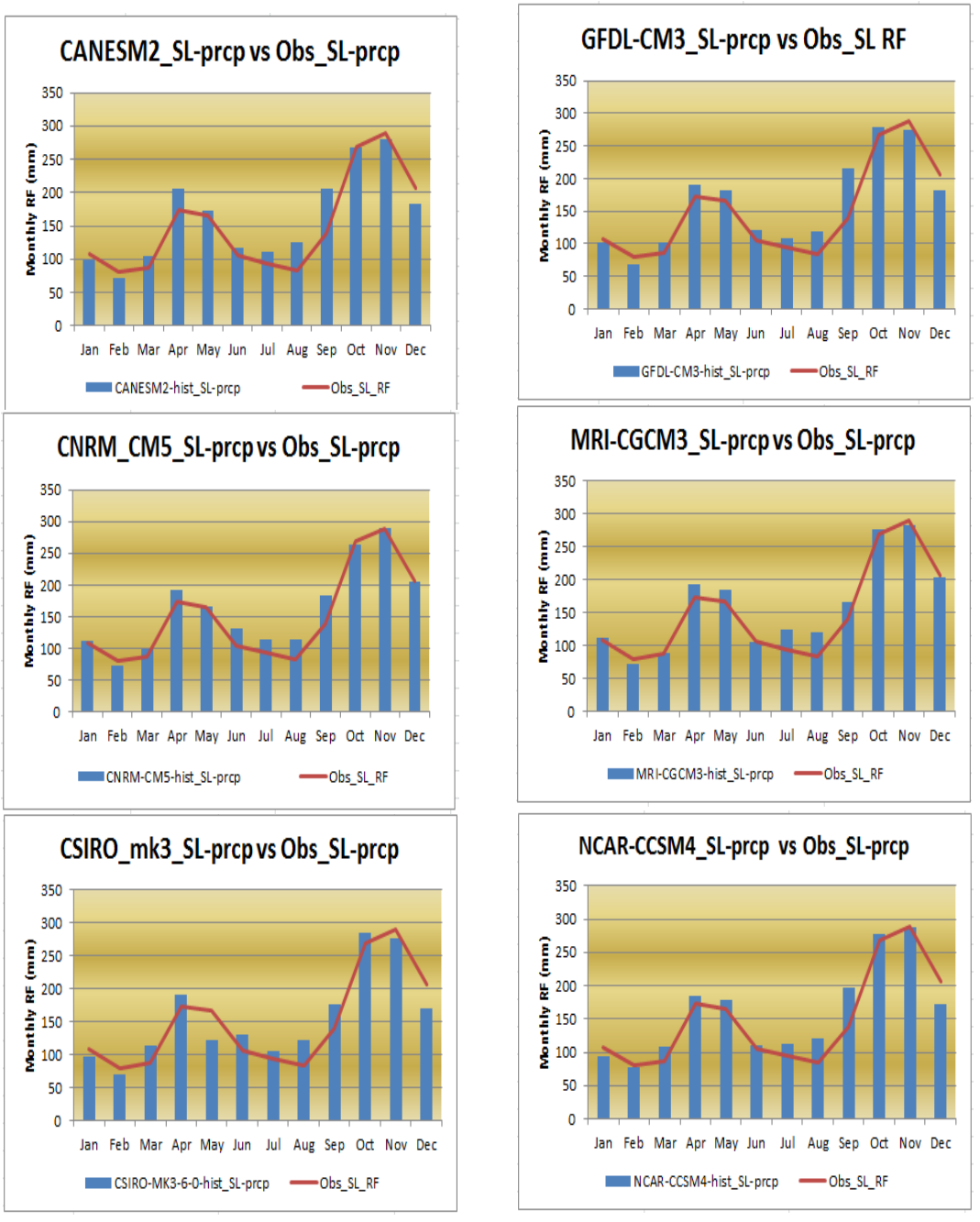

Figure 5 : Monthly Variation of Model historical Precipitation of statistical downscaling of NEX GDDP (1975-2005) (bars) Vs Observed Precipitation (Red Line)

Figure 6 : Monthly Variation of Model historical Maximum Temperature (left) and Minimum Temperature (right) of statistical downscaling of NEX GDDP (1975-2005) (bars) Vs Observed Maximum and Minimum Temperature (red line)

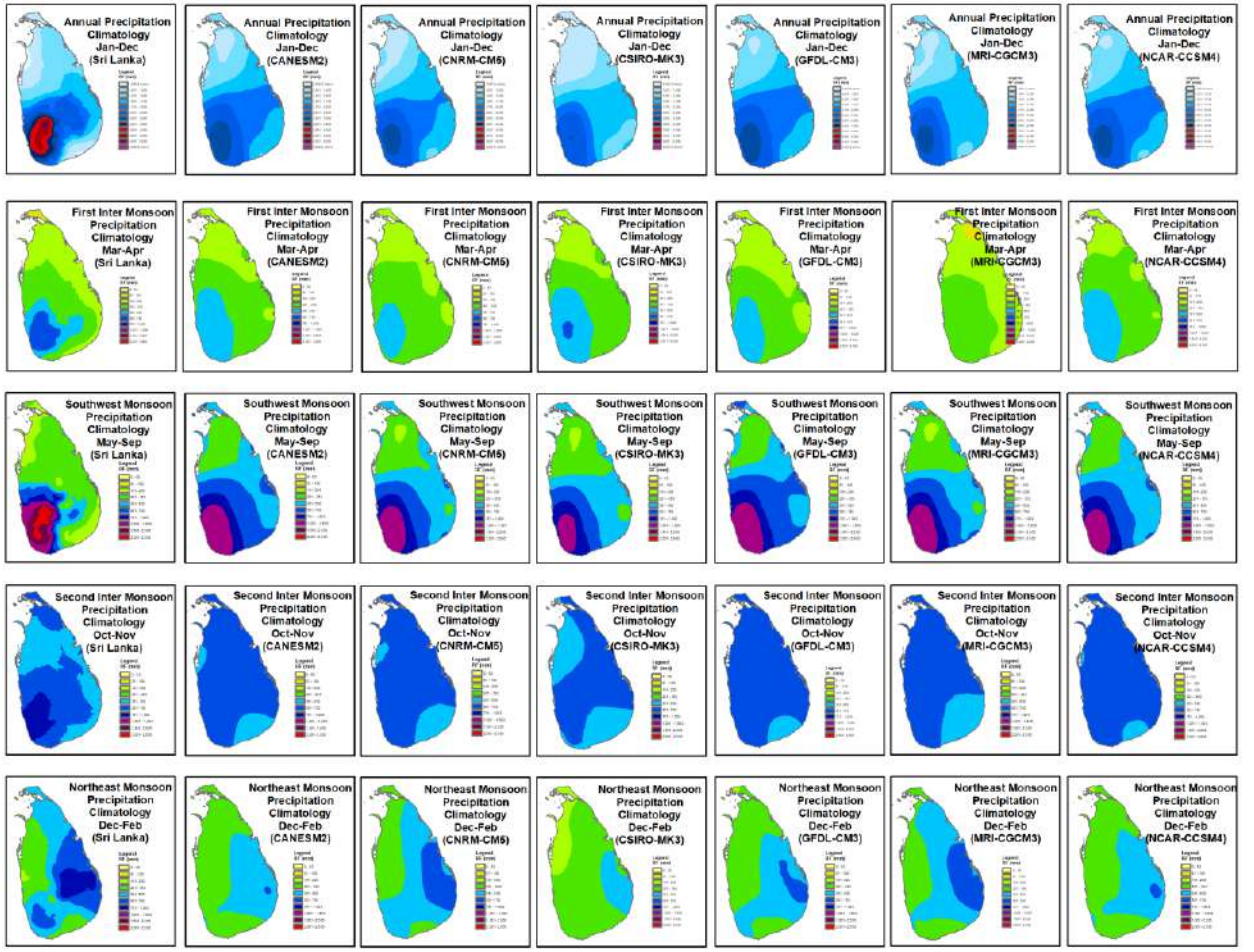

Figure 7 : Spatial variation of Model historical precipitation of Statistical downscaling of NEX-GDDP (1975-2005) Vs Observed precipitation of Annual average, Southwest Monsoon season and Northeast Monsoon Season. First Inter-monsoon season and Second Inter-monsoon season

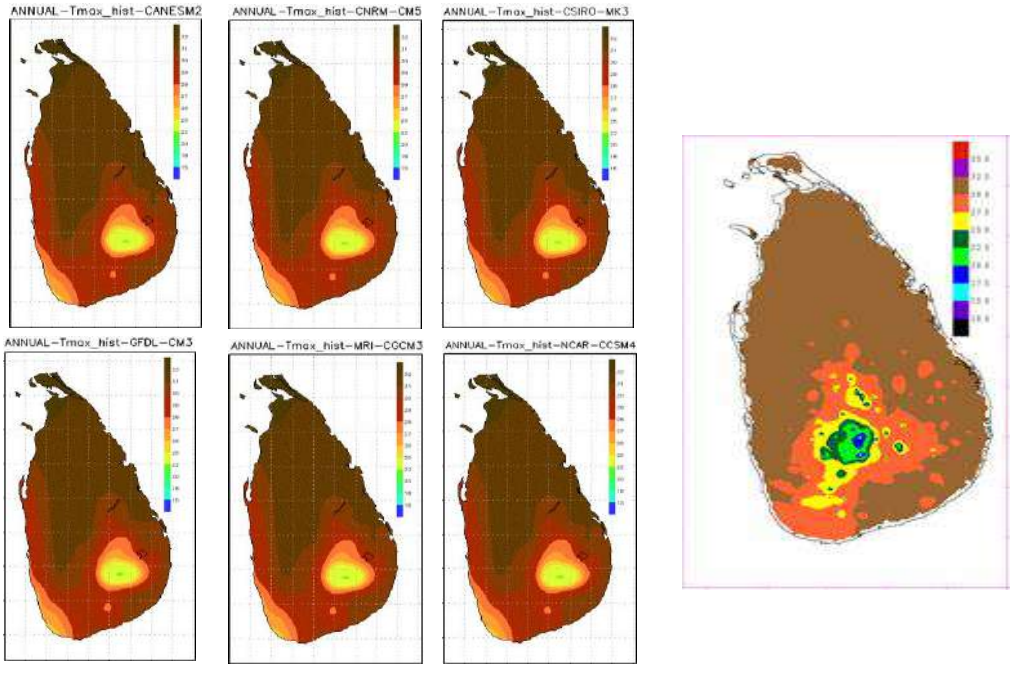

Figure 8 : Spatial variation of Model historical Maximum Temperature of Statistical downscaling of NEX-GDDP (1975-2005) Vs Observed Maximum Temperature of Annual average,

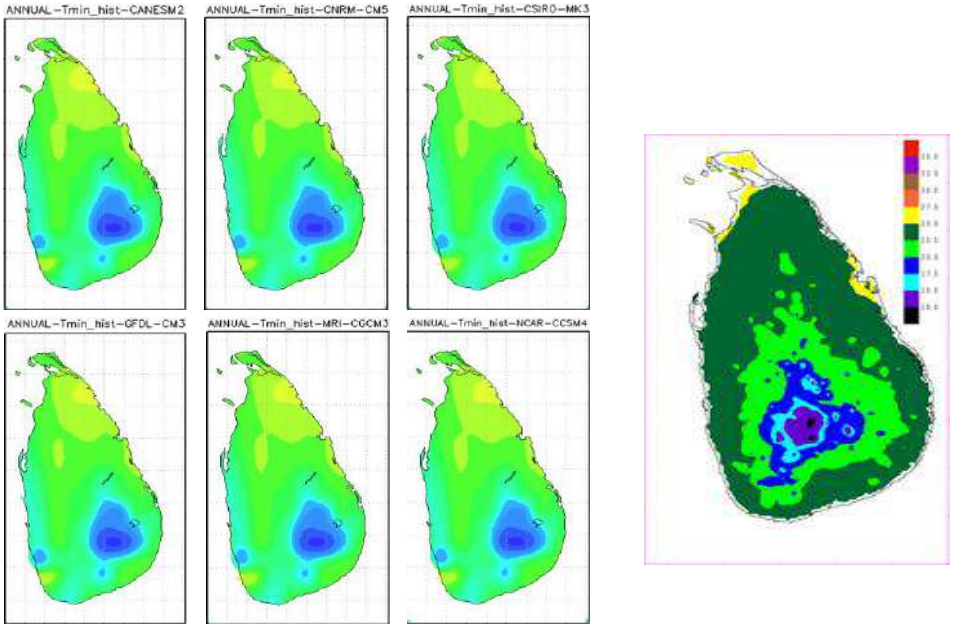

Figure 9 : Spatial variation of Model historical Minimum Temperature of Statistical downscaling of NEX-GDDP (1975-2005) Vs Observed Minimum Temperature of Annual average,

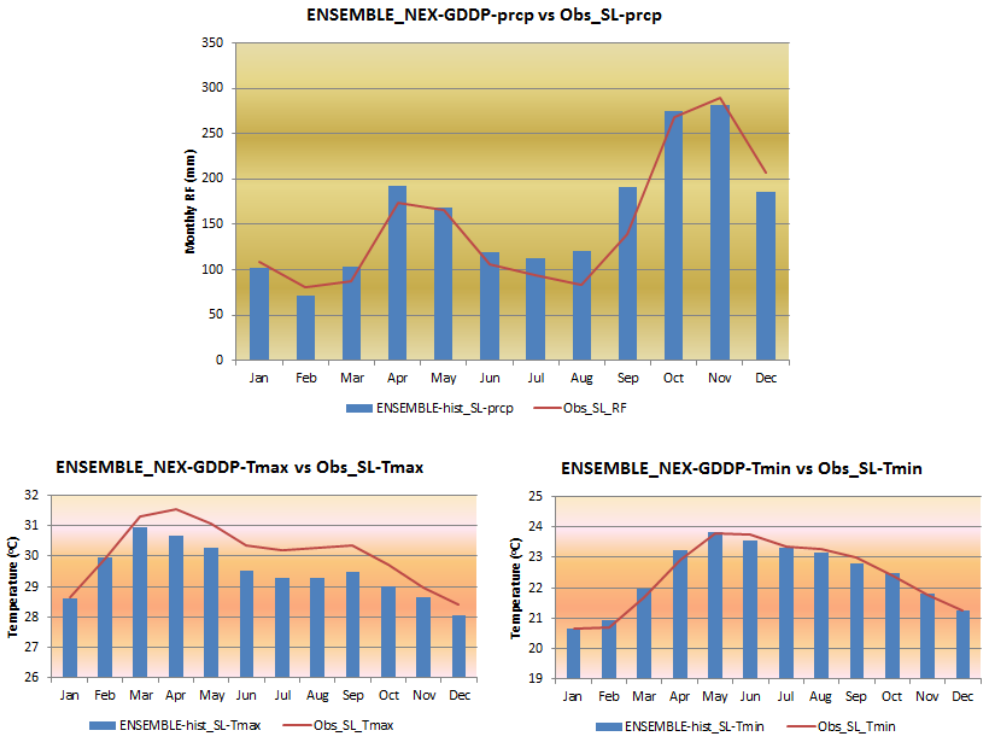

Figure 10 : Monthly Variation of Model historical precipitation (above), Maximum Temperature (left) and Minimum Temperature (right) of statistical downscaling of Ensemble NEX-GDDP (1975-2005) (bars) Vs Observed Maximum and Minimum Temperature (red line)

Table 2 - % of departure_ ENSEMBLE Climatology from Observed Climatology (Sri Lanka)			
	Precipitation	Tmax	Tmin
Jan	-6%	0%	0%
Feb	-10%	0%	1%
Mar	18%	-1%	1%
Apr	11%	-3%	1%
May	1%	-3%	0%
Jun	13%	-3%	-1%
Jul	19%	-3%	0%
Aug	44%	-3%	0%
Sep	37%	-3%	-1%
Oct	2%	-2%	0%
Nov	-3%	-1%	0%
Dec	-10%	-1%	0%
Annual	7%	-2%	0%

Conclusion

NASA Earth Exchange Global Daily Downscaled Projections data with 25km grid spacing and Coordinated Regional Climate Downscaling Experiment (CORDEX) data with 50km grid spacing of 6 GCM models were used to evaluate models suitability for Sri Lanka. Annual mean precipitation and seasonal mean precipitation for four climatic seasons namely Southwest Monsoon, Northeast Monsoon, First Inter monsoon and Second Inter-Monsoon, of model historical runs (1975-2005) were compared with observed climatological average of precipitation to evaluate the models' performance.

CORDEX downscaled models were unable to capture the bi-modal pattern of annual cycle of precipitation in Sri Lanka and the spatial pattern of precipitation.

NEX-GDDP downscaled models captured the bi-modal pattern of annual cycle of precipitation in Sri Lanka and the spatial pattern of precipitation of annual average as well as seasonal average. Based on the model performance of historical runs NASA Earth Exchange Global Daily Downscaled Projections of 6 GCM models (CanESM2, CNRM-CM5, CSIRO-MK3-6-0, GFDL-CM3, MRI-CGCM3and NCAR-CCSM4) with 25km grid spacing were selected to develop future projections for Sri Lanka.

Based on the model performance of historical runs NASA Earth Exchange Global Daily Downscaled Projections of 6 GCM models (CanESM2, CNRM-CM5, CSIRO-MK3-6-0, GFDL-CM3, MRI-CGCM3and NCAR-CCSM4) with 25km grid spacing were used future projections for Sri Lanka.

Acknowledgement

Technical support provided by RIMES under the "Capacity building on generation and application of downscaled climate change projections" project funded by UN ESCAP Trust Fund for Tsunami, Disaster and Climate Preparedness in Indian Ocean and Southeast Asian Countries (LOA No. 2014-0036) is acknowledged.

REFERENCES

Chandrapala, L., 1996. Long term trends of rainfall and temperature in Sri Lanka. *Climate variability and agriculture*, pp.153-162.

Giorgi, F., Jones, C. and Asrar, G.R., 2009. Addressing climate information needs at the regional level: the CORDEX framework. *World Meteorological Organization (WMO) Bulletin*, *58*(3), p.175.)

Hartmann, D.L., Tank, A.M.G.K. and Rusticucci, M., 2013. IPCC fifth assessment report, climate change 2013: The physical science basis. *IPCC AR5*, pp.31-39.

Maraun, D., Wetterhall, F., Ireson, A.M., Chandler, R.E., Kendon, E.J., Widmann, M., Brienen, S., Rust, H.W., Sauter, T., Themeßl, M. and Venema, V.K.C., 2010. Precipitation downscaling under climate change: Recent developments to bridge the gap between dynamical models and the end user. *Reviews of Geophysics*, *48*(3).

Maurer, E.P. and Hidalgo, H.G., 2008. Utility of daily vs. monthly large-scale climate data: an intercomparison of two statistical downscaling methods.

Prudhomme, C., Reynard, N. and Crooks, S., 2002. Downscaling of global climate models for flood frequency analysis: where are we now?. *Hydrological processes*, *16*(6), pp.1137-1150.

Taylor, K.E., Stouffer, R.J. and Meehl, G.A., 2012. An overview of CMIP5 and the experiment design. *Bulletin of the American Meteorological Society*, *93*(4), pp.485-498.

Thrasher, B. and Nemani, R., NASA Earth Exchange Global Daily Downscaled Projections (NEX-GDDP) 2015 1. Intent of This Document and POC.)

Trzaska, S. and Schnarr, E., 2014. A review of downscaling methods for climate change projections. *United States Agency for International Development by Tetra Tech ARD*, pp.1-42.

Van Vuuren, D.P., Edmonds, J., Kainuma, M., Riahi, K., Thomson, A., Hibbard, K., Hurtt, G.C., Kram, T., Krey, V., Lamarque, J.F. and Masui, T., 2011. The representative concentration pathways: an overview. *Climatic change*, *109*(1-2), p.5.

Wilby, R.L. and Wigley, T.M.L., 1997. Downscaling general circulation model output: a review of methods and limitations. *Progress in physical geography*, *21*(4), pp.530-548.)

Wood, A.W., Leung, L.R., Sridhar, V. and Lettenmaier, D.P., 2004. Hydrologic implications of dynamical and statistical approaches to downscaling climate model outputs. *Climatic change*, *62*(1), pp.189-216.

Zorita, E. & von Storch, H. (1999). The Analog method as a simple statistical downscaling technique: comparison with more complicated methods. Journal of Climate 12(8), 2474-2489.

Multi Model Ensemble climate change projections for annual and seasonal rainfall in Sri Lanka

D W T T Darshika ,
I M S P Jayawardane
D M S C Disanayake
Department of Meteorology
Colombo 07

ABSTRACT

Statistically downscaled data into 25kmx25km grid resolution of 6 earth system models namely CanESM2, CNRM-CM5, CSIRO-MK3-6-0, GFDL-CM3, MRI-CGCM3, and NCAR-CCSM4 under coupled model inter-comparison project 5 (CMIP5) are analysed to see the future Changes in annual as well as seasonal Rainfall over Sri Lanka for 3 time periods; 2020–2040, 2040-2060 and 2070-2090 relative to baseline climatology period 1975-2005 for two emission scenarios; Rcp 4.5 representing low emission and Rcp 8.5 representing high emission scenario. The results of Rainfall changes are indicated that annual rainfall anomaly is negative in North-eastern parts, and positive in South-western parts for the period 2020-2040 and positive and increasing thereafter under RCP 4.5 scenario. Annual rainfall anomaly is positive and increasing for all 3 time periods under RCP 8.5 scenario . Southwest monsoon rainfall anomaly is positive and increasing in both RCP 4.5 and RCP 8.5 scenarios with significant increase in rainfall over the wet zone. North-east monsoon rainfall anomaly negative and negative trend is observed in RCP 4.5 and RCP 8.5. Decrease in rainfall is significant in the dry zone.

First Inter Monsoon rainfall anomaly is negative in 2020-2040, slightly negative in 2040-2060 and positive except North-eastern parts under RCP 4.5. First Inter Monsoon rainfall anomaly is negative in all 3 time periods under RCP 8.5 scenarios No significant trend is evident in RCP 8.5. Second Inter Monsoon rainfall anomaly is negative in North eastern parts, and positive in South-western parts in 2020-2040 and positive and increasing after that under RCP 4.5. Second Inter Monsoon rainfall anomaly is positive and increasing in 8.5 scenarios with increase in rainfall is significant in the South-western and South-eastern parts.

1. Introduction

Climate models are currently the most credible tools for making projections of future climate over the next 100 years. A range of different climate models exist, from the simplest energy balance models to the most sophisticated global circulation models (GCMs; see, for example, McGuffie and Henderson-Sellers, 2004). Uncertainty in climate change projections include representation of the GHG emissions scenarios, uncertainties associated with future estimates of population growth, changes in land use, and the economic growth ect. Further uncertainties in climate modelling arise from uncertainties in initial conditions, boundary conditions, observational uncertainties, uncertainties in model parameters and structural uncertainties resulting from the fact that some processes in the climate system are not fully understood or are impossible to resolve due to computational constraints (IPCC, AR4).

The Intergovernmental Panel on Climate Change (IPCC) Fourth assessment report (AR4) stated that the current understanding of future climate change in the monsoon regions remains one of considerable uncertainty with respect to circulation and precipitation (IPCC AR4 Sections 3.7, 8.4.10 and 10.3.5.2).

Multi-model ensembles are defined in these studies as a set of model simulations from structurally different models, where one or more initial condition ensembles are available from each model and it is identified that projections have higher reliability and consistency when several independent models are combined (Doblas-Reyes et al. 2003; Yun et al. 2003). Multi-model projections for long-term climate change were used in reports of the Intergovernmental Panel on Climate Change (IPCC), where unweighted multi-model means rather than individual model results were often presented as best guess projections (IPCC 2001).

According to previous studies, an increase in precipitation is projected in the Asian monsoon (along with an increase in inter-annual season-averaged precipitation variability) and the southern part of the West African monsoon with some decrease in the Sahel in northern summer, as well as an increase in the Australian monsoon in southern summer in a warmer climate. Differently from precipitation, Asian monsoon circulation was projected to decrease by 15 % (Tanaka et al. 2005; Ueda et al. 2006).

The main objective of this paper is to to develop CMIP5-based short-term (2030s representing climatology over 2021–2040), medium-term (2050s representing climatology over2041–2060) and long-term (2080s representing climatology over 2071–2090 (climate change projections in Rainfall for Sri Lanka based on a multi-model ensemble of 6 models.

The remainder of the paper is organized as follows. Descriptions of the data and analysis method used are presented in section 2. In section 3, Future climate projections for annual and seasonal rainfall in Sri Lanka using CMIP5 models are investigated. Conclusion is presented in section 4.

2. Data and Methodology

NASA Earth Exchange Global Daily Downscaled Projections (NEX-GDDP) dataset is comprised of downscaled climate scenarios for the globe that are derived from the General Circulation Model (GCM) runs conducted under the CMIP5 and across two of the four greenhouse gas emissions scenarios known as Representative Concentration Pathways (RCPs). The CMIP5 GCM runs were developed in support of the Fifth Assessment Report of the Intergovernmental Panel on Climate Change (IPCC AR5). The NEX-GDDP dataset includes downscaled projections for RCP 4.5 and RCP 8.5.

Table1 Earth System models used to evaluate

CanESM2	The Second Generation Coupled Global Climate Model Canadian Centre for Climate Modelling and Analysis (2.8*2.8)
CNRM-CM5	National Centre for Meteorological Research/ Meteo-France (1.4 * 1.4)
CSIRO-MK3-6-0	Commonwealth Scientific and Industrial Research Organization (CSIRO) and the Queensland Climate Change Centre of Excellence (QCCCE). (1.895*1.875)
GFDL-CM3	Geophysical Fluid Dynamic Laboratory NOAA, USA Coupled Climate Model (2 * 2.5)
MRI-CGCM3	Global Climate Model of the Meteorological Research Institute, Japan (1.132*1.125)
NCAR-CCSM4	National Center for Atmospheric Research, USA Coupled Climate Model (0.942 * 1.25)

Based on the model performance of historical runs NASA Earth Exchange Global Daily Downscaled Projections of 6 GCM models (CanESM2, CNRM-CM5, CSIRO-MK3-6-0, GFDL-CM3, MRI-CGCM3 and NCAR-CCSM4) with 25km grid spacing were used future projections for Sri Lanka (Herath.2016). Future change of precipitation for 3 time periods 20-year centered on 2030s, 2050s and 2080s (2020-2040, 2040-2060 and 2070-2090) for 2 emission scenarios RCP 4.5 and RCP 8.5 were constructed by comparing climatological means during the historical run period (1975–2005). Spatial patterns of precipitation for all three futures are discussed on Seasonal and annual basis. Never the less this work is giving good initial idea about the future climate changes in precipitation over Sri Lanka.

3. Results

Three time slices incorporating 20-year cantered on 2030s, 2050s and 2080s were examined to gain some insight into the range of future prediction of temperature and precipitation for Rcp8.5 and Rcp4.5 scenarios. Spatial patterns of precipitation and temperature for all three futures are discussed on Seasonal and annual basis. Never the less this work is giving good initial idea about the future climate changes in temperature and precipitation over Sri Lanka.

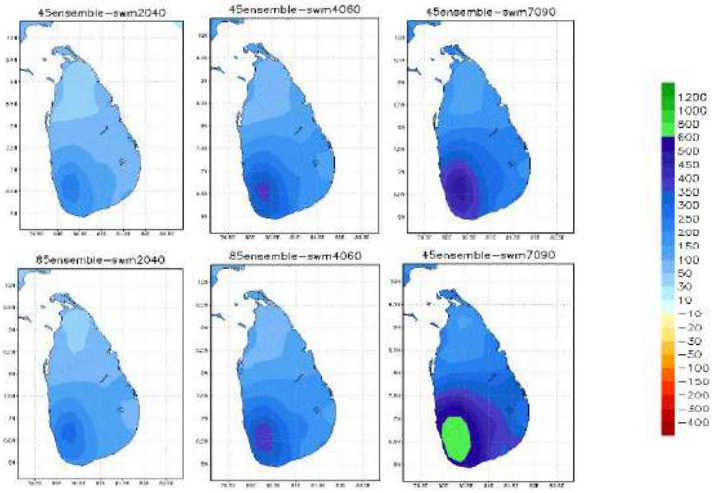

Figure 1: Multi model ensemble of change in Southwest Monsoon Rainfall, relative to 1975-2005 for moderate emission scenario (RCP 4.5) (upper) and high emission scenario (RCP 8.5) for time periods (2020-2040), (2040-2060), (2070-2090).

For the period from 2020 to 2040 positive anomaly rainfall is predicted over most parts of the island by multi-model ensemble prediction under moderate and high (Figure. 1) emission scenarios.

For the period from 2040 to 2060, and 2070 to 2090 positive anomaly rainfall is predicted over most parts of the island by multi-model ensemble prediction under moderate and high (Figure.1) emission scenarios. Higher positive values are clearly apparent in the wet zone. It is evident that the intensity as well as areal extension of the positive rainfall anomaly over the wet zone increases with time (Figure1)

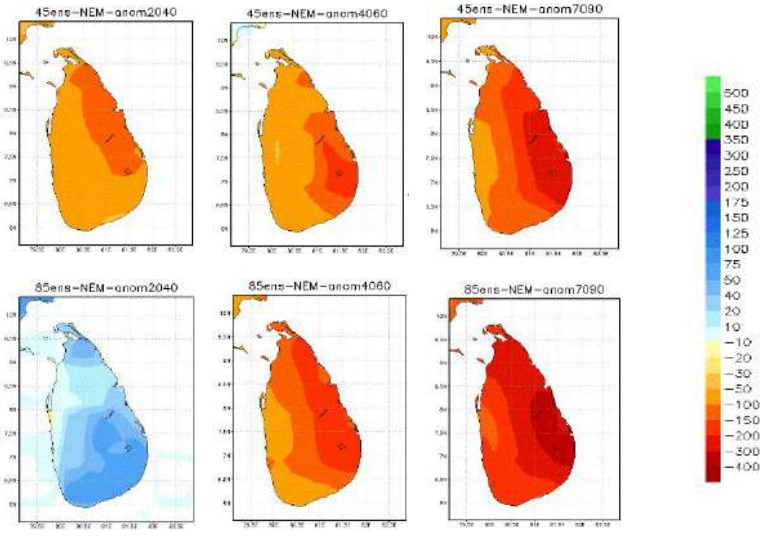

Figure2: Multi model ensemble of change in Northeast -Monsoon Rainfall, relative to 1975-2005 for moderate emission scenario (RCP 4.5) (upper) and high emission scenario (RCP 8.5) for time periods (2020-2040), (2040-2060), (2070-2090).

For Northeast monsoon season, the multi-model ensemble product predicted negative anomaly over the entire island under moderate emission scenario and slightly positive anomaly over the most parts of the island under high emission scenario for 2020-2040 period (Figure2)**.**

For the period from 2040 to 2060, multi-model ensemble product predicted negative rainfall anomaly over the most parts of Sri Lanka for both moderate and high emission scenarios (Figure2).

For the period from 2070 to 2090, multi-model ensemble product predicted negative rainfall anomaly over Sri Lanka for both moderate and high emission scenarios with more negative values can be seen dry zone (Figure2).

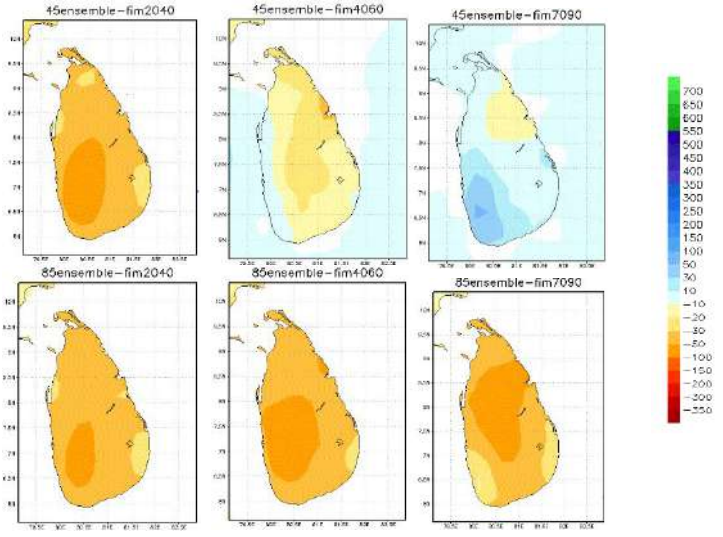

Figure 3: Multi model ensemble of change in First Inter-Monsoon Rainfall, relative to 1975-2005 for moderate emission scenario (RCP 4.5) (upper) and high emission scenario (RCP 8.5) for time periods (2020-2040), (2040-2060), (2070-2090).

When consider about the First inter-monsoon season (Figure3), negative rainfall anomaly is evident in 2020-2040 period, slightly negative rainfall anomaly is evident in 2040-2060 period and positive rainfall anomaly is evident in 2070-2090 period according to the medium emission scenario. But according to the results of the high emission scenario it shows negative anomaly rainfall in 2020-2040, 2040-2060 and 2070-2090.

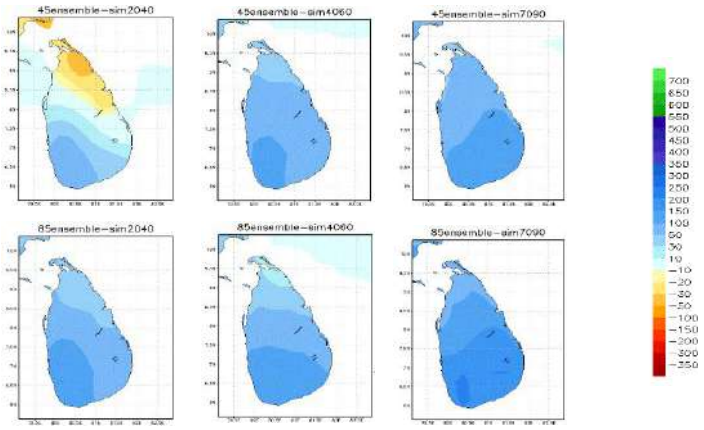

Figure 4. Multi model ensemble of change in Second Inter -Monsoon Rainfall, relative to 1975-2005 for moderate emission scenario (RCP 4.5) (upper) and high emission scenario (RCP 8.5) for time periods (2020-2040), (2040-2060), (2070-2090).

For second-inter monsoon season, the multi-model ensemble product predicted negative anomaly over the northeastern parts while slightly positive anomaly elsewhere (Figure4) for moderate emission scenario for 2020-2040 period**.** For high emission scenario, the multi-model ensemble product predicted positive anomaly rainfall over most parts of the island (Figure4) for 2020-2040 period. For the period from 2040 to 2060, the multi-model ensemble product predicted positive rainfall anomaly over Sri Lanka for both moderate and high emission scenarios (Figure 4). The multi-model ensemble prediction predicted positive rainfall anomaly over the entire country for 2070-2090 period under moderate and high emission scenario (Figure 4).

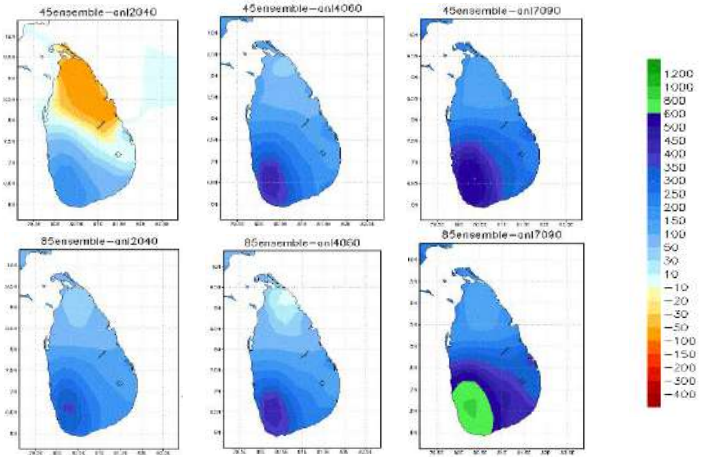

Figure 5: Multi model ensemble of change in Annual Rainfall, relative to 1975-2005 for moderate emission scenario (RCP 4.5) (upper) and high emission scenario (RCP 8.5) for time periods (2020-2040), (2040-2060), (2070-2090).

The multi-model ensemble product indicated negative anomaly over the dry zone and positive anomaly over the dry zone for 2020-2040 period under moderate emission scenario. Multi-model ensemble predicted positive anomaly over most parts of the island for 2020-2040 period under high emission scenario (Figure 5). Increasing rainfall is significant over the wet zone in most models.

The multi-model ensemble product indicated positive rainfall anomaly over the entire country for 2040-2060 period under both moderate and high emission scenarios with significant increase in rainfall over the wet zone.

The multi-model ensemble product indicated positive rainfall anomaly over the entire country for 2070-2090 period under both moderate and high emission scenarios with significant increase in rainfall over the wet zone. Increase in rainfall over the wet zone is more significant in high emission scenario than moderate emission scenario.

The nonlinear and chaotic nature of the climate system imposes natural limits on the extent to which skillful predictions of climate statistics may be made. Model-based 'predictability' studies, which probe these limits and investigate the physical mechanisms involved, support the potential for the skillful prediction of annual to decadal average temperature and, to a lesser extent precipitation (IPCC, AR5 Synthesis report). Even though the Near-term (2020-2040) climate projections are important to decision makers in government and industry, the uncertainty during this period is high due to the climate is more reliance on the initial state of internal variability and less reliance on external forcing from emission scenarios.

4. Conclusion

NASA Earth Exchange Global Daily Downscaled Projections (NEX-GDDP) data GCM 6 climate models (25-kilometer (km) grid resolution) were compared with model historical runs and observed data from 1975-2005 to evaluate model performance. NEX-GDDP downscaled models were captured the bi-modal pattern of annual cycle of precipitation in Sri Lanka as well as the spatial pattern of precipitation of annual average as well as seasonal average.

NEX-GDDP data of GCM 6 climate models were used to develop figure climate projections.

The Representative Concentrated Pathways (RCP) RCP 8.5 and 4.5 scenarios from of the IPCC AR5 2013, representing high and medium futures, respectively, were adopted, with three time periods—2030s, 2050s, and 2080s.

The results indicated that the Annual rainfall anomaly is negative in North-eastern parts, and positive in Southwestern parts in 2020-2040, while Annual rainfall anomaly is positive and increasing thereafter under moderate emission scenario RCP 4.5. Southwest monsoon rainfall anomaly is

positive and increasing in both moderate (RCP 4.5) and high (RCP 8.5) emission scenario. Northeast monsoon rainfall anomaly is negative for short term, medium term and long term projections observed under moderate emission scenario RCP 4.5. Northeast monsoon rainfall anomaly slightly positive in short term projection 2020-2040, and negative thereafter for medium term and long term projections under high emission scenario.

First Inter Monsoon rainfall anomaly is negative in 2020-2040, slightly negative in 2040-2060 and positive except North-eastern parts under moderate emission scenario RCP 4.5. First Inter Monsoon rainfall anomaly is negative in all 3 time frames with no significant trend under high emission scenario 8.5.

Second Inter Monsoon rainfall anomaly is negative in North-eastern parts, and positive in Southwestern parts in 2020-2040. Positive and increasing after that under RCP 4.5.
Second Inter Monsoon rainfall anomaly is positive and increasing in 8.5 scenarios with significant increase of positive rainfall anomaly over the Southwestern and South-eastern parts.

Acknowledgment

Technical support provided by RIMES under the "Capacity building on generation and application of downscaled climate change projections" project funded by UN ESCAP Trust Fund for Tsunami, Disaster and Climate Preparedness in Indian Ocean and Southeast Asian Countries (LOA No. 2014-0036) is acknowledged. Climate scenarios used were from the NEX-GDDP dataset, prepared by the Climate Analytics Group and NASA Ames Research Center using the NASA Earth Exchange, and distributed by the NASA Center for Climate Simulation (NCCS) .

REFERENCES

Cayan, D.R., Maurer, E.P., Dettinger, M.D., Tyree, M. and Hayhoe, K., 2008. Climate change scenarios for the California region. *Climatic change*, *87*, pp.21-42.

Doblas-Reyes, F. J., Pavan, V. & Stephenson, D. B. 2003 The skill of multimodel seasonal forecasts of the wintertime North Atlantic Oscillation. Clim. Dynam. 21, 501–514. (doi:10.1007/s00382- 003-0350-4)

Gbode, I.E., Akinsanola, A.A. and Ajayi, V.O., 2015. Recent Changes of Some Observed Climate Extreme Events in Kano. *International Journal of Atmospheric Sciences*, *2015*.

IPCC 2001 In Climate change 2001: the scientific basis. Contribution of working group I to the third assessment report of the Intergovernmental Panel on Climate Change (eds J. T. Houghton, Y. Ding, D. J. Griggs, M. Noguer, P. J. van der Linden, D. Xiaosu, X. Dai, K. Maskell & C. A. Johnson), p. 881. Cambridge, UK: Cambridge University Press.

Karmacharya, J., Shrestha, A. and Shrestha, M.L., 2007. Climate change scenarios for South Asia and Central Himalayan region based on GCM ensemble. *Department of Hydrology and Meteorology, Kathmandu*.

Lee, J.Y. and Wang, B., 2014. Future change of global monsoon in the CMIP5. *Climate Dynamics*, *42*(1-2), pp.101-119.

McGuffie, K. and Henderson-Sellers, A., 2005. *A climate modelling primer*. John Wiley & Sons.

Tanaka, H.L., Ishizaki, N. and Nohara, D., 2005. Intercomparison of the intensities and trends of Hadley, Walker and monsoon circulations in the global warming projections. *SOLA*, *1*, pp.77-80.

Vera, C., Silvestri, G., Liebmann, B. and González, P., 2006. Climate change scenarios for seasonal precipitation in South America from IPCC-AR4 models. *Geophysical Research Letters*, *33*(13).

Yun, W. T., Stefanova, L. & Krishnamurti, T. N. 2003 Improvement of the multimodel supersensemble technique for seasonal forecasts. J. Clim. 16, 3834–3840.

Modulation of Monthly Rainfall in Sri Lanka by ENSO and ENSO Modoki Extremes

H. A. S. U. Hapuarachchi
I. M. S. P. Jayawardena
Department of Meteorology
Colombo 07

ABSTRACT

The ENSO phenomenon is responsible for strong inter annual variability of rainfall the tropics. A new type of ENSO event called ENSO-Modoki is also responsible for strong inter annual variability of rainfall the tropics, similar to the ENSO phenomenon.

Investigating the nature of monthly rainfall variability with ENSO and ENSO Modoki extreme provides useful information that may lead to enhance of monthly rainfall forecasting skill. The main objective of this study is to investigate the nature of the monthly rainfall variability with ENSO and ENSO Modoki extreme events in Sri Lanka and to compare the impact changes between ENSO and ENSO Modoki extremes on Sri Lanka monthly rainfall.

The influence of El Niño and La Niña on monthly rainfall and El Niño Modoki and La Niña Mooki on monthly rainfall over Sri Lanka was assessed using 61 year monthly rainfall data for the period from 1950 to 2011 from 90 rainfall stations, Oceanic Niño Index (ONI) and El Niño Modoki Index (EMI) respectively. Composite maps of monthly rainfall anomaly maps for ENSO and ENSO Modoki extremes were created.

Out of 12 months, strongest impacts with reduction (enhancement) of rainfall across the country were clearly evident in Months of February during El Niño (La Niña) years. Conversely enhancing (reduction) of rainfall is evident in month of May, October and November during the El Niño (La Niña).

Key words: *El Niño Southern Oscillation (ENSO), El Niño, La Niña, Ocean Nino Index, Modoki event*

1. Introduction

Large-scale climate events, such as the El Niño -Southern Oscillation (ENSO), exert an appreciable impact on the socio-economic well-being of the country. A prolonged drought causes severe water supply crises, disrupts agricultural activities, and destroys rain-fed crops while severe floods often results in massive evacuation and destruction of public and private properties, damage to crops, and even leads to the loss of lives. Hence, the importance and need for accurate and useful climate prediction schemes are clear. The skilful forecast of monthly rainfall with appreciable lead-time provides useful information for decision makers to better manage resources, establish mitigation plans, and enhance response strategies related to flood and drought disasters.

The most important component of ocean atmospherics system is the ENSO (El Niño Southern Oscillation) cycle, which refers to the coherent, large-scale fluctuation of ocean temperatures, rainfall, atmospheric circulation, vertical motion and air pressure across the tropical Pacific(Troccoli, 2008). El Niño and La Niña events are associated with the inter-annual extreme rainfall variability, especially in the tropical and sub-tropical regions of the Pacific basin (Ropelewski and Halpert, 1987; Philander, 1990; Manson, S. and Goddard,L. 2001; Dewitte et al., 2013). The events of La Niña are associated with unusual cold temperatures in the equatorial Pacific Ocean, while El Niño is characterized by unusual high temperatures in the same region. Both of them have an important impact on precipitation patterns, which can increase or decrease the occurrence of extreme dry/precipitation events.

El Niño Modoki is another coupled ocean-atmosphere phenomenon in the tropical Pacific Ocean, which is quite different from the El Niño regarding their spatial and temporal characteristics as well as their teleconnection patterns (Ashok et al. 2007; Weng et al. 2007). Modoki in Japanese means "a similar but different thing". El Niño Modoki is also named as "Date Line El Niño" (Larkin and Harrison 2005), "Central Pacific El Niño" (Yu and Kao 2009) or "Warm Pool El Niño" (Kug et al. 2009). El Niño Modoki is characterized by a warm tropical sea surface temperature anomaly (SSTA) in the central equatorial Pacific and cold SSTA in the western and eastern Pacific (Feng et al, 2011). During an El Niño Modoki event, there are two anomalous Walker Circulation cells in the troposphere, instead of the single-celled pattern of the conventional El Niño (Weng et al. 2007). The principal rising branch of the double-celled Walker Circulation is located over the central equatorial Pacific, and the associated western descending branch is located over Indonesia and Northern Australia and associated western descending branch is located over Eastern equatorial Pacific. Its impacts on the tropical and mid-latitude climate are distinct from these of normal El Niño because the intensity and locations of their associated SST-induced heating are different (e.g. Larkin and Harrison 2005; Ashok et al. 2007; Weng et al. 2007 and 2009; Cai and Cowan 2009;).

The influences of El Niño Modoki during different El Niño phases over East Asia have been documented and compared with these of canonical El Niño (Weng et al. 2007 and 2009; Ashok et al. 2007; Feng and Li 2011; Feng et al. 2011; Zhang et al. 2011). Weng et al. (2007, 2009) and Ashok et al. (2007) analyzed the impacts of El Niño Modoki in boreal summer and winter of the El Niño developing year. The composite and partial correlation analyses illustrated that El Niño Modoki greatly influences the rainfall anomalies over the maritime regions, India, southern Japan, and eastern Australia in summer, while its influences on rainfall in China in summer are weak (Ashok et al. 2007).

As the Impacts of El Nino and La Nina on seasonal rainfall for four climatic seasons in was discussed in the previous journal SLJOM Vol 1, 2016, the aim of this paper is to investigate the monthly rainfall variability with ENSO and ENSO Modoki extreme events. Knowledge of the monthly rainfall connection to ENSO and ENSO Modoki extremes may lead to enhanced monthly forecasting skill, because the predictability of an ENSO event is approximately 3-4 months in advance.

The remainder of the paper is organized as follows. Descriptions of the data and analysis method used are presented in section 2. In section 3, the variation of monthly rainfall with respect to the ENSO and ENSO Modoki extremes are investigated. And in section 4 discussed about different impacts among these two extreme events; finally, a summary and conclusions are presented in section 5.

2. Data and Methodology

For this study, monthly rainfall data from 90 stations for the period from 1950 to 2011 in Sri Lanka were used (Fig 1). Seasonal mean was calculated using data from 1961 to 1990.

El Niño and La Niña episodes are categorized using Ocean Nino Index (ONI) based on 3 month running mean of SST anomalies in the Niño-3.4 region (5oN-5oS, 120o-170oW) (Fig 2). Based on the ONI, National Oceanic and Atmospheric Administration (NOAA) defines El Niño as positive ONI greater than or equal to 0.5°C and La Niña as a negative ONI less than or equal to -0.5°C. An El Niño episode is classified when these conditions are satisfied for a period of at least five consecutive months (Climate Prediction Center).

El Niño Modoki and La Niña Modoki episodes are categorized using El Niño Modoki Index (EMI) defined by Ashok et al. (2007) as: {EMI based on SST anomalies in the Region A (165°E-140°W, 10°S-10°N), Region B(110°W-70°W, 10 15°S-5°N),and Region C(125°E-145°E, 10°S-20°N)} (Fig 3).

EMI={Region A (Mean SST)-0.5* Region B (Mean SST)- 0.5* Region C(Mean SST)}
Accordance as JAMSTEC-APL (S.Varlamov), 2009-2010.

El Niño Modoki defines as positive 3 month running mean of EMI greater than or equal to 0.5°C and La Niña Modoki defines as a negative 3 month running mean of EMI less than or equal to -0.5°C.

An El Niño Modoki and La Niña Modoki episode are classified when these conditions are satisfied for a period of at least five consecutive months.

The ENSO being a major source of global predictability on the monthly time scale, anomaly composites provide useful information for monthly prediction. ‘‘anomaly composites’’ for monthly rainfall are generated with monthly rainfall data for the period from 1950 to 2011 by calculating rainfall deviation from mean during ENSO and ENSO Modoki extreme events, separately to form a composite anomaly maps.

Spatial Distribution of thirty year mean rainfall for each month is given in Figure 4.Spatialdistributions of anomaly rainfall for each month under the influence of El-Nino,La-Nina, El-Nino Modoki and La-Nina Modoki are given in Figures5, 6, 7 and 8 respectively.

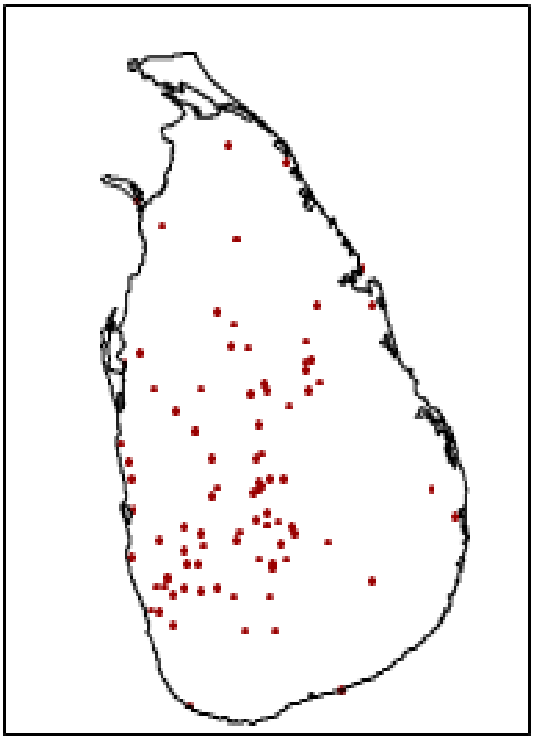

Fig. 1: Locations of 90 Rainfall Stations in Sri Lanka

El Niño and La Niña events during the considered periods are listed in Table 1 below.

Table 1: The number of El Niño and La Niña events, based on ONI Index during the 61 from January to December months recorded from 1950 to 2011.

	Jan	Feb	Mar	Apr	May	Jun	Jul	Aug	Sep	Oct	Nov	Dec
Number of El Niño events	**19**	**17**	**16**	**13**	**14**	**13**	**14**	**16**	**15**	**18**	**18**	**18**
Number of La Niña events	**23**	**18**	**12**	**12**	**11**	**13**	**15**	**14**	**18**	**21**	**22**	**22**

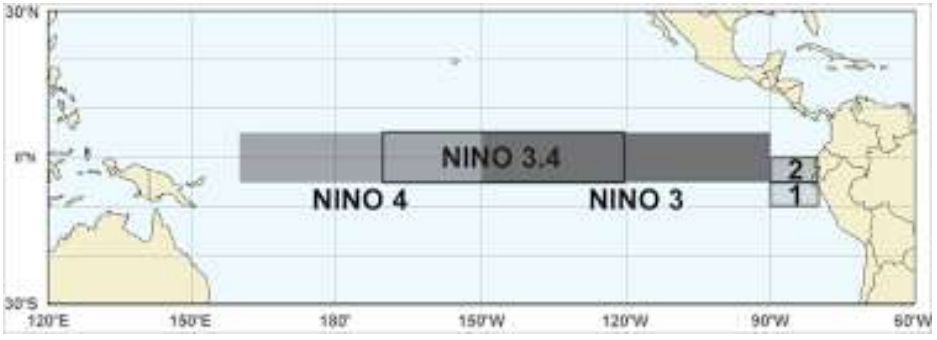

Figure 2 : Ocean Nino Index (ONI) based on 3 month running mean of SST anomalies in the Niño 3.4 region (5°N-5°S, 120°-170°W) (http://www.bom.gov.au/climate/enso/indices/about.shtml)

El Niño Modoki and La Niña Modoki events during the considered periods are listed in Table 2 below.

Table 2: The number of El Niño Modoki and La Niña Modoki events, based on EMI during the 61 from January to December months recorded from 1950 to 2011.

	Jan	Feb	Mar	Apr	May	Jun	Jul	Aug	Sep	Oct	Nov	Dec
Number of El Niño Modoki events	**4**	**4**	**3**	**3**	**3**	**3**	**3**	**3**	**5**	**6**	**7**	**5**
Number of La Niña Modoki events	**9**	**9**	**9**	**8**	**8**	**6**	**4**	**4**	**5**	**6**	**6**	**8**

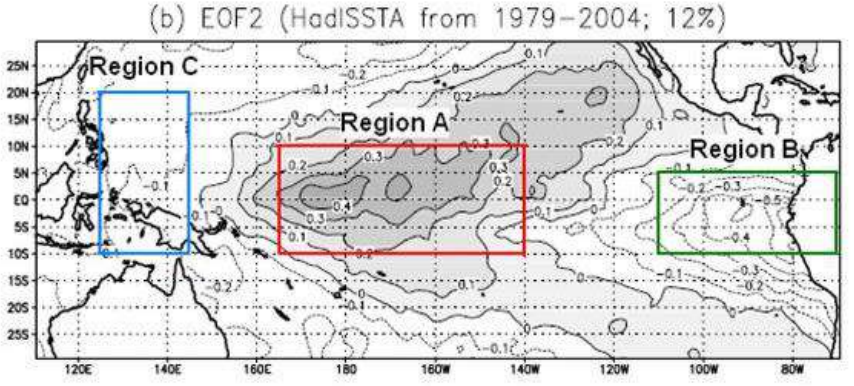

Figure 3: El Niño Modoki Index (EMI) based on SST anomalies in the Region A, Region B, and Region C (EMI=Box_A (Mean SST)-0.5*Box_B (Mean SST)-0.5*Box_C (Mean SST)) (http://www.jamstec.go.jp/frcgc/research/d1/iod/DATA/emi.monthly.txt)

3. Results and Discussion

3.1 Impacts of El-Nino on Monthly Rainfall.

According to the anomaly composites maps, widespread below normal rainfall is evident during months of February, March and September and widespread above normal rainfall is evident during months of October and November (Figure 5). Widespread above normal rainfall is noticeable over most parts of the Island except some parts of southwest quarter in month of May and widespread above normal rainfall is noticeable most parts of the Island except Northern part in month of December. Below normal rainfall is evident except Northern, North Central, North Western and some parts of Eastern of the Island during month of April. In June, above normal rainfall is evident except Southern, South Western, Western and North Western parts.

In general southwest quarter receives more than 400 mm monthly average rainfall during May to September. Reduction of rainfall is noticeable during Interior part of southwest quarter and excess of rainfall over Eastern part of the Island during May to September except month of July. In July, below normal rainfall is evident Northern and North Central, Central and Eastern Part and above normal rainfall in Western, Southern and South western parts (Figure: 5).

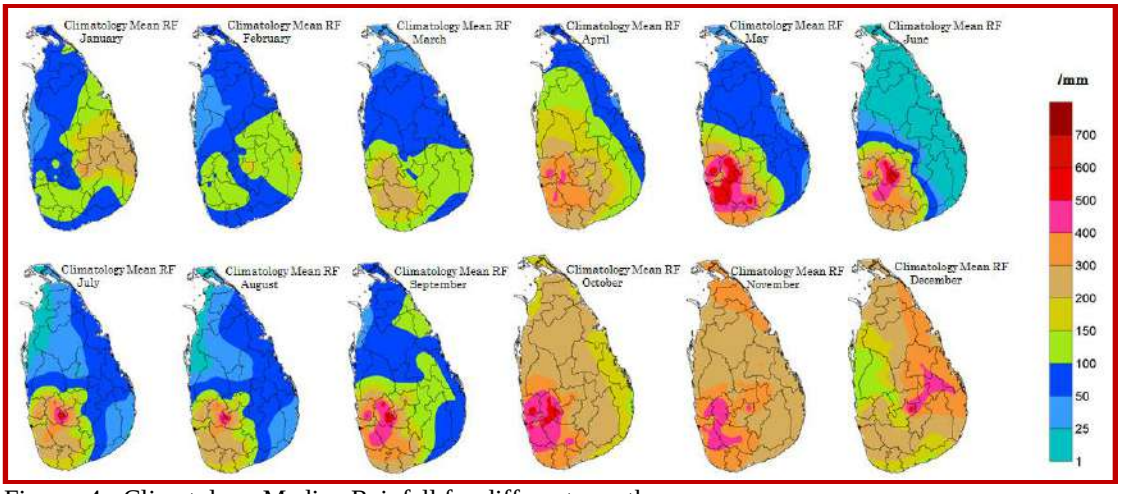

Figure: 4 - Climatology Median Rainfall for different months

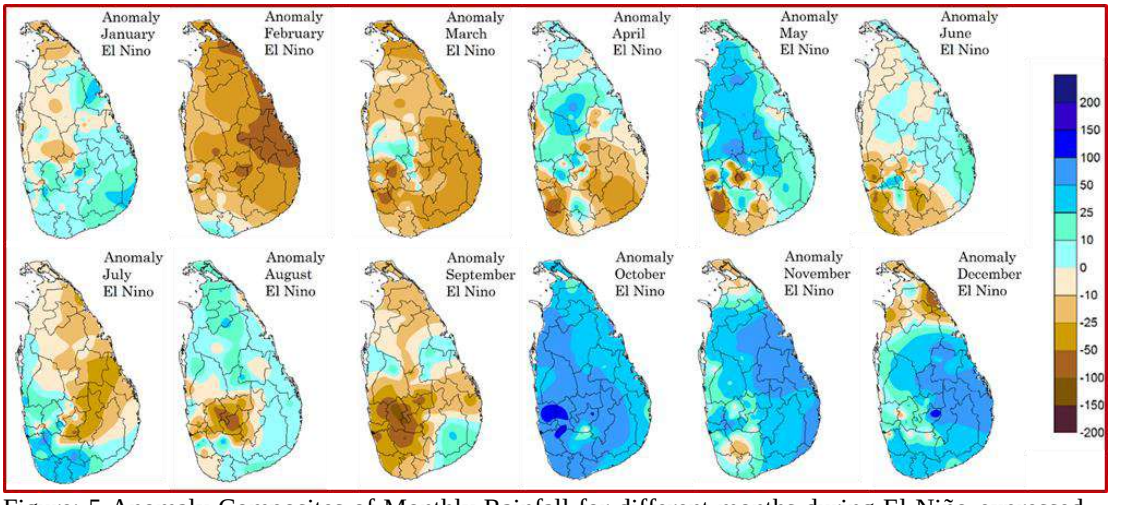

Figure: 5 Anomaly Composites of Monthly Rainfall for different months during El Niño expressed as a percentage

3.2 Impacts of La-Nina on Monthly Rainfall.

During La-Nina years fairly widespread above normal rainfall is noticeable during months of January, February, June, July, and August and fairly widespread below normal rainfall is evident during months of May, October and November. (Figure: 6). Further anomaly composites maps show an excess of rainfall over interior part of southwest quarter during May to August. In months of March and April, above normal rainfall is evident except Eastern, some parts of North Central, Western and central. Below normal rainfall is evident except North Central, North Western and Central parts of the Island during month of September. (Figure: 6)

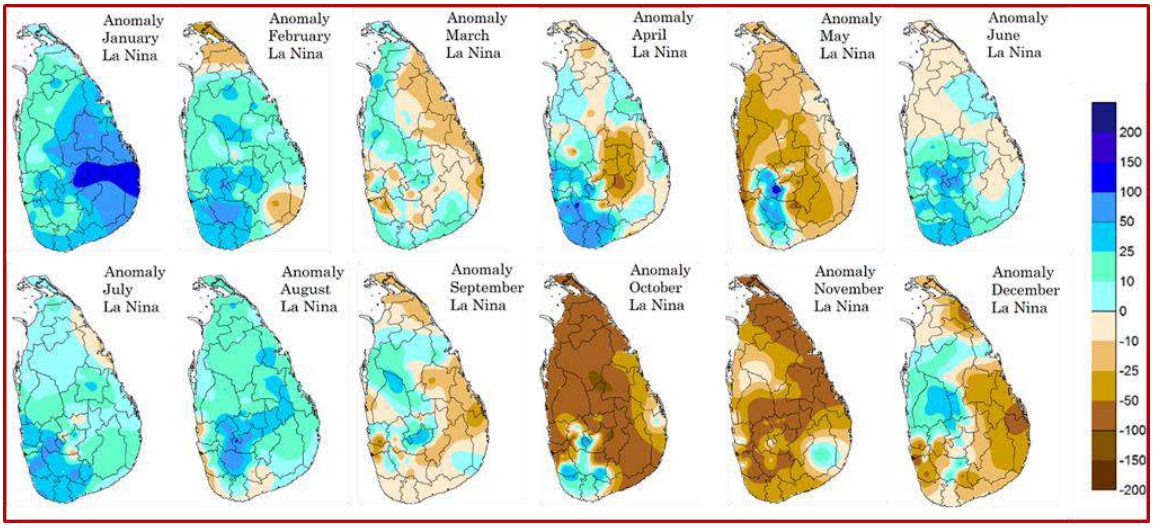

Figure: 6 - Anomaly Composites of Monthly Rainfall for different months during La Niña expressed as a percentage

3.3 Impacts of El-Nino Modoki on Monthly Rainfall.

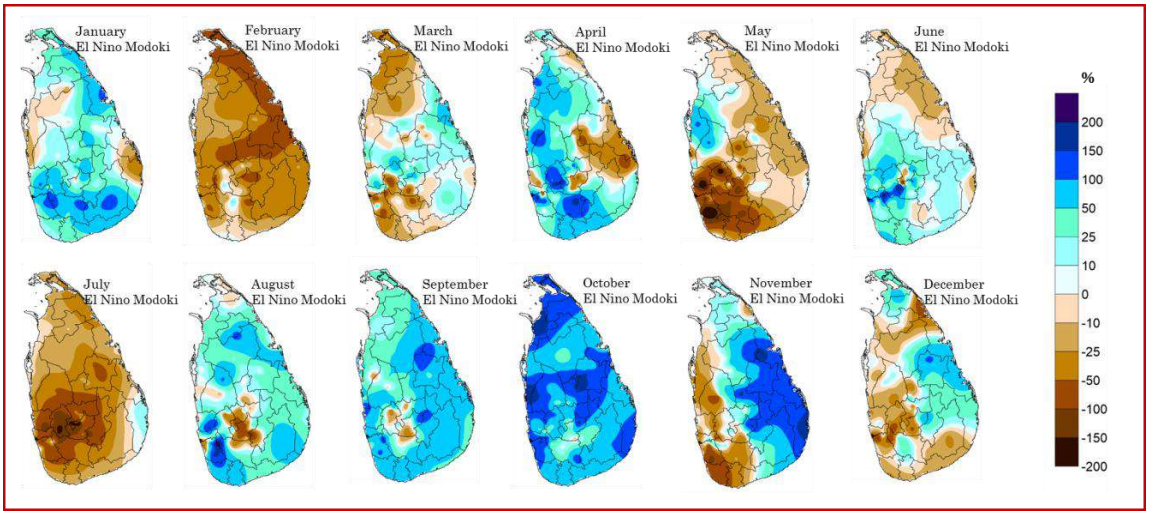

Figure: 7 -Anomaly Composites of Monthly Rainfall for different months during El Niño Modoki expressed as a percentage.

According to the anomaly composites maps, strong impacts of El Niño Modoki are apparent with below normal rainfall during months of February and July and widespread above normal rainfall events during months of August, September and October (Fig 7).

In January above normal rainfall is evident most part of the Island except some area of eastern part and North Western Part .Widespread below normal rainfall is evident during months of February

except some parts of Sabaragamuwa. Above normal rainfall is evident over most part of the Island except Northern, southern and Sabaragamuwa province and some areas of north central and north-western parts in March. Above normal rainfall is evident except some parts of western, northern, central, Eastern and Uva province of the Island during month of April. Widespread below normal rainfall is noticeable most parts of the Island except some parts of western and Wayamba province in month of May and In June, widespread above normal rainfall is noticeable over most parts of the Island except Northern part and some areas in north central and eastern parts of the Island. In month of July below normal rainfall is evident most parts except some part of eastern. Widespread above normal rainfall is evident except inner parts of the country in month of August and September. In month of October Widespread above normal rainfall is evident all over the Island. Above normal rainfall is noticeable in most part of the country except western and southern, Sabaragamuwa and Wayamba provinces. In December above normal rainfall can expect eastern part and below normal rainfall can expect western part of the Island. (Figure 7)

3.4 Impacts of La-Nina Modoki on Monthly Rainfall

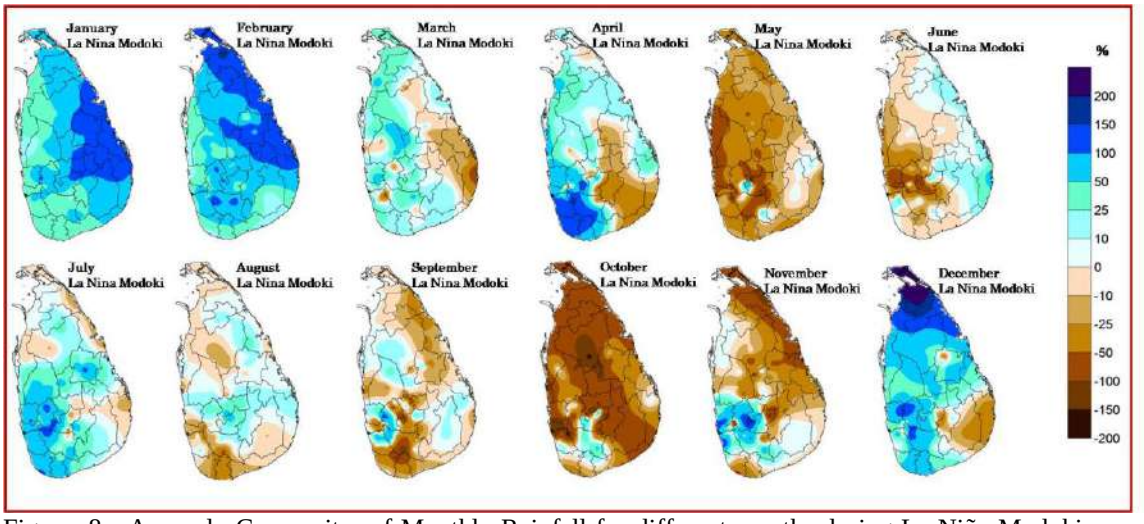

Figure: 8 - Anomaly Composites of Monthly Rainfall for different months during La Niña Modoki expressed as a percentage.

Strong impact in La Niña Modoki conditions are evident during months of January and February with widespread above normal rainfall and during months of May and October with widespread below normal rainfall.

Anomaly composites maps shows During La-Nina Modoki years, widespread above normal rainfall is noticeable during months of January, February, July and December and widespread below normal rainfall during months of May and October. (Figure: 8)

In months of March below normal rainfall can noticeable eastern parts of the country including some parts of central and north western and in April, above normal rainfall is evident except northern , some parts of southern and Uva province. Below normal rainfall is evident during month of June, except northern, northcentral, north-western, western and some part of Sabaragamuwa province. In month of August, September and November, both above normal and below normal rainfall are vitiating over the Island as though (Figure: 8)

Occurrence of extreme rainfall events, notably influence the rainfall anomaly composites in ENSO Modoki events.

3.5 Patently contrast Rainfall Events on ENSO extreme events

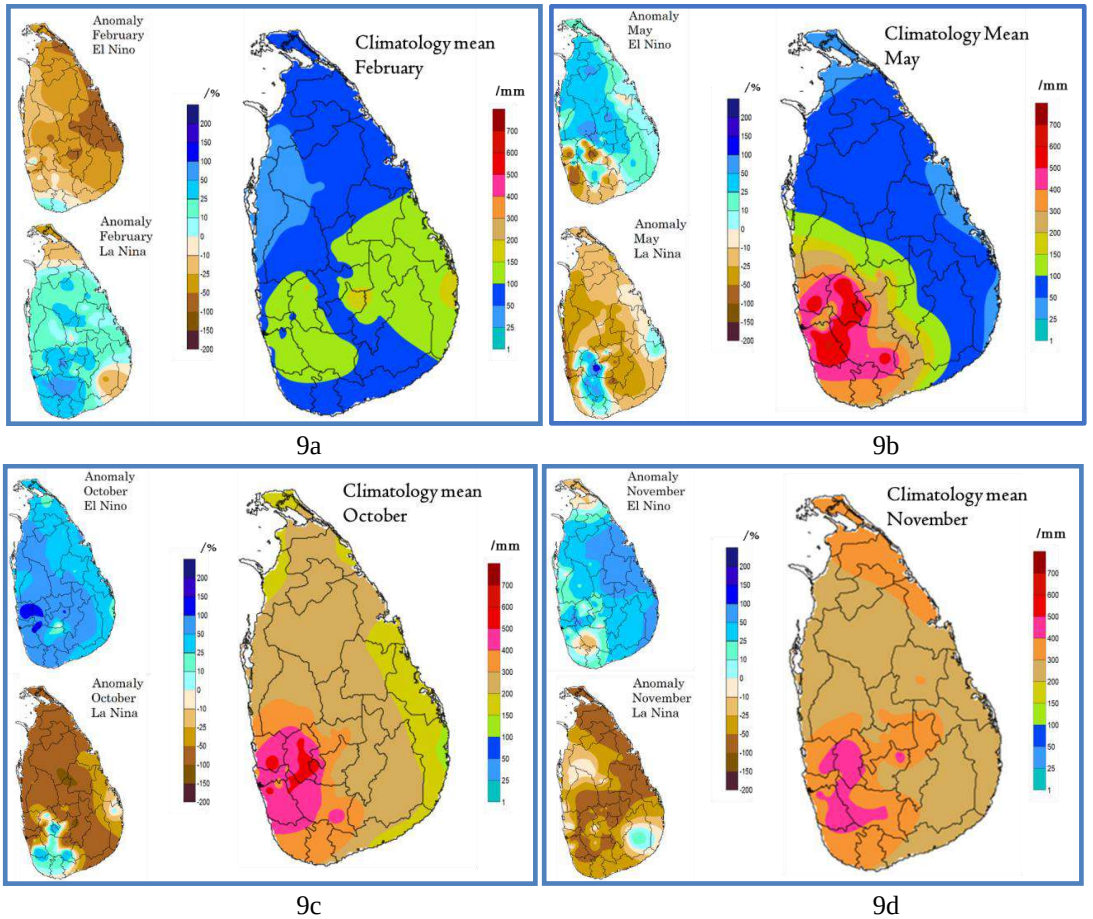

9a 9b

9c 9d

Figure: 9a, 9b, 9c, 9d - Anomaly Composites of El Niño (Upper Left)expressed as a percentage, Anomaly Composites of La Niña (Lower Left)expressed as a percentage. Climatology monthly rainfall for relevant month (Right).

Results of the present study indicate strong influences of extreme phases of the ENSO phenomenon on the monthly rainfall in Sri Lanka. Patently patterns of monthly rainfall in anomaly composites maps of the ENSO phenomenon shows clear contrasts between El Niño and La Niña events as represented in figures 9a, 9b, 9c and 9d. These contrasting spatial patterns are evident in most parts of Sri Lanka, which experience an excess of monthly rainfall in El Niño years and deficit of monthly rainfall in La Niña years during month of May (9b), October (9c) and November (9d). Reduction of monthly rainfall in El Niño years and excess of monthly rainfall in La Niña years is evident during month of February (9a).

3.6 Patently contrast Rainfall Events on ENSO Modoki extreme events

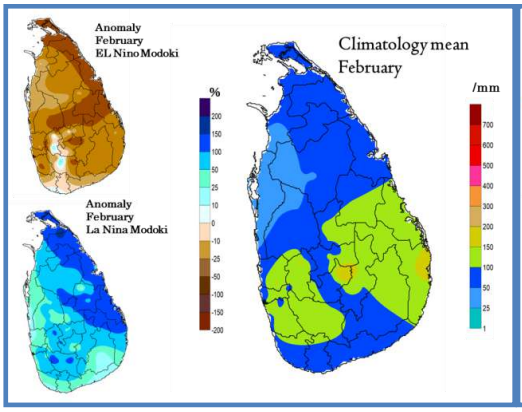

10a

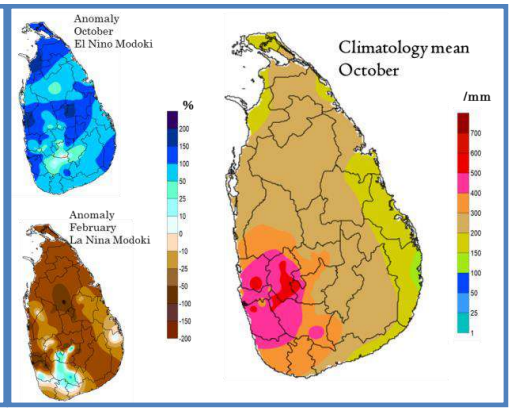

10b

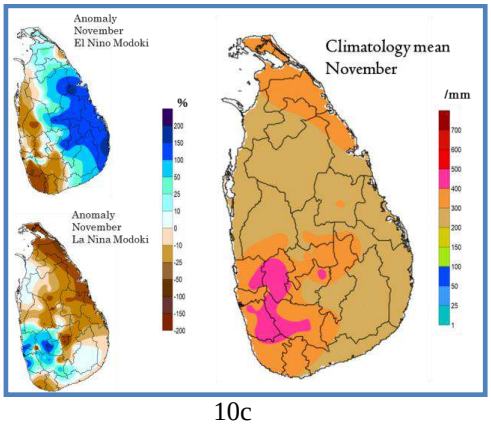

10c

Figure: 10a, 10b, 10c, - Anomaly Composites of El Niño (Upper Left)expressed as a percentage, Anomaly Composites of La Niña (Lower Left) expressed as a percentage. Climatology monthly rainfall for relevant month (Right).

In ENSO Modoki phenomenon, anomaly composites maps shows clear contrasts between El Niño Modoki and La Niña Modoki events as represented in figures 10a, 10b and10c.

According to figures 10a, 10b and 10c, clearly noticeable contrasting pattern of reduction of monthly rainfall in El Niño Modoki years and excess of monthly rainfall in La Niña Modoki years is evident

during month of February (10a). Excess of monthly rainfall in El Niño Modoki years and reduction of monthly rainfall in La Niña Modoki years is evident during month of October (10b).

An excess of rainfall in eastern part and deficit of rainfall in western part of the Island in El Niño Modoki years and excess of rainfall in western part and deficit of rainfall in eastern part of the Island in La Niña Modoki years is evident during month of November (10c)

4. Summary and Conclusion

For this study, monthly rainfall data from 90 stations over Sri Lanka, Ocean Nino Index (ONI) data and El Niño Modoki Index (EMI) data for the period from 1950 to 2011Seasonal mean was calculated using data from 1961 to 1990. ‘‘Anomaly composites’’ for monthly rainfall are generated with monthly rainfall data for the period from 1950 to 2011 by calculating rainfall deviation from mean during ENSO and ENSO Modoki extreme events, separately to form a composite anomaly maps.

Results of the present study indicate the influences of extreme phases of the ENSO and ENSO Modoki phenomenon on the monthly rainfall in Sri Lanka. Contrasting spatial patterns are evident in most parts of Sri Lanka, with an excess of monthly rainfall in El Niño years and deficit of monthly rainfall in La Niña years during month of May, October, and November. Reduction of monthly rainfall in El Niño years and excess of monthly rainfall in La Niña years is evident during month of February.

In ENSO Modoki phenomenon, clearly noticeable contrasting pattern of reduction of monthly rainfall in El Niño Modoki years and excess of monthly rainfall in La Niña Modoki years is evident during month of February while an excess of monthly rainfall in El Niño Modoki years and reduction of monthly rainfall in La Niña Modoki years is evident during month of October. An excess of rainfall in eastern part and deficit of rainfall in western part of the Island in El Niño Modoki years and excess of rainfall in western part and deficit of rainfall in eastern part of the Island in La Niña Modoki years during month of November .

Impact of ENSO and ENSO Modoki on monthly rainfall is similar in February and October but different in May and November.

The ENSO being a major source of global predictability on the seasonal time scale, these information together with accurately predicted ENSO condition can be used to improve the monthly rainfall prediction.

REFERANCES

Ashok, K., and T. Yamagata, 2009 : The El Niño with a difference. Nature. 461, 481-484.

Ashok, K., S. K. Behera, S. A. Rao, H. Weng, and T. Yamagata, 2007 : El Niño Modoki and its possible teleconnection. J. Geophys. Res., 112, C11007, doi:10.1029/2006JC003798. (JGR site)

Bjerknes J. (1969). Atmospheric Teleconnections from the Equatorial Pacific. Monthly Weather Review, 97, 163–172.

Cai, W. and Cowan, T., 2009. La Niña Modoki impacts Australia autumn rainfall variability. Geophysical Research Letters, 36(12).

Dewitte, B., Bourrel, L., and Ambrizzi, T.: Editorial, Adv. Geosci., 33, 1–1, doi:10.5194/adgeo-33-1-2013, 2013.

Diaz, H. F., and G. N. Kiladis, 1992: Atmospheric teleconnections associated with the extreme phases of the Southern Oscillation. In: Paleoclimatic Aspects of El Niño/Southern Oscillation, edited by H.F. Diaz and V. Markgraf. Cambridge University Press, 476 pp

Eugene M. Rasmusson and Thomas H. Carpenter, 1983: The Relationship Between Eastern Equatorial Pacific Sea Surface Temperatures and Rainfall over India and Sri Lanka. Mon. Wea. Rev., 111 517–528.;

Feng, J., Chen, W., Tam, C.Y. and Zhou, W., 2011. Different impacts of El Niño and El Niño Modoki on China rainfall in the decaying phases. International Journal of Climatology, 31(14), pp.2091-2101.

Feng, J. and Li, J., 2011. Influence of El Niño Modoki on spring rainfall over south China. Journal of Geophysical Research: Atmospheres, 116(D13).

HartmutBeherend 1987: Teleconnections of rainfall anomalies and of the Southern Oscillation over the entire tropics

Himesha, D.A (2012), Developing a statistical model to predict the rainfall at onset of Maha season. Master's thesis, University of Colombo, Sri Lanka.

Kug, J.S., Jin, F.F. and An, S.I., 2009. Two types of El Niño events: cold tongue El Niño and warm pool El Niño. Journal of Climate, 22(6), pp.1499-1515.

Kao, H.Y. and Yu, J.Y., 2009. Contrasting eastern-Pacific and central-Pacific types of ENSO. Journal of Climate, 22(3), pp.615-632.

Larkin, N.K. and Harrison, D.E., 2005.Global seasonal temperature and precipitation anomalies during El Niño autumn and winter. Geophysical Research Letters, 32(16).

Manson, S. and Goddard, L.: Probabilistic precipitation anomalies associated with ENSO, B. Am. Meteorol. Soc., 82, 619–638, 2001.

María Carolina Pinilla Herrera1,2 and Carlos Andrés Pinzón Correa2 - Adv. Geosci., 42, 23–33, 2016 doi:10.5194/adgeo-42-23-2016

McPhaden, M. J. (2004), Evolution of the 2002–2003 El Niño, Bull. Am. Meteorol. Soc., 85, 677–

Nicholls N. and K. K. Wong, 1990: Dependence of Rainfall Variability on Mean Rainfall, Latitude, and the Southern Oscillation. J. Climate, 3, 163–170.

Philander 1990 S. G.El Niño, La Niña, and the Southern Oscillation. Ix + 293 pp. San Diego, New York, Berkeley, Boston, London, Sydney, Tokyo, Toronto: Academic Press (Harcourt Brace Jovanovich). Price £42.50 (hard covers). ISBN 0 12 553235 0.International Geophysics Series Vol. 46.

Premalal, K.H.M.S. 2013, Change and Behavior of Rainfall Pattern in Sri Lanka with Southern Oscillation (SO) - El Niño and La Niña , SAARC Meteorological Research Centre, Dhaka, Bangladesh

Punyawardena BVR, Cherry NJ. 1999. Assessment of the predictability of the seasonal rainfall in Ratnapura using Southern oscillation and its two extremes. Journal of the National Science Council of Sri Lanka, 27(3): 187–195.

Ratnam J. V., S. K. Behera, Y. Masumoto, K. Takahashi and T. Yamagata, 2010 : Pacific Ocean origin for the 2009 Indian summer monsoon failure. Geophys. Res. Lett., 37, L07807, doi:10.1029/2010GL042798. (GRL site)

Ropelewski, C. F. and Halpert, M. S. (1987). Global and regional scale precipitation patterns associated with the El Niño/Southern Oscillation. Monthly Weather Review, 115(8), 1606-1626.

Ropelewski, C. F. and Halpert, M. S. (1989). Precipitation patterns associated with the high index phase of the Southern Oscillation. Journal of climate, 2(3), 268-284.

Sumathipala WL, Punyadeva NBP. 1998. Variation of the rainfall of Sri Lanka in relation to El Niño .In Proceedings of the Annual Sessions of the Institute of Physics, Sri Lanka, Colombo.
Suppiah, R. 1989. 'Relationships between the southern oscillation and the rainfall of Sri Lanka', Int. J. Climatol., 9, 601–618.

Suppiah, R. 1996. 'Spatial and temporal variations in the relationships between the Southern Oscillation phenomenon and the rainfall of Sri Lanka', Int. J. Climatol., 16, 1391–1408.

Suppiah, R. and Yoshino, M. M. 1984a.'Rainfall variations of Sri Lanka.Part 1.Spatial and temporal patterns', Arch. Meteorol.Geophys.

Suppiah, R. and Yoshino, M. M. 1984b.'Rainfall variations of Sri Lanka.Part 2.Regional fluctuations', Arch. Meteorol.Geophys.

Troccoli, A. (2008). Seasonal climate: forecasting and managing risk (Vol. 82). Springer Science & Business Media.

Weng, H., Ashok, K., Behera, S.K., Rao, S.A. and Yamagata, T., 2007. Impacts of recent El Niño Modoki on dry/wet conditions in the Pacific rim during boreal summer. Climate Dynamics, 29(2-3), pp.113-129.

Weng, H., G. Wu, Y. Liu, S. K. Behera, and T. Yamagata, 2009 : Anomalous summer climate in China influenced by the tropical Indo-Pacific Oceans. Climate Dynamics.DOI 10.1007/s00382-009-0658-9.

Weng, H., S. K. Behera, and T. Yamagata, 2009 : Anomalous winter climate conditions in the Pacific rim during recent El Niño Modoki and El Niño events. Climate Dynamics, 32, 663-674.

Yoshino, M.M. &Suppiah, R. (1984).Rainfall and paddy production in Sri Lanka. Journal of Agricultural Meteorology, 40, 9–20.

Influence of the ENSO to the following year southwest monsoon dry/wet conditions in Sri Lanka

A.M.A.H.D. Alagiyawanna,
I.M.S.P. Jayawardane
D M S C Disanayake
Department of Meteorology
Colombo 07

ABSTRACT

El Niño–Southern Oscillation (ENSO) is the dominant mode of climate variability tends to cause wide range of weather changes around the world. Typically, El Niño develops during boreal summer, peaks during early winter, and decays the following spring. The purpose of this study is to find out the influence of El-Nino to the subsequent southwest monsoon season (May to September) rainfall in Sri Lanka. Southwest Monsoon (SWM) is the major rainy season in Sri Lanka. It influences many sectors like agriculture, power generation, heath etc. Southwest monsoon following an El-Nino event can be categorized into three such as El-Nino -SWM, La-Nina-SWM or Neutral-SWM. So this study has been based on these three categories. For the analysis 18 El-Nino episodes were considered from 1950 to 2015. It has been recognized 4 El-Nino-SWM periods, 9 La-Nina-SWM periods and 9 Neutral -SWM periods.

According to the analysis it shows that during El-Nino –SWM rainfall tends to decrease most parts of the country and it is most evident in the southwest parts of the country. During Neutral-SWM deficit rainfall can be expected most parts of the country and during La-Nina- SWM periods it is expected increase of rainfall south west parts of the country.

But when considering La-Nina events separately it was found that some events clearly shows increase of rainfall, some years with decrease of rainfall as well as some years shows average rainfall most parts of the country.

Key words: Southwest monsoon; ENSO, El-Nino, La-Nina, El-Nino-SWM, La-Nina-SWM, Neutral-SWM

Introduction

El-Nino southern oscillation (ENSO) is a climatic phenomenon, which originate in the Pacific Ocean and has a wide impacts on weather patterns globally. ENSO describes the fluctuation in temperature between the ocean and atmosphere in the east equatorial Pacific. El-Nino is a warm phase of ENSO and La-Nina is the cold phase of ENSO.

According to the past records El-Nino and La-Nina episodes typically last for nine to twelve months. But some El-Nino and La-Nina episodes had been prolonged for years. The frequency of the events is quite irregular. El-Nino and La-Nina events occur on average every two to seven years. But El-Nino occurs more frequently than La-Nina. Xie et al 2009 found that significant climate anomalies persist through the summer (June–August) after El Niño dissipates in spring over the equatorial Pacific. Some of those significant climate anomalies persist through the summer after dissipation of El Nino is the tropical Indian Ocean sea surface temperature (SST) warming, increased tropical tropospheric temperature, an anomalous anticyclone over the subtropical northwest Pacific, and

increased mei-yu–baiu rainfall (Chang 2004) over East Asia. As Sri Lanka is located in the Indian Ocean, tropical Indian SST warming may significantly influence the rainfall variability during following SWM rainfall. These results have important implications for the predictability of SWM rainfall.

Impact of ENSO on the climate of various countries had been studied. And also the studies had been carried out to find the impact of ENSO on the climate of Sri Lanka. It has found that the ENSO has a clear influence on Sri Lanka rainfall. Suppiah (1989, 1997) examined the influence of extreme phases of the Southern Oscillation phenomenon, *El Niño* and *La Niña* on the seasonal rainfall of Sri Lanka and found strong links between rainfall anomalies and the ENSO events. ENSO relationships to the Sri Lanka rainfall has been examined and revealed that El-Nino conditions tends to droughts and La-Nina conditions are associated with floods during southwest monsoon season. The second inter-monsoon season showed strong opposite tendency that of the southwest monsoon (Kane, 1998). Another study found significantly greater amounts of second inter-monsoon (October-November) precipitation during El-Nino years at most of the climate stations, and increased southwest monsoon precipitation (May-September) during La-Nina years at a few climate stations. Influences of El Niño Southern Oscillation (ENSO) extremes such as El Niño and La Niña events on the seasonal rainfall for four climatic seasons in Sri Lanka are examined and found that strongest impact can be seen during the SIM season with probability of receiving above - median rainfall over most parts of the Island is high (low) on El Niño (La Niña) events. Western slope of the central hills has a considerable influence during ENSO extremes with suppressed seasonal rainfall during El Niño events and enhanced seasonal rainfall during La Niña events in SWM season. Enhanced and suppressed rainfall activity is evident in North western parts of the island during La Niña and El Niño events respectively during NEM season. Weakest impact of ENSO extremes can be seen during the FIM season (Hapuarachchi & Jayawardana, 2015).Jayakody P.M. (2015) examined the Influence of La Nina on Sri Lanka Rainfall and found that the strongest impact of La Niña is evident during Northeast Monsoon (NEM) with positive rainfall anomaly.

This study is mainly focused on the impact of an El-Nino condition on the following year southwest monsoon rainfall in Sri Lanka region. Study has carried out according to the prevailed El-Nino, La-Nina or Neutral condition during said monsoon period. Therefore it has mentioned these three categories here after as El-Nino-SWM, La-Nina-SWM, and Neutral-SWM.

Data and Methodology

Data

For the analysis, monthly rainfall data of 72 stations from Department of Meteorology and wind data from JRA55 (Kobayashi et al 2015) of different pressure levels were used. 1950 to 2015, and 1958 to 2015 time periods were considered for rainfall and wind analysis respectively. These 72 stations

were selected as they have continuous climate records from 1950 and those stations represent 21 districts in Sri Lanka. There were no continuous climate records from 1950 in Northern Province districts Jaffna, Kilinochchi, Mulathivu and Mannar. Locations of the rainfall stations used for the study were indicated in figure 01.

South west monsoon season (May- September) rainfall was used in the analysis and it was obtained by computing total rainfall for the period.

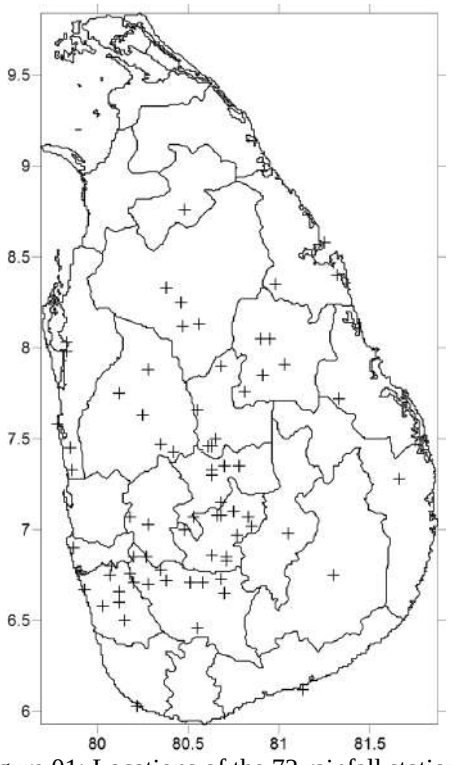

Figure 01: Locations of the 72 rainfall stations

Upper air winds information also used in the analysis. Therefore wind data were obtained from the Japanese 55 year reanalysis (JRA -55) data using Interactive Tool for Analysis of the Climate System (ITACS). Which is a web-based application to assist National Meteorological and Hydrological services (NMHS) to monitor climate status and to analyses extreme climate events. In these JRA -55 data set, data were available from 1958. Wind data of 500 hpa and 850 hpa levels were considered in the analysis.

El-Nina and La-Nina episodes from 1950 to 2015 were obtained by the Climate prediction center of the NOAA National Weather Service. URL:

http://www.cpc.ncep.noaa.gov/products/analysis_monitoring/ensostuff/ensoyears.shtml.

El-Nino (warm) and La-Nina (cold) periods were categorized according to the Ocean Nino Index (ONI). Warm and cold periods are relative to below and above normal Sea Surface Temperatures and it is based on a threshold of +/- 0.5^{o}C for the Oceanic Niño Index. ONI calculate using 3 month

running mean of ERSST.v4 SST anomalies in the Nino 3.4 region (5^oN-5^oS, 120^o-170^oW)], based on centered 30-year base periods updated every 5 years.

Statistical Analysis

For the analysis SWM seasons of the years as indicated in Table 01 were considered. According to the ONI we were able to identify strong, moderate or weak El-Nino periods before these selected SWM periods. These SWM periods can again be an El-Nino, La-Nina or Neutral periods according to the ONI. Therefore according to above categorization El-Nino-SWM, La-Nina-SWM or Neutral=SWM years were indicated in Table 01.

Table 01: Selected El-Nino, La-Nina and Neutral Southwest Monsoon years.

El-Nino	Neutral	La-Nina
1953	1952	1954
1958	1959	1964
1969	1966	1970
1987	1977	1973
	1980	1988
	1983	1995
	1992	1998
	2003	2007
	2005	2010

According to the ONI values it has been recognized 4 El-Nino-SWM periods, 9 La-Nina-SWM periods and 9 Neutral-SWM periods.

Software

The Grid Analysis and Display system (GrADS) is an interactive desktop tool for easy access, manipulation and visualization of earth science data. Therefore GrADS software has been used to visualize wind data of different pressure levels.

Surfer is software for scientific data mapping, modelling and analysis. It has been used to digitize the results.

Results and Discussion

According to the NOAA National Weather Service it was found 4 El-Nino-SWM years (1953, 1958, 1969 and 1987), 9La-Nina-SWM years (1954, 1964, 1970, 1973, 1988, 1995, 1998, 2007 and 2010) and 9 Neutral-SWM years (1952, 1959, 1966, 1977, 1980, 1983, 1992, 2003 and 2005) from 1950 to

2015. JRA-55 reanalysis data were available from 1958 and therefore 1950 to 1958 years were not included in the wind analysis. So in the wind analysis year 1952 is excluded in El-Nino-SWM years, 1953 is excluded in Neutral-SWM years and the year 1954 is excluded in La-Nina-SWM years. For the rainfall analysis it was considered data from 1950 to 2015.

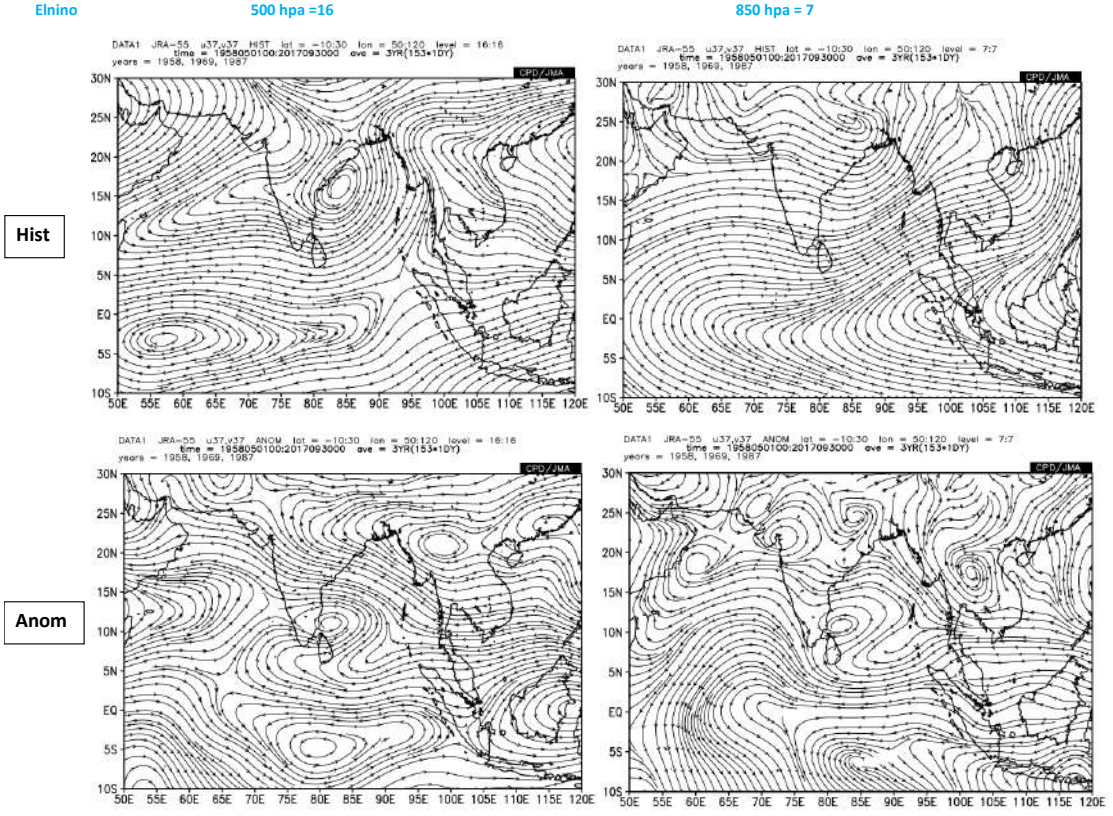

Fig 2: Wind at 500hpa (top left), wind anomaly at 500hpa (bottom left), wind at 850hpa (top right) and wind anomaly at 850hpa (bottom right) in El-Nino-SWM years.

In general the winds at low levels during the south west monsoon season are characterized by the strongest westerlies in the tropics at 850 hPa over the Arabian Sea. It is known as the low-level westerly jet. In figure 2(upper right) tropical low level westerly jet is visible. But in the anomaly maps of the figure 2(bottom left and bottom right) it can be identified east west oriented anomalous ridge in 850hPa as well as 500hPa over the Southern part of Sri Lanka region. The air is often sinking within a ridge and it tends to bring warmer and drier weather. Also there can be seen an anomalous divergence in 850hPa layer. (Figure 2-bottom right). Anomalous cyclonic circulation appeared in north of Sri Lanka adjacent to Jaffna peninsula may have responsible for above normal rainfall over northern part of Sri Lanka during SWM El Nino years.

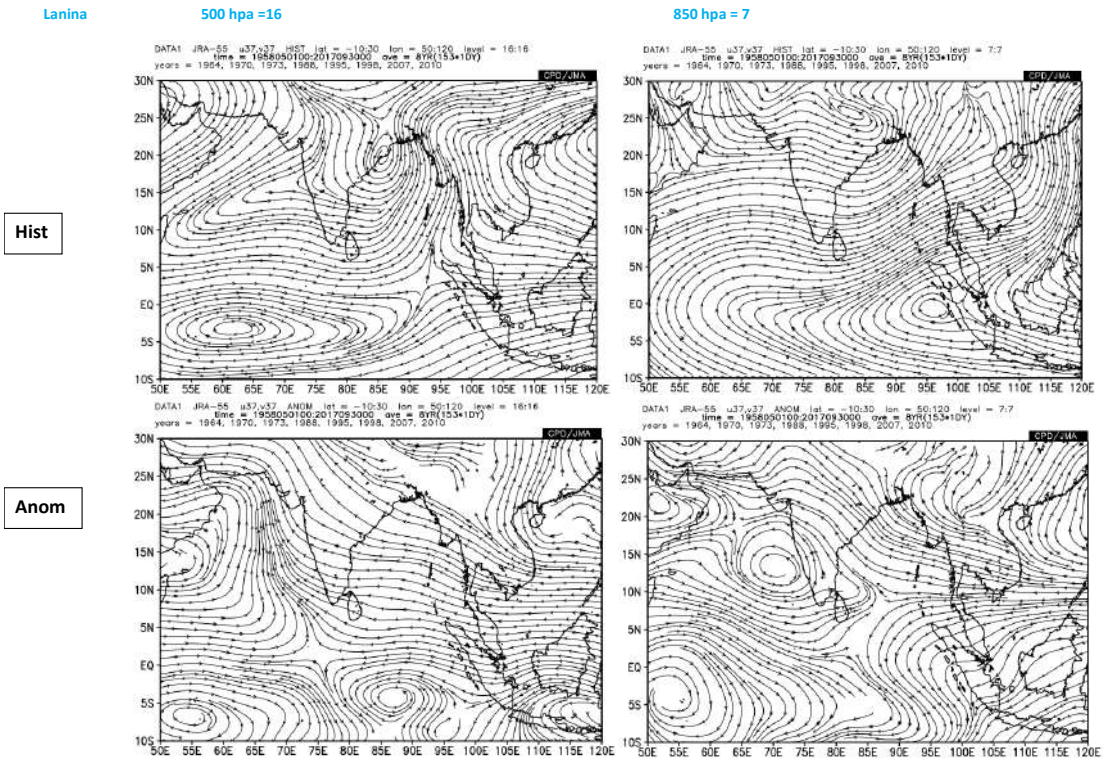

Fig 3: Wind at 500hpa (top left), wind anomaly at 500hpa (bottom left), wind at 850hpa (top right) and wind anomaly at 850hpa (bottom right) in La-Nina-SWM years.

Anomalous south westerly flow appears in 850mb layer. It may be favourable in south west monsoon rains and may expect above normal rainfall over southwest parts.

Anomalous south easterly flow appeared over Sri Lanka in 500mb may have weaken monsoon flow at mid-level by providing favourable conditions of afternoon thunder showers in eastern parts of Sri Lanka resulting above normal rainfall over that region.

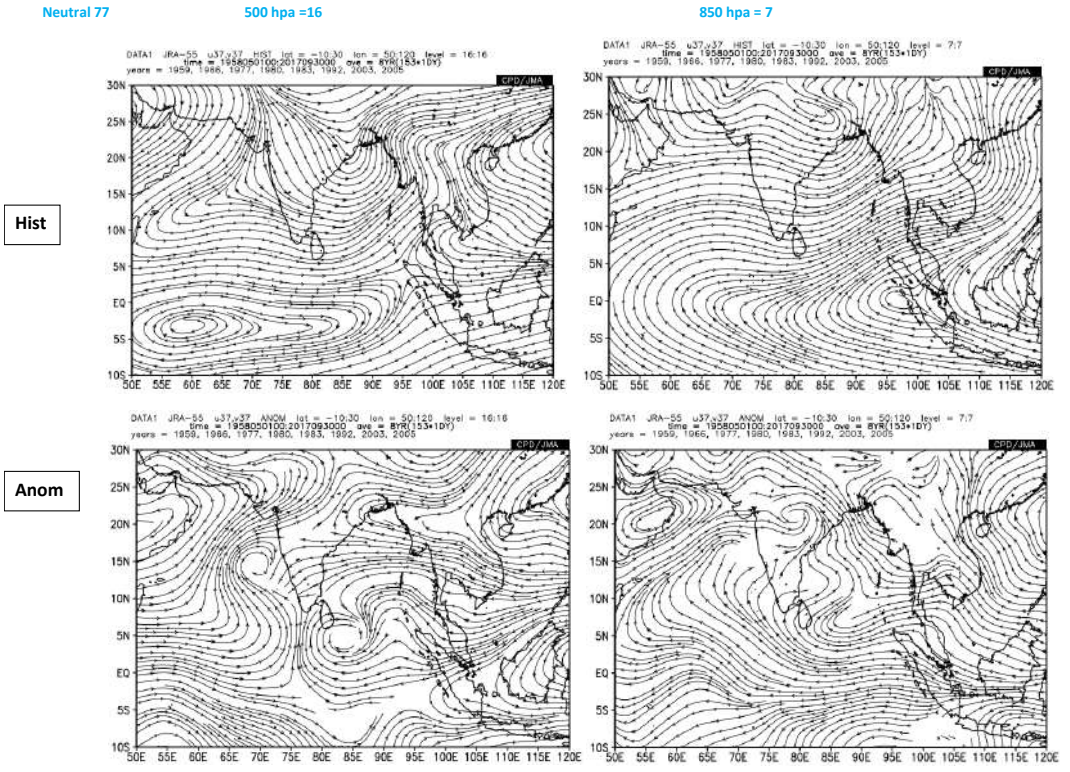

Fig 4: Wind at 500hpa (top left), wind anomaly at 500hpa (bottom left), wind at 850hpa (top right) and wind anomaly at 850hpa (bottom right) in SWM Neutral years.

In figure 4 northwest-southeast oriented ridge axis lies over Sri Lanka in anomalous 850mb layer and anomalous anti-cyclonic circulation is appeared in southeast of Sri Lanka in 500mb level. Together of above it can be bring dry condition over Sri Lanka region.

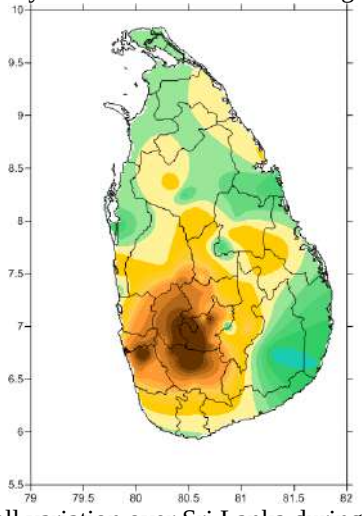

Figure 5: Average anomaly rainfall variation over Sri Lanka during After El-Nino-SWM periods

According to the Figure 5 it can be seen below average rainfall anomaly not only in south west parts but also many others parts of the country. Above average rainfall is evident in south eastern, north-western, and northern and few other parts only.

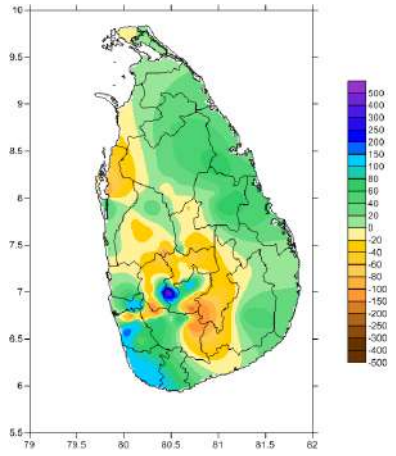

Figure 6: Average anomaly rainfall variation over Sri Lanka during After La-Nina SWM periods

According to the Figure 6 most of the southwest parts of the island has received average to above average rainfall during after La-Nina periods. Central and north western parts of the country shows deficit rainfall anomaly, but eastern and north eastern parts of the country shows average to little above average rainfall anomaly.

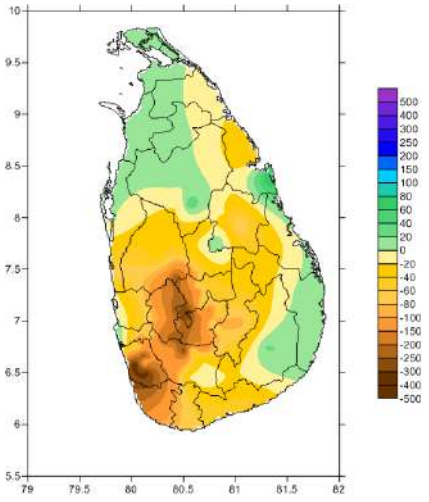

Figure 7: Average anomaly rainfall variation over Sri Lanka during Neutral-SWM periods

According to the Figure 7 it can be seen that most parts of the country has received deficit of average anomaly rainfall variation during Neutral-SWM years. Only in the north-western and south eastern parts of the Island has received nearly average anomaly rainfall.

Conclusion

Analysis was carried out to investigate how the ENSO influenced the south west monsoon rainfall which occurred after an ENSO period. Considered southwest monsoon periods has categorized as

El-Nino-SWM, La-Nina-SWM and Neutral-SWM. The results clearly showed that ENSO modulates rainfall over Sri Lanka region. According to the analysis it showed that, during El-Nino-SWM the rainfall over the country tends to decrease and during the neutral-SWM also showed decrease of rainfall over the most parts of the country than the long term averages.

When it has considered La-Nina-SWM, it showed that averagely increase of rainfall over the country. But when it has been considered that La-Nina-SWM events separately it was found that some events clearly shows increase of rainfall, some years with decrease of rainfall as well as some years shows average rainfall most parts of the country.

Acknowledgement

The JRA-55 reanalysis dataset was provided by the JMA and is available at http://jra.kishou.go.jp/JRA-55/index_en.html. Preliminary analysis in the present study used the ITACS system developed by the JMA.

REFERANCES

Chang, C.P., 2004. *East Asian Monsoon* (Vol. 2). World Scientific.

Eugene M. Rasmusson and Thomas H. Carpenter, 1983: The relationship between Eastern Euatorial Pacific Sea Surface Temperatures and Rainfall over India and Sri Lanka, Monthly Weather Review, 111, 517-528.

Hapuarachchi, H.A.S.U., and Jayawardena I.M.S.P., 2015: Modulation of Seasonal Rainfall in Sri Lanka by ENSO Extremes, Sri Lanka Journal of Meteorology, 1, 3-11.

http://journals.ametsoc.org/doi/full/10.1175/JCLI3670.1

http://oceanservice.noaa.gov/facts/ninonina.html

http://www.livescience.com/3650-el-nino.html

Hyo-SeokPark, John C.H. Chiang, and Guang J. Zhang, 2009: The Delayed Effect of Major El Nino Events on Indian Monsoon Rainfall, Journal of Climate, 23, 932-946.

Jayakody, P.M., 2015: The Influence of La Nina on Sri Lanka Rainfall, Sri Lanka Journal of Meteorology, 1, 41-49.

Kane, R.P., 1998: ENSO relationship to the rainfall of Sri Lanka, International Journal of Climatology, 18(8), 859-871.

Kobayashi, S., Ota, Y., Harada, Y., Ebita, A., Moriya, M., Onoda, H., Onogi, K., Kamahori, H., Kobayashi, C., Endo, H. and Miyaoka, K., 2015. The JRA-55 reanalysis: General specifications and basic characteristics. *Journal of the Meteorological Society of Japan. Ser. II*, *93*(1), pp.5-48.

Malmgren A. Bjorn, Hulugalla R., Hayashi Y., and Mikami T., 2003: Precipitation trends in Sri Lanka since the 1870s and relationships to El-Nino Southern Oscillation, International Journal of Climatology, 23, 1235-1252.

Suppiah R., 1989: Relationships between the southern oscillation and the rainfall of Sri Lanka. InternationalJournal of Climatology 9(6): 601 − 618.

Suppiah, R., 1997: Extremes of the southern oscillation phenomenon and the rainfall of Sri Lanka, International Journal of Climatology, 17(1), 87-101.

Zubair, L., & Ropelewski, C. F., 2006: The strengthening relationship between ENSO and northeast monsoon rainfall over Sri Lanka and southern India, Journal of Climate, 19(8), 1567-1575.

Zubair, L., 2002: El Nino–southern oscillation influences on rice production in Sri Lanka, International Journal of Climatology, 22(2), 249-260.

Assessment of the behaviour of K-Index, Lifted Index and Convective Availability Potential Energy (CAPE) in development of thunderstorms in Sri Lanka

Malith Fernando and Malinda Millangoda,
K. H. M. S. Premalal
Department of Meteorology
Colombo 7

ABSTRACT

The aim of this study is to evaluate the relationship of some of the instability indices with the atmospheric instability in the troposphere around Sri Lanka. There are numerous instability indices developed to assess the instability of the atmosphere for the purpose of forecasting thunderstorms which results in the occurrence of lightning and thunder. Although there are various instability indices which combine thermodynamic and/or kinematic parameters utilized to forecast thunderstorms, effectiveness of these indices for this region have not been studied. In this study, K-Index, Lifted index and Convective Availability Potential Energy (CAPE) processed products of NCEP FNL (Final) Operational Global Analysis data for the month of November 2016. Then statistical methods were used to test the correlation of the computed three indices with meteorological observation data of lighting and thunder from twenty two principal meteorological stations in Sri Lanka and Vaisala Global Lightning Dataset (GLD 360) data for the same region. This study will be broadened further in the next stage by comparing more instability indices with data length of a year compared to the data length of a month used in the current study to improve the forecasting ability of thunderstorms.

Introduction

Thunderstorms are deemed to be one of the major sources of water in the North and Eastern parts of the country except the North East monsoon period where most of the country's agricultural land are spread out. In Sri Lanka, thunderstorms mostly occur during the inter-monsoon periods (March – April & October – November) where the winds does not carry a specific dominant direction. Thunderstorms contribute to almost half of the annual rainfall during this period throughout the country(Department of Meteorology, Sri Lanka, 2016).

Apart from being a useful factor in one part of the country's economy and livelihood of the people, severe thunderstorms also bring great devastation and destruction in many ways. They have badly affected sectors such as marine, civil aviation and agriculture apart from the day to day to lives of the general public. On 17 May 2003, heavy rainfall (around 700mm) associated with a mesoscale convective system around Deniyaya triggered a landslide which claimed around 200 lives. On 14 November 2014, heavy intense rainfall (56mm within 20 minutes) associated with a thunderstorm

resulted in a flash flood situation in the Colombo metropolitan area which caused great inconvenience and economic loss for the country(Warnasooriya et al, 2016.). The Meeriyabadda landslide in the Koslanda estate in the district of Badulla which occurred in 29 October 2014 which caused 12 deaths and 23 disappearances while completely destroying all the estate line houses in the area was also a result of continuous rainfall exceeding 500mm received within 3 days of the catastrophic event (Somarathne, 2014). This high intense rainfall was also triggered by a thunderstorm during this period over the Badulla district (Rupasingheet al, 2016.).According to the stated events above it is evident that even though thundershowers are small in spatial and temporal scales effects of the thunderstorms and associated hazards has caused great damage. Around 50 reported deaths occur due to lightning strikes in Sri Lanka specially people who are working outdoors (Kumarasinghe, 2008). Most of the people who die are farmers who work outdoors. These deaths have impacted the family livelihoods and the agriculture sector in general.

Thunderstorms are considered to be one of the most challenging weather phenomena to predict in the field of meteorology. Thundershowers being small in scale in temporal and spatial distribution(Perler andMarchand, 2009) and the chaotic nature of the atmosphere has made it hard to predict than the large scale phenomenon(Elmore et al, 2002). It is learnt that in most of the situations, forecasters around the world use surface observations with satellite and radar images to predict the occurrence of thundershowers in the short term in now casting basis. This requires experience, understanding of relevant synoptic pattern recognition and climatology (Perler andMarchand, 2009). This of course is not adequate considering both the magnitudes of the positive and negative impacts on the relevant sectors and communities by thunderstorms. Therefore, the use of instability indices derived by Numerical Weather Prediction (NWP) outputs to ascertain the possibility of thundershowers ahead in days is essential to mitigate the negative impact and to improve the capacity of utilizing thundershowers to acquire the most of its positive impacts.

Instability indices have long being used in the field of meteorology to assess the instability of the atmosphere which is a critical factor in development of thunderstorms. In this study, K-Index(George, 1960) , Lifted Index(Galway, 1956) and Convective Availability Potential Energy (CAPE) was used to identify the effectiveness of these indexes in forecasting thunderstorms. According to the founder of the K-Index it is defined as,

$$\textbf{K-Index} = (T_{850}-T_{500})+D_{850}-(T_{700}-D_{700})$$

Where T_{850}, T_{700}, and T_{500} are the temperatures of the 850hPa, 700hPa and 500hPa layers of the atmosphere respectively. D_{850} and D_{700} are dew point temperatures of the 850hPa and 700hPa layers of the atmosphere respectively. It has been stated that the founders research on this index has identified that the occurrence of thunderstorm probability is 50% when the K-Index value is more than 26^0C (Tajbakhsh et al, 2012).The K-index is initially used to help forecast continental

summertime air mass thunderstorm potential (Peppler, 1988). Air mass thunderstorms are defined as thunderstorms that develop in areas of weak winds without apparent frontal or cyclonic influence.

Lifted Index is defined as the following by J.G. Galway,

$$\textbf{Lifted Index} = T_L - T_{500}$$

Where $T_L$is the temperature (°C) of a parcel lifted from 850hPa to 500hPa, dry-adiabatically to saturation and moist-adiabatically above that. Lifted index is a modification of the Showalter Index and has a strong resemblance of it except for the determination of the level from which the parcel is lifted and the Lifted Index is an index used to forecast whereas the Showalter Index is an observed static index (Peppler, 1988). Lifted index was originally created as a latent instability predictor in forecasting severe thunderstorms. It is stated to be extensively used in analysis and forecasting thunderstorms in the United States.(Peppler, 1988). In 1956 in Galway's study on Lifted Index (LI), it was stated that negative LI shows that the boundary layer is unstable compared to the middle troposphere. Galway in his study declared that LI values between -3 and -5 shows marginal instability.

CAPE is an indicator of the quotient of energy present for convection. Value of CAPE is directly proportional to the maximum potential vertical speed of an updraft which relates to severe weather occurrence. CAPE is defined as,

$$\textbf{CAPE} = \int_{p_f}^{p_n} R_d (T_{vp} - T_{ve})\, d \ln p$$

CAPE is indicated as a vertical integration of the parcel-to-environment temperature difference between the Level of Free Convection (LFC) to the Level of Neutral Buoyancy (LNB) which are the levels where the parcel freely rises. It is stated that it quantifies the energy a parcel will have when lifted (in J kg^{-1}) and indicates the potential strength of updrafts within a thunderstorm (DeRubertis, 2006). When considering CAPE, it is accepted that more than 1000 J kg^{-1} indicates that the atmosphere is moderately unstable. The atmospheric instability increases with the increase of CAPE.

In operational meteorology, forecasters around the world use various threshold values for each of these indices to assess the instability of the atmosphere. The Weather Forecast Office of the National Weather Service of the United States of America under the National Oceanic and Atmospheric Administration uses the following criteria to assess instability using K-Index, Lifted Index and CAPE (US Department of Commerce, n.d.).

KI below 30:	**Thunderstorms with heavy rain or severe weather possible.**
KI over 30:	Better potential for thunderstorms with heavy rain.
KI = 40:	Best potential for thunderstorms with very heavy rain.

(KI denotes K-Index in the above table).

LI over 0:	Stable but weak convection possible for LI = 1-3 if strong lifting is present.
LI = 0 to -3:	Marginally unstable.
LI = -3 to -6:	Moderately unstable.
LI = -6 to -9:	Very unstable.
LI below -9:	Extremely unstable.

(LI denotes Lifted Index in the above table).

CAPE below 0:	Stable.
CAPE = 0 to 1000:	Marginally unstable.
CAPE = 1000 to 2500:	Moderately unstable.
CAPE = 2500 to 3500:	Very unstable.
CAPE above 3500-4000:	Extremely unstable.

Although the above threshold values are used as "universal" threshold values, there is a lack of research to support these threshold values. Studies and research analyzing the dependence of geographic location, time of day and seasons of the year on the variability of severe weather triggering threshold values are limited as well. However, it is widely accepted that increasing atmospheric instability increases the possibility of severe weather. Therefore, an array of threshold values have been selected to test for this region.

Since it was recognized that increasing instability increases the chance for severe weather, it could be identified that higher values for K-Index and CAPE and negative values for Lifted Index will increase the atmospheric instability which will in turn increase the chance for occurrence of thunder.

The objective of this study is to evaluate the relationship of some of the instability indices such as K-Index, Lifted index and Convective Availability Potential Energy (CAPE) with occurrence of thunder and lightning activity in Sri Lanka and seek the possibility of use the instability indices derived from numerical models for the purpose of forecasting thunderstorms which results in the occurrence of lightning and thunder. Although there are various instability indices which combine thermodynamic and/or kinematic parameters utilized to forecast thunderstorms, effectiveness of these indices for this region have not been studied. In this study, processed products of NCEP FNL (Final) Operational Global Analysis data for the month of November 2016.

Methodology

Global Data Assimilation System (GDAS) National Centre for Environmental Prediction (NCEP) Final (FNL) data of the resolution of 0.25 degree on a 3 hourly basis was downloaded for the month of November, 2016. The considered parameters K-Index, Lifted Index and CAPE were extracted utilising GRADS software for the 23 principal meteorological stations of Sri Lanka.

The FNL data used in this study is 0.25 degree and that constitutes an area of approximately 800 sqkm which will encompass a square of a side length 28 km. When extracting data, the latitude and longitude for each station was collected. Data of 4 adjoining grid points to that point of the station was selected as per the following diagram.

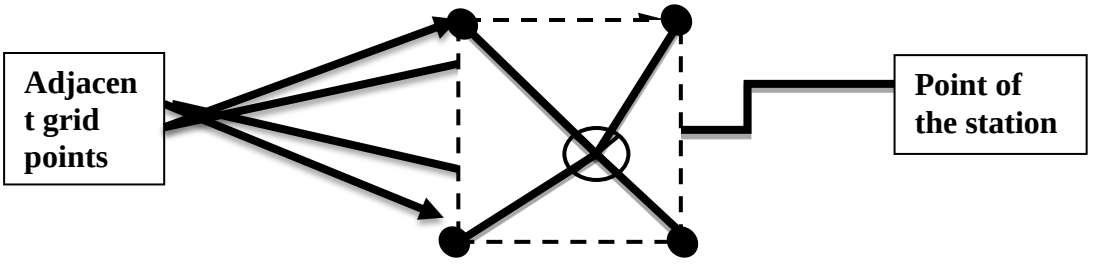

After the selection of the 4 adjacent grid points, the considered parameters were extracted for each of the grid points. Then the minimum, maximum and average values from 4 of these grid point values were selected for each of the considered parameters. 3 hourly synoptic observation data were taken from the Department of Meteorology, Sri Lanka (DoMSL) for the respective principal meteorological stations and Global lightning detection database (GLD 360) data which were provided by the Finnish Meteorological Institute under the Severe Storm Warning Services for Sri Lanka (SSWSS) project.VaisalaGLD360 was established in 2009. It consists of VLF (Very Low Frequency) sensors strategically placed around the world for optimal detection of cloud-to-ground (CG) lightning strokes using magnetic direction finding (MDF) and time-of arrival (TOA) methodologies combined with proprietary lightning recognition algorithms in the band. GLD360 is

the first ground-based lightning detection network capable of providing both worldwide coverage and uniform, high performance without severe detection differences between daytime and night time conditions (Pohjola. and Mäkelä, 2013; Demetriades et al 2010). Lightning data which corresponds to the above meteorological stations were extracted from GLD360 as per the previous selection criteria using MS Excel. After extraction and preparation of data, the GDAS FNL data was compared with synoptic observation data and GLD360 data.

The comparison was done separately for each minimum, maximum and average values that were extracted which constituted six scenarios as shown in the table below.

		1	2
1	**Minimum**	**synoptic observation data**	**GLD 360 data**
2	**Maximum**		
3	**Average**		

As it was established in the introduction part of this text, higher values for K-Index and CAPE and lower values for Lifted Index can be identified as increase chance for occurrence of thunder. Considering this the following four cases were defined to further broaden the analyses.

Case 1: The extracted average values for KI, CAPE and LI were compared with synoptic observation data/GLD 360 data for both occurrence and non-occurrence of thunder.

Case 2: The extracted maximum values for KI and CAPE and minimum values for LI were compared with synoptic observation data/GLD 360 data for both occurrence and non-occurrence of thunder.

Case 3: The extracted minimum values for KI and CAPE and maximum values for LI were compared with synoptic observation data/GLD 360 data for both occurrence and non-occurrence of thunder.

Case 4: Maximum values for KI and CAPE with minimum value for LI for the instances where thunder occurred and minimum values for KI and CAPE with maximum value for LI for the instances where thunder was not observed were compared separately.

Considering previous research on KI, CAPE and LI for instability which were stated in the introduction above, a minimum threshold value was selected for each of these parameters. The selected minimum threshold value for each parameter for CAPE, KI and LI respectively was 1000, 20 and -2. The step values were determined as 1000, 10 and -2 which constituted the following combinations of values.

	1	**2**	**3**
CAPE	**1000**	2000	3000
KI	**20**	30	40
LI	**-2**	-4	-6

According to the output of this comparison case 2 was selected for further analysis.

Results& Discussion

Observational data selection test

The criteria for selection mentioned in the methodology provided eight cases all together since the GDAS FNL data was compared with two observational data sets.

The following table shows the outcome of these four cases for each observation datasets.

Synoptic observation			
	Hit rate (%)	**Correct rejection (%)**	**Total (%)**
Case1	2.1	83.4	85.5
Case2	4.0	70.4	74.5
Case3	0.7	90.2	90.9
Case4	4.0	72.8	76.8

GLD 360 observation			
	Hit rate (%)	**Correct rejection (%)**	**Total (%)**
Case1	2.3	86.6	88.8
Case2	4.1	75.4	79.6
Case3	0.7	91.7	92.4
Case4	4.1	91.7	95.8

Considering the total of both hit rate and correct rejections for each dataset, it is evident that the GLD 360 dataset has provided with more accuracy than its counterpart. The average score for the GLD 360 dataset for all cases is superior to overall average score of synoptic observations. GLD 360 dataset has also provided almost more than 80% for each case considered and more than 90% in almost 3 of 4 cases considered whereas the synoptic observations has passed 90% only in one case. Therefore, GLD360 was selected as the observation dataset to carry out the analysis.

In the selected dataset of GLD 360, the highest total percentage of hit rate and correct rejections are provided in case 4 with a total in excess of 95%. The case with the highest percentage of hit rate was selected since the aim of this study is to identify the occurrence of thunder and lightning rather than correctly predicting non-occurrence. Therefore, case 2 was selected for further analysis.

After the initial trial and error method analysis was concluded, the optimum combination that provided the maximum total hit rates for CAPE, KI and LI respectively was 1000, 20 and -3. This

prompted for an increase of variations and combinations to identify the optimum combination for the occurrence and non-occurrence of thunder. Accordingly, the following combinations were selected for the next analysis.

CAPE	KI	LI
0-500	21-24	(-1.5) – (-2.5)
500-1000	24-27	(-2.5) – (-3.5)
1000-1500	27-30	(-3.5) – (-4.5)
1500-2000	30-33	(-4.5) – (-5.5)
2000-2500	33-36	
2500-3000	36-39	

By using the above combinations, it could be found that more relevant combinations for thunder occurrence and non-occurrence events are as follows

Thunder occurrence

Minimum Cape	Maximum Cape	Minimum K Index	Maximum K Index	Minimum Lifted Index	Maximum Lifted Index	Number of events
0	1000	0	27	-2	-3	1262
0	1000	0	27	-3	-4	868
0	1000	0	27	-1	-2	799
0	1000	0	27	0	-1	400
1000	2000	0	27	-3	-4	602
1000	2000	0	27	-2	-3	222
1000	2000	0	27	-1	-2	26
1000	2000	0	27	0	-1	1

Thunder non-occurrence

Minimum Cape	Maximum Cape	Minimum K Index	Maximum K Index	Minimum Lifted Index	Maximum Lifted Index	Number of events
500	2500	27	33	-2.5	-4.5	124
500	2500	33	39	-2.5	-4.5	79
500	2500	21	27	-2.5	-4.5	74
500	2500	21	27	-0.5	-2.5	8
500	2500	27	33	-0.5	-2.5	3
500	2500	33	39	-0.5	-2.5	2

The following ranges of criteria have the highest combined thresholds for event representation.

Best for occurrence,

CAPE 500-2500 KI 27-33 LI (-2.5) – (-4.5)

From the total of 376 events of total thunder events, 124 events were in this region which constituted the highest percentage among the thunder occurring cases. 32.4% of thunder events that occurred during this period was inside the above region of CAPE, KI and LI.

Considering for non-occurrence,

CAPE 0-1000 KI 0-27 LI (-2.0) – (-3.0)

From the total of 5144 non occurring events considered in this, 1262 were in this region which constituted the highest percentage among the non-occurring cases. 24.5% of non-occurring events were in the above criteria.

Summary and conclusions

The relationship of instability indices such as K-Index, Lifted index and Convective Availability Potential Energy (CAPE) with occurrence of thunder and lightning activity in Sri Lanka was evaluate using of NCEP FNL (Final) Operational Global Analysis data, manual observation of thunder activity from 23 meteorological stations owned by DoMSL, GLD360 dataset provided under Severe Storm Warning Services for Sri Lanka (SSWSS) project for the month of November 2016. It is important to note that as data length used in this study is very limited (one month) findings of this study might change with a longer period dataset.

This study revealed that impact of CAPE in occurrence in thunder which is a direct outcome of atmospheric instability is low, although it is widely accepted that CAPE is a good measure to identify instability. But when it comes to the non-occurrence thunder scenario, CAPE range which captured most of the cases were 0-1000. This is parallel with the literature. It is evident that the impact of KI for tropical region is good. This study also showed that the Higher KI values for occurrence of thunder and lower KI values for non-occurrence. When considering LI, again the outcome of this study are not in line with the normal threshold values which are generally accepted.

This study was conducted using NCEP FNL data of 0.25degree resolution. Since, Sri Lanka is an Island which is having a complex geography, a higher resolution observational data is required to examine these kinds of indices more accurately. Another major reason of not having a significant outcome would be the lack of upper air observations in the selected region, which can increase the accuracy and reliability of data. Therefore, assimilated FNL data may not be accurate enough and

can lead to false observations. Since, this study was conducted only for a month, data density is lesser. This may also not enough to find a good statistical relationship of thunder and instability indices. Another factor that limit the data density is the 23 observational points (meteorological stations owned by DoMSL) that were selected in the study going in line with the observation stations which is relatively a low number.

Broadening of this study to consider a longer period will provide a more comprehensive results for the corresponding instability indices. Since thunder is not a large scale phenomenon more high resolution data would improve the results as well. A comparison of every grid point rather than 23 selected grid points with the GLD360 dataset might yield better results, since it can increase the data density.

Acknowledgments

Technical support and GLD360 dataset provided by Finnish Meteorological Institute (FMI) and VAISALA oyj under Severe Storm Warning Services for Sri Lanka (SSWSS) project is acknowledge.

REFERENCES

Demetriades, N.W., Murphy, M.J. and Cramer, J.A., 2010, April.Validation of Vaisala's global lightning dataset (GLD360) over the continental United States.In *Preprints, 29th Conf. on Hurricanes and Tropical Meteorology, Tucson, AZ, Amer. Meteor.Soc. D* (Vol. 16).

Department of Meteorology, Sri Lanka (n.d.).Climate of Sri Lanka. Retrieved from http://www.meteo.gov.lk/index.php?option=com_content&view=article&id=13&Itemid=132&lang=en#4-northeast-monsoon-season-december-februaryservations.

DeRubertis, D, 2006. Recent trends in four common stability indices derived from US radiosonde observations. *Journal of Climate* 19(3), pp.309–323.

Elmore, K. L., Stensrud, D. J., & Crawford, K. C., 2002. Explicit cloud-scale models for operational forecasts: A note of caution. *Weather and Forecasting*, 17(4), 873–884.

Galway, J.G., 1956. The *Lifted Index as a Predictor of Latent Instability. Bulletin of the American Meteorological Society*, Vol. 37, pp. 528-529.

George, J.J., 1960. Weather Forecasting for Aeronautics. *Quarterly Journal of the Royal Meteorological Society*, Vol. 87, Issue 371, 120.

KumarasingheNuwan, 2008. A low cost lightning protection system and its effectiveness. Department of Meteorology, Sri Lanka

Peppler, R. A., 1988. A review of static stability indices and related thermodynamic parameters. Illinois State Water Survey. Retrieved from https://www.ideals.illinois.edu/handle/2142/48974

Perler, D. &Marchand, O., 2009. A Study in Weather Model Output Post processing: Using the Boosting Method for Thunderstorm Detection. *Weather and Forecasting*, 24(1), 211–222.

Pohjola, H. and Mäkelä, A., 2013. The comparison of GLD360 and EUCLID lightning location systems in Europe. *Atmospheric research*, *123*, pp.117-128.

Rupasinghe, W.N.S. &Premalal, K.H.M.S. 2016. Possible early warning for landslide in Sri Lanka using "Anticedent Daily Rainfall Index": A case study of Meeriyabadda Landslide on 29 October 2014.*Mitigation of Disaster due to Severe Natural events: from Policy to Practice 2015 workshop proceedings*.

Somarathne, M., 2014, December. Challenges to overcome: An Overview of Recent Landslides. *GSSL Newsletter*, 31(2), 7–10.

Tajbakhsh, S., Ghafarian, P. &Sahraian, F., 2012. Instability indices and forecasting thunderstorms: the case of 30 April 2009. *Natural Hazards and Earth System Sciences*.

US Department of Commerce, (n.d.).Env Parameters and Indices. Retrieved March 3, 2018, from https://www.weather.gov/lmk/indices

Warnasooriya, A.R., Rodrigo, A.C.M. &Premalal, K.H.M.S, 2016, August. Case Study of Flash Flood Event on 14th November 2014 in Colombo due to Short Period High Intense Rainfall. Department of Meteorology, Sri Lanka.

Investigation of combine effects of El Nino , Positive IOD and MJOon Second Inter-Monsoon Rainfall 2015 in Sri Lanka

K A K T W Weerasinghe and I M S P Jayawardena
P. A. Athula Priyantha
Department of Meteorology
Colombo 07

ABSTRACT

2015/2016 El-Nino episode is a one of the very strong El-Nino among 1982/1983, 1997/1998 and 2015/2016 El-Nino episodes. Together with El Nino , a positive Indian Ocean Dipole also occurred over the Indian Ocean. Strong convective phase of MJO activity also exist over the Indian Ocean during SIM 2015. To analyse the influence of global teleconnections such as El Nino, Positive IOD and MJO on SIM rainfall 2015 and corresponding large scale circulation anomalies, daily rainfall data from 250 rain gauge stations, GLD 360 data provided by the Finnish Meteorological Institute under the Severe Storm Warning Services for Sri Lanka (SSWSS) project, JRA 55 Reanalysis data, ONI data, DMI data, and RMM index data were used in this study.

Composites of large scale circulation anomalies over the South Asian region associated with El Nino year, Positive IOD years and simultaneous years of El Nino and positive IOD were constructed to explain the observed changes in large scale circulation pattern during SIM 2015.

Significantly above normal rainfall has been received over most parts of the country during SIM 2015. Some parts such as northern part receive more than 200% of their climatological average and 90% of its annual average exceeding 1000mm surplus rainfall during SIM 2015. Total accumulated rainfall during SIM 2015 shows three regions of rainfall maxima and rainfall maxima in west-south-western part is associated with the zone of maximum lightning strokes.

80% of heavy rainfall events (daily rainfalls exceeding 100mm), 90% very heavy rainfall events (daily rainfalls exceeding 150mm) were reported in MJO phase 2 and 3. So the influence of MJO on occurrence of extreme rainfall events is significant during SIM 2015providing favourable conditions to develop multi-scale cloud convective clusters.

During SIM 2015, semi permeant twin vortices located are apparent at low levels, one located over south-eastern part of Sri Lanka, and the other to the west of Sri Lanka between 65^0E to 70^0E. The vortex over south-eastern part of Sri Lanka provided a favourable environment for the occurrence of excessive rainfall over Sri Lanka with high positive vorticity and strong uplift at low levels. The semi-permanent vortex over south-eastern part of Sri Lanka appeared in SIM 2015 may be a combine effect of EL Nino , Positive IOD and MJO convective phase in the Indian Ocean.

The cross section of the relative divergence and pressure vertical velocity reveals that in SIM 2015, anomalous Walker type east-west circulation cell and Hadley type circulation cell appeared in the Indian Ocean with rising motion over Sri Lanka and sinking motion over Maritime continent and south of Sri Lanka between 4^0S and 7^0S respectively. This setup allows evacuation of the ascending air mass, therefore aiding its intensification.

Key words: Monsoon, El Nino, Positive IOD, MJO, Hadley Cell and Walker Cell

1. Introduction:

The Second Inter Monsoon (SIM)period from October to November period rainfall is very important to the economy of Sri Lanka as most parts of the country receives significant amount of rainfall during this period.Almost the entire island receives in excess of 400 mm of rain during this season, with the Southwestern slops receiving higher rainfall in the range 750mm to 1200 mm (Weweltalawa Estate in Yatiyantota recording 1219 mm) in SIM season according to the Department of Meteorology records (www.meteo.gov.lk).

SIM rainfall occur in association with the respective northward and southward migrations of the inter-tropical convergence zone (ITCZ) over Sri Lanka (Malmgren et al.,2003). ITCZ is the convergence zone of trade winds blowing from northern hemisphere and southern hemisphere, also known as the low pressure belt. With the conjunction of ITCZ, SIM rainfall is influenced by low pressure areas, depressions and tropical cyclones formed in the Bay of Bengalas well as locally induced thunderstorms. In the SIM period extreme weather events are frequent experiencing strong winds with widespread rain, floods and landslides.

SIM rainfall and its variability is important for agricultural activities in Sri Lanka as onset of main agricultural season “Maha” season is associated with SIM rainfall. Hence the predictability of SIM rainfall as well as its intra-seasonal variability is important for agricultural planning activities, disaster preparedness and water resources management. Intra seasonal-to-inter annual rainfall variability of SIM rainfall has been linked to a variety of processes, mostly tropical in origin.

Influence of the El Niño–Southern Oscillation (ENSO) on SIM rainfall is well documented (Rasmussen and Carpenter, 1983; Suppiah and Yoshino, 1986; Ropelewski and Halpert, 1987; 1989; Suppiah, 1997; 1998, Malmgren*et al.*, 2003; Zubair and Repolewski, 2006, Chandimala and Zubair, 2007; Hapuarachchi and Jayawardena, 2015). Using rainfall data from 90 stations and ONI index from 1950-2011, Hapuarachchi et al 2015 identified that the strongest influence of ENSO extremes is evident during SIM with contrasting spatial patterns are evident in most parts of Sri Lanka, which experience an excess of seasonal rainfall during El Nino years and a deficit of seasonal rainfall in La Nina years (Fig 1).

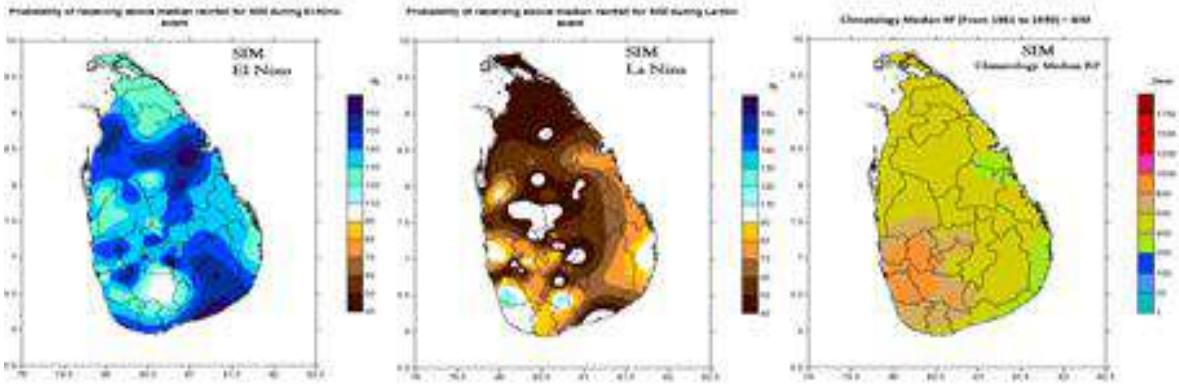

Fig. 1. Composites of Seasonal rainfall probabilities (shading) for SIM season during El Nino (left) and La Nina (Middle). Rainfall probabilities refer to the chance of seasonal rainfall exceeding the median, expressed as a ratio with the mean probability (nominally 50%). Climatological SIM seasonal median rainfall (mm) (right) (Adopted from Hapuarachchi and Jayawardena 2015).

According to Zubair et al 2003 Indian Ocean dipole (IOD) also plays a significant role in inter annual rainfall variability of SIM rainfall. Investigating September to December Rainfall associated with Maha rice growing season, Zubair et al 2003 documented that the strong modulation of the *Maha* rainfall is evident by the IOD phenomenon. The convection arising from this convergence leads to enhanced rainfall over Sri Lanka. The opposite mechanism is at work during negative IOD events (Fig 2). These results show the direct influence of the IOD phenomenon on the Asian monsoon during the boreal fall: the season with the strongest IOD intensity.

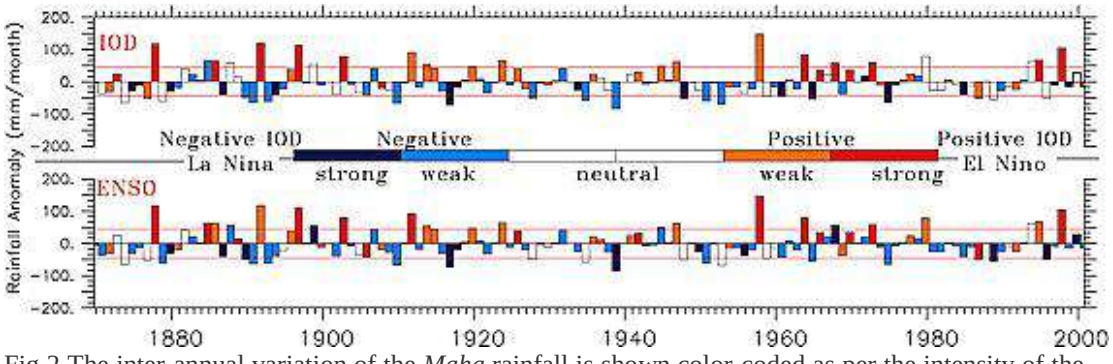

Fig 2 The inter-annual variation of the *Maha* rainfall is shown color-coded as per the intensity of the IODMI (top) and as per the intensity of NINO3 (bottom). Its standard deviation (σ) is shown as horizontal lines. Weak and strong events are taken to be departures of index exceeding 0.25σ and σ respectively. σ for IODMI and NINO3 is 0.30°C and 0.89°C respectively (Adopted Zubair et al, 2003).

The Madden Julian Oscillation (MJO) is a global, tropical, eastward-propagating, quasi-regular circulation anomaly with a 30–60 day period. Convection is strongly coupled to the MJO in the Indian Ocean and the West Pacific (Madden and Julian 1971). The importance of the MJO to tropical and global weather and climate has become increasingly apparent. As intra-seasonal time scale lies between daily weather and seasonal climate (20-90 days), the direct impacts of the MJO on tropical weather and climate phenomena have been widely documented (Zhang 2013). Using 30 years of data from 1981–2010. Jayawardena 2016 and Jayawardena et al 2017 identified that the greatest impact of MJO on rainfall variability occurs during SIM season with well-marked wet signal in phases 1 to 3 and dry signal in phases 5 to 7.The wet signal in MJO phase 2 and 3 is due to the direct influence of the MJO's tropical convective anomalies and associated low-level circulations in the vicinity of Sri Lanka. While analysing extreme rainfall events exceeding the 90^{th} percentile, Jayawardena 2016 found that more frequent extreme rainfall events occur over Sri Lanka when MJO convective phase is in 1, 2 or 3 during SIM season. A simultaneous combination of local phenomena of terrain effects, cold surge at low levels, MJO wet phase and a vortex to southeast Sri Lanka causes heavy rainfall that leads to flood phenomena over Eastern and North eastern parts of Sri Lanka in December 2014 (Jayawardena et al 2017).

Objective of this study is to analyse the influence of global teleconnections such as El Nino, Positive IOD and MJO on SIM rainfall 2015 and large scale circulation anomalies associated with SIM 2015.

2. Data and Methodology

Daily rainfall data from 250 rain gauge stations are used for this study. Global lightning detection database (GLD 360) data provided by the Finnish Meteorological Institute under the Severe Storm Warning Services for Sri Lanka (SSWSS) project are used to see the distribution of lightning strokes during SIM 2015. Vaisala GLD360 is the first ground-based lightning detection network capable of providing both worldwide coverage and uniform, high performance without severe detection differences between daytime and night time conditions (Pohjola. and Mäkelä, 2013; Demetriades et al 2010).Japanese 55-year Reanalysis (JRA-55; Ebita et al. 2011) are used for analysis of large scale circulation patterns. JRA-55 is a third generation reanalysis spans 1958-2012. Japanese 55-year Reanalysis (JRA-55) project was conducted by the Japan Meteorological Agency (JMA) for the period from 1958 onward (Kobayashi et al. 2015) with horizontal resolution of 1.25^0 x 1.25^0.

El Nino episode are categorized using Ocean Nino Index (ONI) based on 3 month running mean of SST anomalies in the Niño. The ONI (Oceanic Niño Index) is defined as 3-month running-mean

values of SST departures from average in the Niño-3.4 region (5^oN-5^oS, 120^o-170^oW). Based on the ONI , NOAA defines El Niño as *positive* ONI greater than or equal to 0.5°C. El Niño episode is classified when these conditions are satisfied for a period of at least five consecutive months (Climate Prediction Center).

Composites of large scale circulation anomalies over the South Asian region associated with El Nino and Positive IOD years (Table 1) were constructed to explain the observed changes in large scale circulation pattern during SIM 2015.

El-nino years	1972, 1976, 1982, 1986, 1987, 1991, 1994, 1997, 2002, 2004, 2006
Positive IOD years	1972 1982 1994 1997 2006 2011
Occurrence of positive IOD and El Nino in simultaneous years	1972 1982 1994 19972006

Table 1.

Dipole Mode Index (DMI) calculated as the anomaly in SST gradient between two particular regions of rectangular shape in the western (50^oE-70^oE and 10^oS-10^oN) and south-eastern (90^oE-110^oE and10^oS-0^oN) tropical Indian Ocean was introduced by Saji in 1999 (Saji et al., 1999). Monthly dipole mode index was used to identify the IOD condition for SIM 2015.

MJO index

The MJO index, a real-time multivariate MJO (RMM) index developed by Wheeler and Hendon (2004), from 01stOctober to 30th November 2015 is used to see the MJO activity during SIM season 2015. The RMM1 and RMM2 index defines a 2D phase space. This phase space is used to define eight ‘‘strong’’ MJO phases, each corresponding to the geographical position of its active convective center (labeled 1–8 in Fig3), and a ‘‘weak MJO’’ category defined when the amplitude is less than 1. These phases make up a full MJO cycle originating from the western Indian Ocean and decaying over the central Pacific. For instance, phases 2 and 3 mark the time when the MJO’s convective envelopes are centered in the Indian Ocean and phases 6 and 7 mark the time when it is in the Western Pacific.

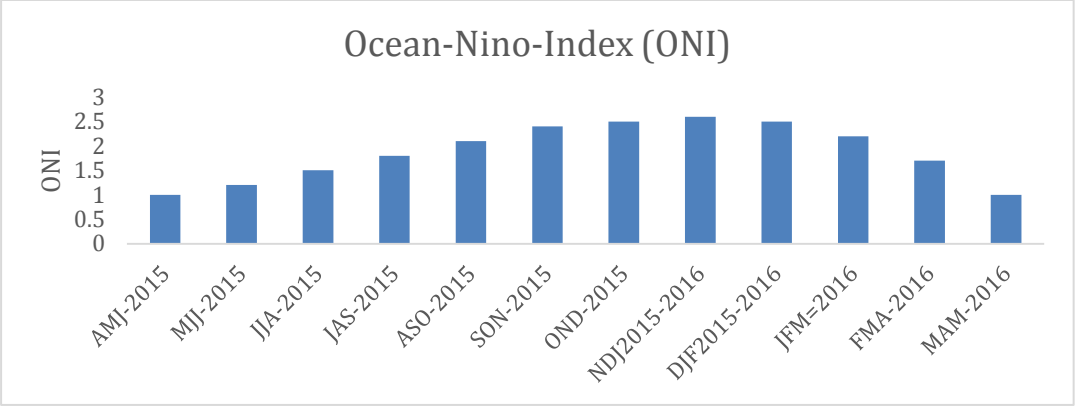

Figure 3.Time series of Ocean Nino Index from April-May-June (AMJ) 2015 to March-April-May (MAM) 2016 (Data from CPC website :www.cpc.ncep.noaa.gov/)

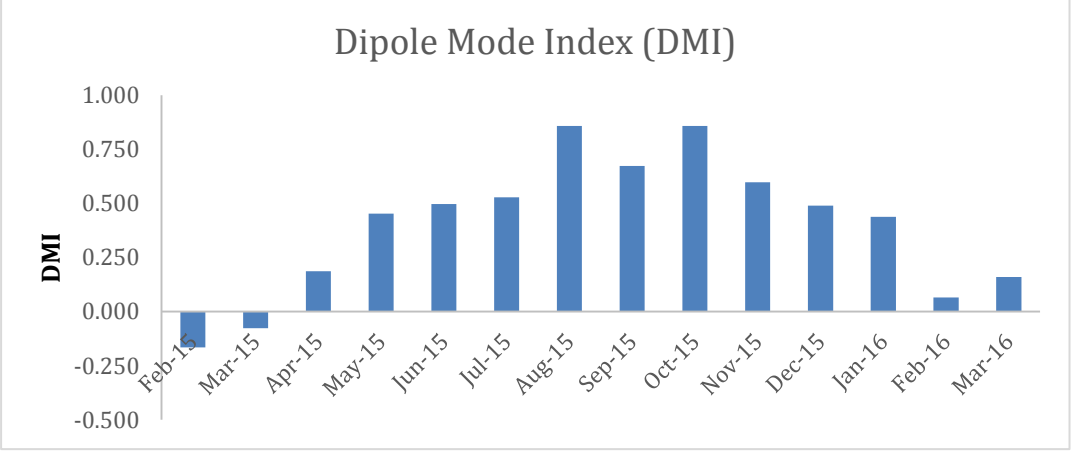

Figure 4. Time series of Dipole Mode Index (DMI) from February 2015 to March 2016 (Data from Jamstec website: http://www.jamstec.go.jp/frcgc/research/d1/iod/e/iod/about iod.html.).

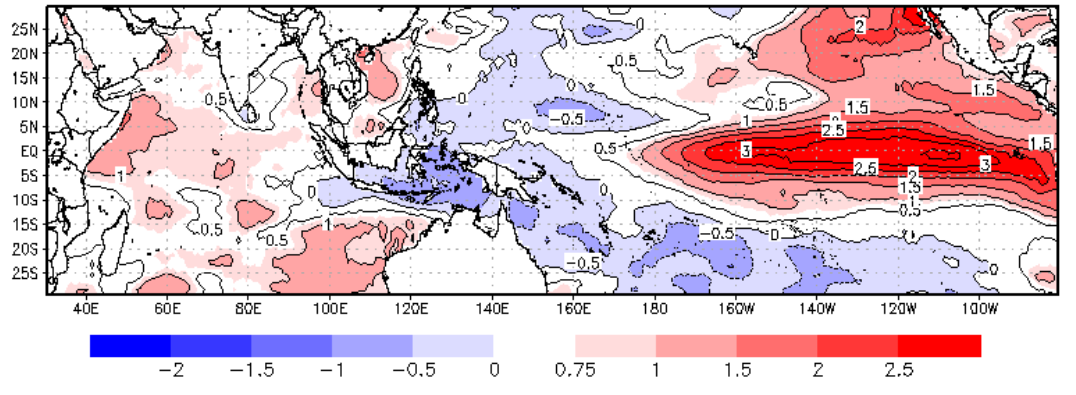

Fig 5. Sea surface Temperature (SST) anomalies during SIM 2015

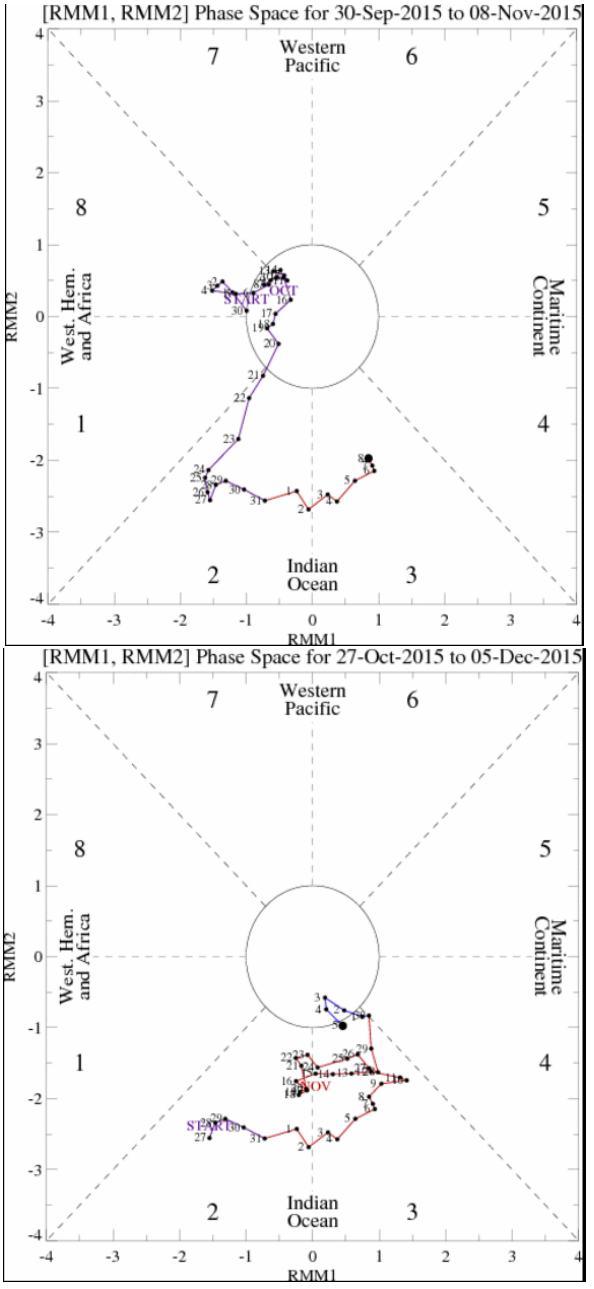

Figure 6. Phase diagram of RMM index (Wheeler and Hendon 2004) from 30th September to 05 December 2015. Each point represents a day. Eight phases and corresponding approximate locations of enhanced convective signals of the MJO are labelled. Points within the circle represent weak or no MJO (Adopted from CPC website :www.cpc.ncep.noaa.gov/)

3. Results and Discussion

3.1 Global Climate conditions during SIM 2015

2015/2016 El-Nino episode is a one of the very strong El-Nino among 1982/1983, 1997/1998 and 2015/2016 El-Nino episodes. ONI index is above 1 from April May June season 2015 to March April May season 2016 indication strong persisting warming occurred over the equatorial eastern Pacific in year 2015 (Fig. 3). Dipole Mode Index (DMI) is above 0.5 from August 2015 to November 2015 (Fig 4) .Further strong El Nino conditions over the equatorial eastern pacific together with positive IOD (Fig 4) conditions over the tropical Indian Ocean were prevailed during SIM season (Fig 5). According to the MJO index, strong MJO is present in the Indian Ocean from 22 October to 30th November 2015 (Fig 6). MJO activity is defined when the intensity of MJO index is larger than 1.

3.2 SIM 2015 Rainfall distribution

Significantly above normal rainfall has been received over most parts of the country during SIM 2015 (Fig 7(A and B)). Some parts such as northern part receive more than 200% of their climatological average (fig 7 (A)) exceeding 1000mm surplus rainfall (Fig 7(B)) in SIM 2015. It is noteworthy to mention that northern part received more than 90% of it's annual average during SIM 2015 season. During SIM 2015 highest seasonal rainfall recoded is 2106.8 mm from Dabar estate in Kegelle district which is nearly 210% of it's seasonal average. Kirklees Estate received 1881 mm which is nearly 306 % of it's seasonal average. It is worthy mentioning that nearly 100% of annual average is received during SIM 2015 at some stations such as Kannukkeni Tank, Nachchaduwa, Karukkuwa Estate and Iranamadu Tank over northern part of the country.

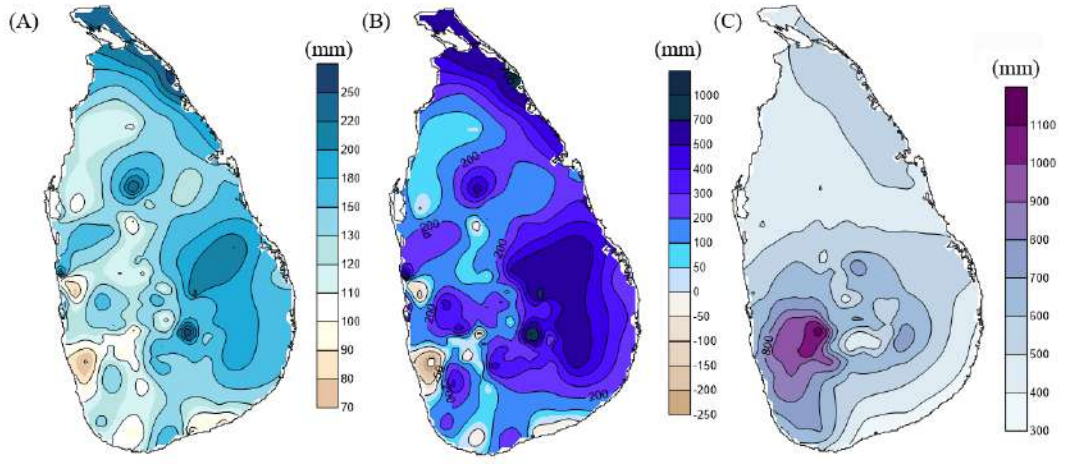

Fig 7.Percentage of departure from seasonal mean during SIM 2015(A), Rainfall anomaly during SIM2015 (B) and Climatology of SIM Rainfall (1981 to 2010) (C).

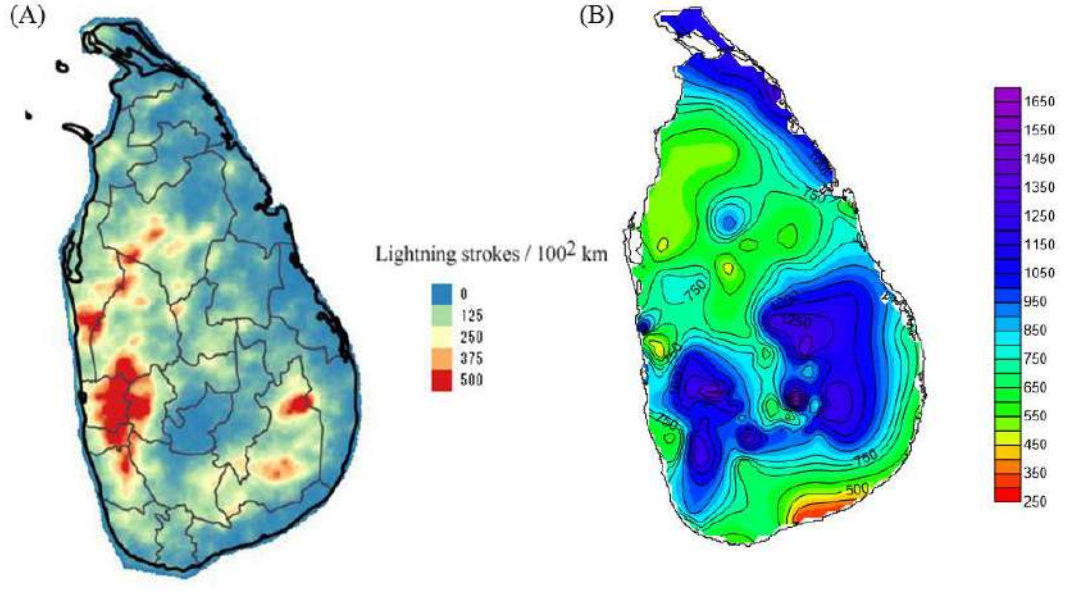

Fig 8 : Lightning flash density (Strokes per 100 km^2) using GLD360 data (A) and total accumulated rainfall (B) for October-November 2015.

Table 2 : Stations received more than 100mm daily rainfall in month of October 2015

Month	Day	Stations received more than 100mm daily rainfall
10	2	Beauvais Estate
10	7	Kirindiwela (Coconut)
10	12	Mattala
10	13	OkkampitiyaDiyabeduma, Mihintale W/S, Wellewala, Madutugama, Hathmaththa
10	14	Canawarella Group, Mapakadawewa, Sita Eliya, Vincit Estate, Thalapathkanda, Mahadowa Estate
10	16	Bandara Eliya Estate, Dambatenne, Padukka Estate, Pussella S.P., Poonagala Group, Factory, PitaratMalai Estate
10	18	Athuela Hakbellawaka LabuduwaVincit Estate Baddegama Estate Depedena Group Dunedin Estate Kirindiwela (Coconut) Pallegama ,Rathnayake Gp Weweltalawa Estate, Nittambuwa Hathmaththa Stinsford Chesterford Ruwanwella Rest House, Moralioya Gonagamuwa
10	19	Balangoda Post Office, Detanagalla, Sirikandura Estate
10	20	Eppawala Water Supply, Owella – Rattota, Giddawa, Batalagoda Tank
10	21	Hakbellawaka
10	22	Dickoya, Bopekanda Estate, Eheliyagoda S.P, Pussella S.P., Passikuda, Rammala Kanda, Suriyawewa, Gangeyaya
10	23	
10	24	Batuwangala, Batticaloa, DalkethEst,(Baduraliya), Katandola, Rugam Tank, Poonagala Group, Factory
10	25	Batticaloa, Mylambavelly Estate, Thumpenkeni Tank, Unichchai Tank, Rugam Tank, Sagamam Tank, Vakaneri, Samanthurai
10	26	Vakaneri, Mylambavelly Estate, Thumpenkeni Tank, Passikuda, Addalachenai, Horowupatana,Aga Office
10	27	Hakgala Botanical Gdns, Trincomalee, Kal Aar, Kannukkeni Tank, Welikanda Singhapura, Vakaneri, Kirklees Estate
10	28	Kuchchaveli
10	29	Mutwagalla Estate

Rainfall from atmospheric deep convection is a very common weather phenomenon during SIM. The character of convective precipitation is influenced by the complex interactions of atmospheric circulations, land surface process, moisture and heat energy. Figure 8 (A) represents the spatial distribution of lighting strokes occurred during SIM 2015. In general higher lightning activity has confines to western, north-western and south-eastern parts of the country during SIM 2015. The major region of strongest lightning activity during SIM 2015 is evident over the inland areas of western coast over the boundary between Gampaha and Kegalle districts, and Colombo and Ratnapura districts. According to situation report of the Disaster Management Centre (DMC), four casualties two from Batticaloa on 18th and two from Buththla on 12th during month of October and five casualties (4 from Northern, Northcentral and Eastern provinces and another one from Kegalle district) were reported during the month of November due to lightning strikes.

Table 3 : Stations received more than 100mm daily rainfall in month of November 2015

Month	Day	Stations received more than 100mm daily rainfall
11	1	Hiripitiya Hospital, Inginimitiya, Parasangahawewa Farm, Anuradhapura, Nachchaduwa, Rambewa, Vavunikulam
11	2	Crystal Hill Estate, Trincomalee, Imbulandanda, Kalawewa Tank, Mahailluppallama S/F, Medapihilla, Mediyawa Tank, Mihintale W/S, Parasangahawewa Farm, Batticaloa, MahaIlluppallama, Warakapola(Niyadurupola), Yakawewa, Anuradhapura, Katunayake, Wellewala, Huruluwewa, Eppawala Water Supply, Poottwala Estate, RidibendiEla, MolaEliya, DickoyaMahagalkadawla,Galgamuwa, Palampoddar,Thambalagamu, AlutOya, Delta Estate,EastDiv, Delta North, Elahera, Watawala,Railway Station, NachchaduwaChesterford, Bowatenna, Kirindiwela (Coconut), Wewelmada, WariyapolaExptl.Station, Dampellassa – Narammala,
11	3	Passikuda, Thumpenkeni Tank, Bandarawela, Mylambavelly Estate, Lunuwila (Bandirippuwa), Karukkuwa Estate, Loolkade Division
11	4	Delwala, Eheliyagoda S.P, Katunayaka, Wellewala, Huruluwewa, Eppawala Water Supply, Poottwala Estate, RidibendiEla, MolaEliya, Mahagalkadawla,Galgamuwa
11	5	Annfield Estate, Dunedin Estate, Kirklees Estate, Canyon, Upper UgraOya, Samanala Power Station, Mutwagalla Estate, Padukka Estate, Lellopitiya Estate , Weweltalawa Estate, Halwatura, Summerset, Embilipitiya,CoconutNur, Labukelle, Dickoya
11	6	Batuwangala, Undugoda, DalkethEst,(Baduraliya)
11	7	Rayigama, Kamalasram (Udubaddawa), PannalaViridiyawaEst, Vincit Estate, Bopitiya Co
11	8	Labuduwa, Galle, Middeniya
11	9	Middeniya
11	11	Pulmudei
11	12	Gomara, Pannala, ViridiyawaEst, Frocestor Estate, Pulmoddai
11	13	Ehetugaswewa, EthawetunuWewa, Mundalama, PalaviSaltern, Palugaswewa Estate, PannalaViridiyawaEst, RathmalgahaWewa Hospital, Mannar, Horowupatana,Aga Office, Puttalam, Vavuniya, Huruluwewa, Poottwala Estate, Singhapura, Padawiya, Devisipura, Uhana Coconut, Parangiyawadiya, Wahalkada, Morawewa Irrigation, Amparai Tank, Vavunikulam, Karukkuwa Estate, MutuIyankaddu, Kannukkeni Tank
11	14	EthawetunuWewa, Medapihilla, Passikuda, Akkarayankulam, Kankesanturai, Padawiya, WahalkadaKariyalainagapoduwan, Chilaw-P.W.D, , Alambil, Point Pedro, Bakamuna, Elahera, Kalawediulpota, Jaffna, Atchuvely, Karukkuwa Estate, MutuIyankaddu, St. Annes Estate, Daluwa, Kannukkeni Tank
11	15	Hiripitiya Hospital, KimbulwanaOya, Hakwatuna-Oya, Palugaswewa Estate, Mannar, Point PedroIranamadu Tank, Poottwala Estate, Norochcholai, , Jaffna, Atchuvely, Loolkade Division
11	16	Akkarayankulam, Iranamadu Tank, Kariyalainagapoduwan
11	18	Handapangala, Giritale, Dambatenne
11	19	Poonagala Group, Factory Pattipola, St.Catherine Division, Loolkade Division
11	20	Negombo, Undugoda
11	25	Deegala
11	28	Illukkumbura
11	29	Galoola Estate, Rantembe, Randenigala, Kirklees Estate, Tambuttegama, Giritale (Wild Life), Diyabeduma, Kandaketiya, Aluthnuwara
11	30	Marigold Factory, PannalaViridiyawaEst, NalandaExper.Station

Table 4: Stations received very heavy rainfall (more than 150mm daily rainfall (mm)) during October and November 2015

Station Name	Month	day	Daily Rainfall (mm)	Station Name	month	day	Daily Rainfall (mm)
Mannar	11	15	350.9	PannalaViridiyawaEst	11	12	166.7
Kannukkeni Tank	11	13	330.0	Atchuvely	11	14	166.6
Pulmoddai	11	11	304.3	Trincomalee	10	27	166.4
Karukkuwa Estate	11	14	274.0	Jaffna	11	14	166.3
MutuIyankaddu	11	13	262.0	Dunedin Estate	10	18	166.2
PoonagalaGrou	11	19	261.0	Mahadowa Estate	10	14	165.1
Iranamadu Tank	11	15	254.6	MutuIyankaddu	11	14	165.0
Pulmoddai	11	12	250.5	Mahailluppallama	11	2	162.1
Nachchaduwa	11	2	243.3	MahaIlluppallama	11	2	162.1
Akkarayankulam	11	14	236.8	Kariyalainagapoduwan	11	14	160.5
Padawiya	11	13	209.9	Chilaw-P.W.D	11	14	160.0
Poottwala Estate	11	13	195.0	BandaraEliya Estate	10	16	160.0
Vakaneri	10	27	191.2	Kirklees Estate	10	27	160.0
Vakaneri	10	25	186.9	Bakamuna	11	14	156.5
Singhapura	11	13	186.5	EthawetunuWewa	11	13	156.0
Batticaloa	10	24	182.9	Dunedin Estate	10	30	155.6
PannalaViridiyawa	11	30	182.3	Horowupatana	10	26	155.5
Poottwala Estate	11	2	182.0	Dambatenne	10	16	155.0
Mylambavelly Estate	10	25	181.6	Passikuda	10	26	155.0
Labuduwa	10	18	180.8	EthawetunuWewa	11	14	154.0
Kannukkeni Tank	11	14	173.0	Mahadowa Estate	11	29	152.0
Ehetugaswewa	11	13	172.0	Loolkade Division	11	19	151.3
Karukkuwa Estate	11	13	170.0	Morawewa Irrigation	10	27	151.0
Karukkuwa Estate	11	3	167.0	Weweltalawa Estate	10	18	150.9
Point Pedro	11	15	167.0	Mylambavelly Estate	11	3	150.7

Total accumulated rainfall during SIM 2015 (Fig 8 (B)) shows 3 precipitation maxima m northern-north-eastern parts, eastern-south-eastern parts and west-southwestern parts. Rainfall maxima in west-south-western part is associated with the zone of maximum lightning strokes (Fig 8(A)), Rainfall maxima in northern-north-eastern part is not associated with the strong lightning activity (Fig 8(A)) indicating possible strati form precipitation over that region. South eastern boundary of eastern-south-eastern rainfall maxima is associated with higher lightning stroke density indication convective precipitation dominating over that area. Rest of the region may have dominated by strati form precipitation.

According to situation report of DMC round 79000 people in 14 districts including N'Eliya, Badulla, Batticaloa, Gampaha, Trincomalee, Matale, Jaffna, Kilinochchie and Mulathive were affected by

heavy rain and 3 casualties also were reported due to flood situation during November 2015. A landslide had been reported from Urubokka in Galle district on 25th November 2015. During this period many stations around the island reported more than 100mm daily rainfall (table 2 and 3). 280 heavy rainfalls exceeding 100mm within 24 hours were reported during SIM 2015 (Table 2 and 3). 50 very heavy rainfall events exceeding 150mm within 24 hours were reported during SIM 2015 (Table 4). Highest reported daily rainfall amount during SIM 2015 was 350.9 mm from Mannar on November 15 and was the ever recorded highest 24 hour rainfall at that station.

3.3 Impact of MJO on SIM 2015

Using 30 years of data from 1981–2010, Jayawardena 2016 identified that the greatest impact of MJO on rainfall variability occurs during SIM season with well marked wet signal in phases 1 to 3 and dry signal in phases 5 to 7. According to the MJO index, strong MJO is present in the Indian Ocean from 21 October to 30th November 2015. MJO activity is defined when the intensity of MJO index is larger than 1. Strong MJO can be seen in phase 2 from 21 October to 02nd November 2015 and in phase 3 from 03rd November to 30th November 2015. MJO is divided into eight phases and on average, each phase of MJO lasts for about 6 days (Wheeler and Hendon 2004). But in 2015 MJO was in phase 2 for 11 days and phase 3 for 28 days.

The MJO is a phenomenon in which cooperation between large-scale dynamics and organized convection is essential, as the multi-scale organization of convection is a key aspect of the MJO (Nakazawa 1988). According to Nakazawa1988 within the MJO active phase, synoptic-scale convection with super cloud clusters with temporal scale of about 10 days were observed to propagate eastwards while convective cloud clusters with temporal scale of about a day move westward. Hence MJO provides favourable conditions to develop multi-scale cloud convective clusters bringing heavy rainfall amounts . Out of 280 daily heavy rainfall events occurred during this period, 227 were reported in MJO phase 2 and 3. Accordingly 80% of heavy rainfall events (daily rainfalls exceeding 100mm) reported in MJO phase 2 and 3 (from 21 October to 30thNovember). Out of 50 very heavy rainfall events (Table 4), 44 were reported in MJO phase 2 and 3 where MJO convective core located in Indian Ocean. So the influence of MJO on occurrence of extreme rainfall events is significant during SIM 2015. More than 250mm daily rainfall events including the highest reported daily rainfall amount 350.9 mm from Mannar were occurred from 11th to 19th November (Table 4) during MJO convective phase 3 . Hence influence of MJO on extreme rainfall events during SIM 2015 is clearly evident.

3.4 Large scale circulation anomalies during SIM 2015

It is well recognized that for deep convection to occur, the troposphere should be convectively unstable for ascent of moist parcel through a relatively deep layer. On synoptic scales, instability to moist convection is a necessary but not sufficient condition for the occurrence of organized convective events. In addition to the thermodynamic conditions, dynamic conditions such as low level convergence, rising motion, suitable wind shear are also necessary (Cohen and Frank, 1989).

The spatial distribution of SIM rainfall varies according to the large- and local-scale atmospheric patterns. However, among that variety of patterns, it could be argued that, from a diagnostic point of view, there are some atmospheric conditions that hold true for a generalized rainfall event and also for extreme cases of precipitation in Sri Lanka during SIM season. As previous studies identified the influence of ENSO and IOD on SIM rainfall, SIM-based composite for the low level wind were constructed for El Nino years (Table 1), positive IOD years(Table 1) and simultaneous years of positive IOD and El Nino (Table 1) during SIM.

During SIM 2015, semi permeant twin vortices located were apparent at low levels; 850 hPa (Fig 9(A)) and 700 hPa (Fig 10(A)), one located over south eastern part of Sri Lanka, and the other to the west of Sri Lanka between 65^0E to 70^0E (Figs 9(A) and 10(A)). The vortex over south eastern part of Sri Lanka provided a favourable environment for the occurrence of excessive rainfall over Sri Lanka with high positive vorticity and strong uplift at low levels.

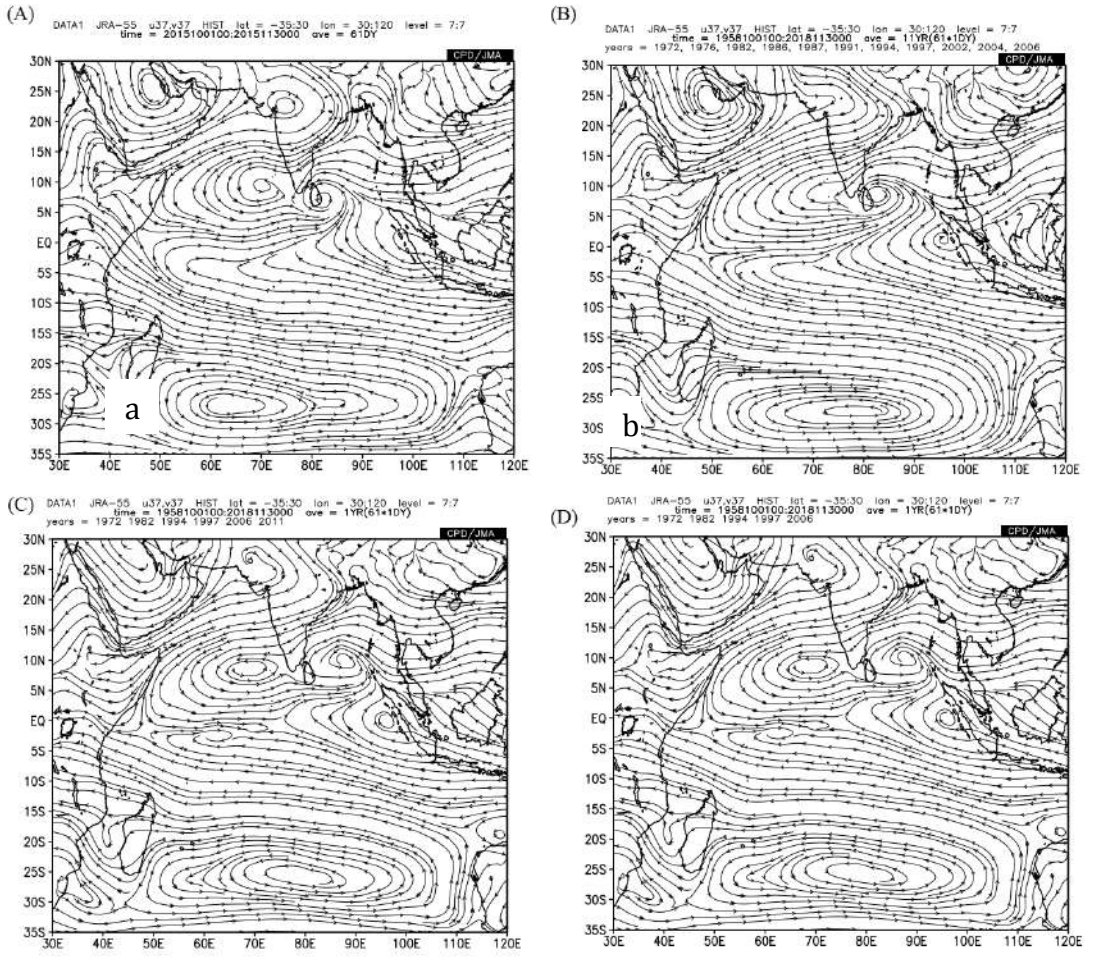

Fig 9.Mean wind at 850hPaduring SIM 2015 (A), Composite of mean wind at 850-hPa (streamlines) for El Nino years during SIM(B), Composite of mean wind (streamlines) at 850-hPa for positive IOD years during SIM(C), and Composite of mean wind (streamlines) at 850-hPa for simultaneous years of positive IOD and El Nino during SIM

During El Nino years a single vortex at low levels was appeared in the Southwest Bay of Bengal (BoB) to the East of Sri Lanka at 850hPa (Fig 9(B)) and at 700 hPa (Fig 10(B)). East-west oriented trough axis associated with the vortex in southwest BoB extended to west of Sri Lanka in 850hPa and 700 hPa (Fig 9(B) and 10(B)).

During positive IOD years as well as simultaneous years of positive IOD and El Nino twin vortices were apparent at low levels; 850 hPa (Figs 9(C)) and 9(D)) and 700 hPa (Figs 10(C)and 10(D)).

One vortex was located over the central BoB to East of Sri Lanka, and the other to the west of Sri Lanka between 65^0E to 70^0E (Figs 9(C),9(D), 10(C), and 10(D)).

The vortex over south-eastern part of Sri Lanka appeared in SIM 2015 may be a combine effect of EL Nino , Positive IOD and MJO convective phase in Indian ocean.

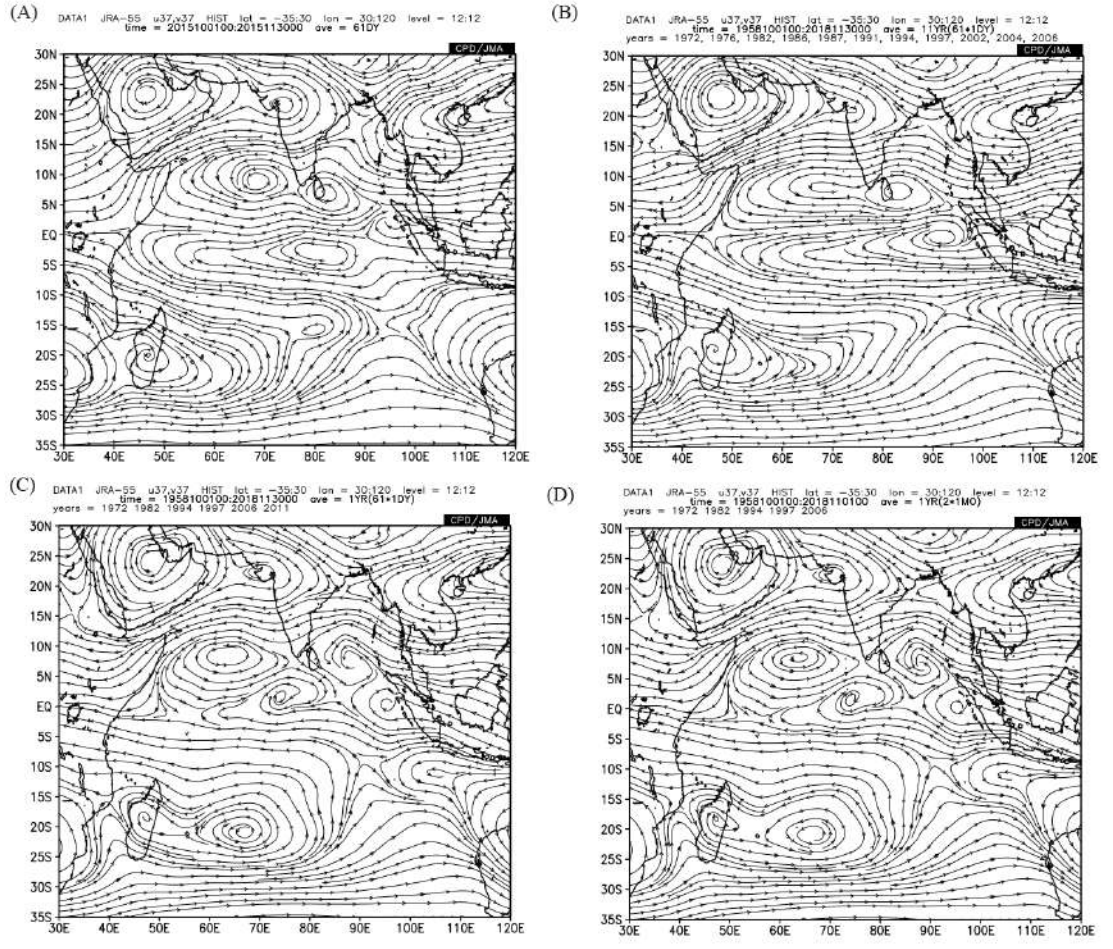

Fig 10.Mean wind at 700hPa during SIM 2015 (A), Composite of mean wind at 700-hPa (streamlines) for El Nino years during SIM(B), Composite of mean wind (streamlines) at 700-hPa for positive IOD years during SIM(C), and Composite of mean wind (streamlines) at 700-hPa for simultaneous years of positive IOD and El Nino during SIM

To see the associated dynamical parameters during SIM 2015, vertical profile of pressure vertical velocity anomaly, and relative divergence anomaly, across (Fig 11) and along (Fig 12) Sri Lanka region are analyzed using JRA55 reanalysis data. Rising motion with negative pressure vertical velocity (Figs. 11 (A) and 12 (A)) is evident from low levels to upper levels with relative maxima around 850hPalevel.Strong lower level convergence is evident between surface to 800 hPa levels (Figs. 11 (B) and 12 (B))in the vicinity of Sri Lanka between 80^0E and 85^0E as well as between the Equator and 10^0N. Strong upper level divergence is evident between 250 hPa to 100 hPa levels (Figs. 11 (B) and 12 (B))in the vicinity of Sri Lanka between 80^0E and 85^0E as well as between the Equator and 10^0N.

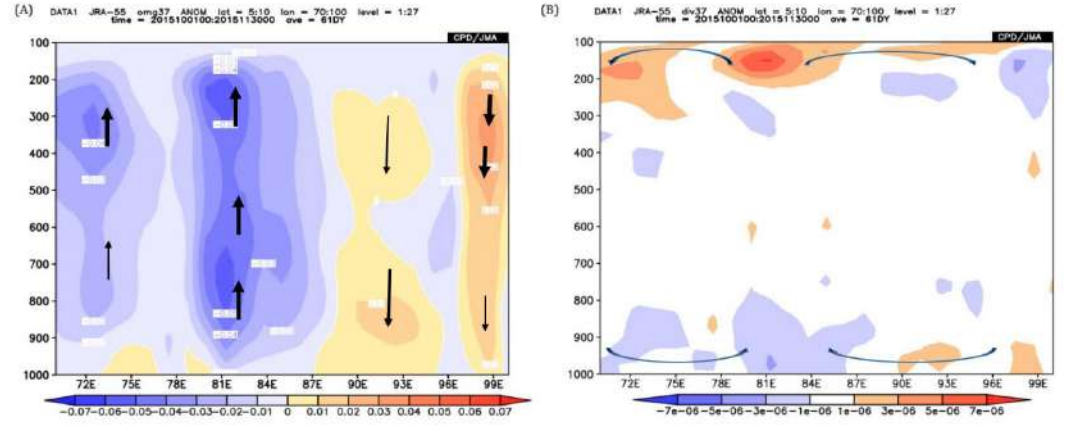

Fig 11.Pressure-longitude cross sections (averaged over Sri Lanka Region from 05°N–10°N) of Pressure vertical velocity anomaly (Pas s^{-1}, shaded) (A) , and Relative divergence anomaly (10^{-6} s^{-1}, shaded)(B) for SIM 2015

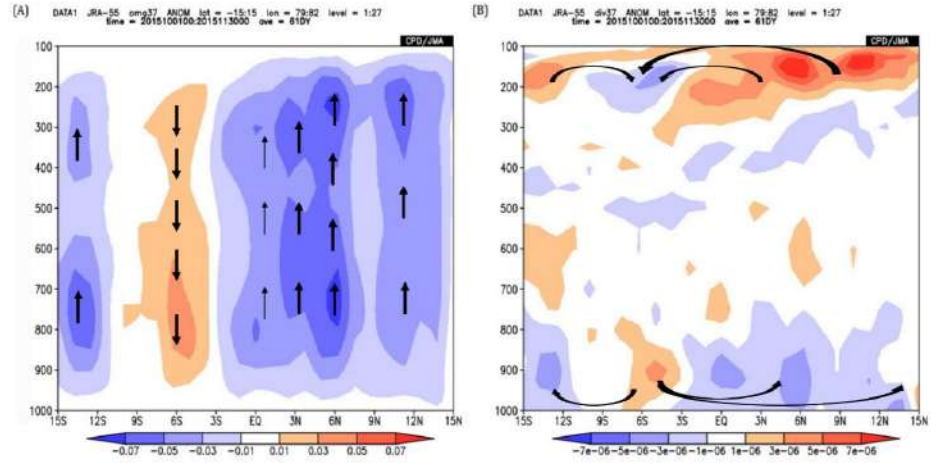

Fig12.Pressure-latitude cross sections (averaged over Sri Lanka Region from 79°E–82°E) of Pressure vertical velocity anomaly (Pas s^{-1}, shaded)(A) , and Relative divergence anomaly (10^{-6} s^{-1}, shaded) (B) for SIM 2015.

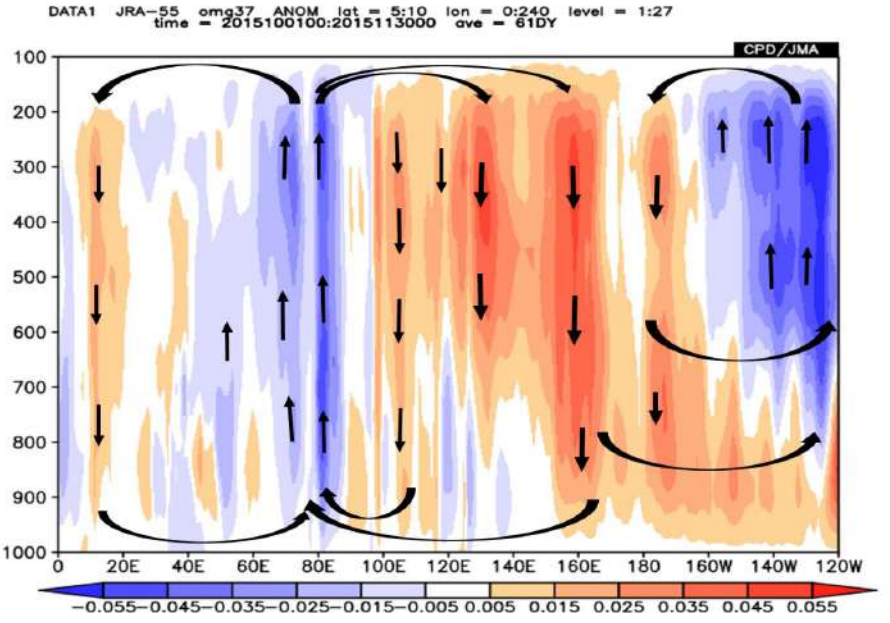

Fig 13.EastWest vertical cross-section of pressure vertical velocity during SIM 2015

Associated with vigorous upward motion in the vicinity of Sri Lanka between 80^0E and 85^0E as well as between the Equator and 10^0N , sinking motion is evident to East of Sri Lanka between 90^0E and 100^0E and south of Sri Lanka between 4^0S and 7^0S (Figs. 11 (A) and 12 (A)). East-west cross-section of pressure vertical velocity from West Indian Ocean to central pacific (Fig 13) indicate the changes in Walker circulation with sinking motion over Western Africa, rising motion over Sri Lanka region, sinking motion over Maritime continent, and rising motion over Eastern Pacific ocean, associated with persisting El Nino conditions in the equatorial Pacific Ocean as well as positive IOD conditions in the Indian Ocean (Fig 13).

The cross section of the relative divergence field in Figures 11 (A) and 12 (A) shows that strong low-level wind divergence and upper level convergence exists over maritime continent beyond 95^0E and south of Sri Lanka between 4^0S and 7^0S associated with sinking motion over those regions. The cross section of the relative divergence and pressure vertical velocity reveals that in SIM 2015, anomalous Walker type east-west circulation cell and Hadley type circulation cell appeared in the Indian Ocean with rising motion over Sri Lanka and sinking motion over Maritime continent and south of Sri Lanka between 4^0S and 7^0S respectively. This setup allows evacuation of the ascending air mass, therefore aiding its intensification. The combination of strong low-level convergence and upper-level divergence is characteristic of deep convection with the low-level moisture source from

the Bay of Bengal provided a favourable environment for the occurrence of excessive rainfall over Sri Lanka with high positive vorticity and strong uplift at low levels.

4. Summary and Conclusion

The purpose of this study is to analyse the influence of global teleconnections such as El Nino, Positive IOD and MJO on SIM rainfall 2015 and large scale circulation anomalies associated with SIM 2015. Daily rainfall data from 250 rain gauge stations, GLD 360 data provided by the Finnish Meteorological Institute under the Severe Storm Warning Services for Sri Lanka (SSWSS) project, JRA 55 Reanalysis data, ONI data, DMI data, RMM index data are used .

Anomaly of Seasonal rainfall and percentage of rainfall departure from seasonal mean were constructed for the period from October 01 to November 30, 2015 to see the seasonal rainfall variability. Composites of large scale circulation anomalies over the South Asian region associated with El Nino year, Positive IOD years and simultaneous years of EL Nino and positive IOD were constructed to explain the observed changes in large scale circulation pattern during SIM 2015.

Significantly above normal rainfall has been received over most parts of the country during SIM 2015. Some parts receive such northern part more than 200% of their climatological average and 90% of it's annual average exceeding 1000mm surplus rainfall during SIM 2015.

Total accumulated rainfall during SIM 2015 shows 3 precipitation maxima and Rainfall maxima in west-south-western part is associated with the zone of maximum lightning strokes.

MJO provides favourable conditions to develop multi-scale cloud convective clusters bringing heavy rainfall amounts . 80% of heavy rainfall events (daily rainfalls exceeding 100mm), 90% very heavy rainfall events (daily rainfalls exceeding 150mm) were reported in MJO phase 2 and 3. So the influence of MJO on occurrence of extreme rainfall events is significant during SIM 2015.

During SIM 2015, semi permeant twin vortices located were apparent at low levels, one located over south-eastern part of Sri Lanka, and the other to the west of Sri Lanka between 65^0E to 70^0E. The vortex over south-eastern part of Sri Lanka provided a favourable environment for the occurrence of excessive rainfall over Sri Lanka with high positive vorticity and strong uplift at low levels. The vortex over south-eastern part of Sri Lanka appeared in SIM 2015 may be a combine effect of EL Nino , Positive IOD and MJO convective phase in Indian ocean.

The cross section of the relative divergence and pressure vertical velocity reveals that in SIM 2015, anomalous Walker type east-west circulation cell and Hadley type circulation cell appeared in the Indian Ocean with rising motion over Sri Lanka and sinking motion over Maritime continent and south of Sri Lanka between 4^0S and 7^0S respectively. This setup allows evacuation of the ascending air mass, therefore aiding its intensification. The combination of strong low-level convergence and upper-level divergence is characteristic of deep convection with the low-level moisture source from the Bay of Bengal provided a favourable environment for the occurrence of excessive rainfall over Sri Lanka in SIM 2015.

Acknowledgement

The JRA-55 reanalysis dataset was provided by the JMA and is available at http://jra. kishou .go.jp/JRA-55/index_en.html. Preliminary analysis in the present study used the ITACS system developed by the JMA. Technical support and GLD360 dataset provided by Finnish Meteorological Institute (FMI) and VAISALA oyj under Severe Storm Warning Services for Sri Lanka (SSWSS) project is acknowledge.

REFERENCES

Chandimala, J. and Zubair, L., 2007, Predictability of stream flow and rainfall based on ENSO for water resources management in Sri Lanka. Journal of Hydrology, 335(3), pp.303-312.

Cohen, C. and Frank, W.M., 1989. A numerical study of lapse-rate adjustments in the tropical atmosphere. *Monthly weather review*, *117*(8), pp.1891-1905.

Demetriades, N.W., Murphy, M.J. and Cramer, J.A., 2010, April.Validation of Vaisala's global lightning dataset (GLD360) over the continental United States.In *Preprints, 29th Conf. on Hurricanes and Tropical Meteorology, Tucson, AZ, Amer. Meteor.Soc. D* (Vol. 16).

Ebita, A., Kobayashi, S., Ota, Y., Moriya, M., Kumabe, R., Onogi, K., Harada, Y., Yasui, S., Miyaoka, K., Takahashi, K. and Kamahori, H., 2011. The Japanese 55-year reanalysis "JRA-55": an interim report. *Sola*, *7*, pp.149-152.

Hapuarachchi H. A. S. U., and I. M. S. P. Jayawardena, 2015. Modulation of Seasonal Rainfall in Sri Lanka by ENSO Extremes , Sri Lanka Journal of Meteorology, 1, 3-11

http://www.jamstec.go.jp/frcgc/research/d1/iod/e/iod/about iod.html (Jamstec Centre website)

http://www.cpc.ncep.noaa.gov (Climate Prediction Centre, USA website)
http://www.meteo.gov.lk (DoM Sri Lanka website)
http://www.dmc.gov.lk(DMC Sri Lanka website)

Jayawardena, I. M. S. P. , W. L. Sumathipala, and B. R S. B. Basnayake 2016. Impact of the Intra-seasonal Oscillations (ISO) on Rainfall Variability during Southwest Monsoon in Sri Lanka. 16th Conference of the Science Council Asia : Science for People : Mobilizing Modern Technologies for Sustainable Development in Asia, Abstracts and Proceedings 31 May-02 June 2016, Colombo, Sri Lanka pp 104-109

Jayawardena, I. M. S. P., W. L. Sumathipala, and B. R S. B. BasnayakeIntra-seasonal rainfall variability during Southwest Monsoon in Sri Lanka 2016 CLIVAR Open Science Conference"Charting the course for climate and ocean research" 18-25 September 2016 Qingdao, China

Jayawardena, I.M.S.P., Sumathipala, W.L. and Basnayake, B.R.S.B., 2017. Impact of Madden Julian oscillation (MJO) and other meteorological phenomena on the heavy rainfall event from 19th− 28th December, 2014 over Sri Lanka. *Journal of the National Science Foundation of Sri Lanka*, *45*(2).

Kobayashi, S., Ota, Y., Harada, Y., Ebita, A., Moriya, M., Onoda, H., Onogi, K., Kamahori, H., Kobayashi, C., Endo, H. and Miyaoka, K., 2015. The JRA-55 reanalysis: General specifications and basic characteristics. *Journal of the Meteorological Society of Japan.Ser. II*, *93*(1), pp.5-48.

Madden, R.A. and Julian, P.R., 1971. Detection of a 40–50 day oscillation in the zonal wind in the tropical Pacific. *Journal of the atmospheric sciences*, *28*(5), pp.702-708.

Malmgren, B.A., Hulugalla, R., Hayashi, Y. and Mikami, T., 2003.Precipitation trends in Sri Lanka since the 1870s and relationships to El Niño–Southern Oscillation. *International Journal of Climatology*, *23*(10), pp.1235-1252.
.

Nakazawa, T., 1988.Tropical super clusters within intraseasonal variations over the western Pacific. *Journal of the Meteorological Society of Japan.Ser. II*, *66*(6), pp.823-839.

Pohjola, H. and Mäkelä, A., 2013. The comparison of GLD360 and EUCLID lightning location systems in Europe. *Atmospheric research*, *123*, pp.117-128.

Rasmusson E. M, & Carpenter, T. H. (1983) The relationship between eastern equatorial Pacific sea surface temperature and rainfall over India and Sri Lanka. *Monthly Weather Review* 110: 354–383.

Ropelewski C. F, &Halpert M. S. (1987) Global and regional scale precipitation patterns associated with the El Nin˜o/southern oscillation. *Monthly Weather Review* 115:

RopelewskiC.F,&Halpert M.S. (1989) Precipitation patterns associated with the high index phase of the southern oscillation. *Journal of Climate* 2(3): 268–284.

Saji N H, Goswami B N, Vinayachandran P N, & Yamagata T (1999) A dipole mode in the tropical Indian Ocean. Nature 401:360–363.

Suppiah R, Yoshino, M M. (1986) Someagroclimatological aspects of rice production in Sri Lanka. *Geographical Review of Japan, Series B* 59(2): 137–153.

Suppiah R. (1997) Extremes of the southern oscillation and the rainfall of Sri Lanka. *International Journal of Climatology* 17(1): 87–101.

Suppiah R. (1998) Spatial and temporal variations in the relationship between the southern oscillation and the rainfall of Sri Lanka.*International Journal of Climatology* 16(12): 1391–1408.

Wheeler, M. C., & Hendon, H. H. (2004) An all-season real-time multivariate MJO index: Development of an index for monitoring and prediction. *Monthly Weather Review*132, 1917–1932.

Zhang C, (2013) Madden–Julian oscillation: Bridging weather and climate. *Bulletin of the American Meteorological Society*, 94, 1849–1870.

Zubair and Repolewski, 2006, Zubair, L., Rao, S.A. and Yamagata, T., 2003.Modulation of Sri Lankan Maha rainfall by the Indian Ocean Dipole. *Geophysical Research Letters*, *30*(2).

Zubair L, Siriwardhana M, Chandimala J, Yahiya Z. Predictability of Sri Lankan rainfall based on ENSO. International Journal of Climatology. 2008 Jan 1;28(1):91-101.

Develop an equation between pan evaporation and meteorological parameters in sri lanka using regression method

M.R.C.Silva
K.H.M.S. Premalal
Department of Meteorology
Colombo 7

ABSTRACT

The Pan Evaporation is influenced by various Meteorological parameters. The influence of meteorological parameters such as Temperature, Relative Humidity, Wind Speed, Solar Radiation were investigated using data collected from the Department of Meteorology, Sri Lanka. To identify the variation of the pan evaporation over the Sri Lanka, the linear regression method was developed. The developed regression model is given positive influence of Temperature, Wind Speed and negative influence of Relative Humidity. The Maximum Temperature and Wind Speed were the most affected to the Pan Evaporation than the other parameters. More than 50% of Evaporation amount on 80% area of the Dry Zone has given by the Maximum Temperature. Relative Humidity was less affected to the Pan Evaporation and afternoon values of Relative Humidity were more affected than the morning values. The calculated evaporation values obtained from the developed regression model of Sri Lanka matched closely with the observed pan evaporation values.

KEYWORDS: *Correlation, Regression, Minitab14, Pan Evaporation, Meteorological Parameters, Sri Lanka, Zones.*

1. Introduction

The hydrological cycle—the cycling of water in the oceans, atmosphere and biosphere (Chahine.et.al, 1992).The hydrological cycle influences climate in a variety of ways. The exchanges of moisture and heat between the atmosphere and the Earth's surface fundamentally affect the dynamics and thermodynamics of the climate system. In the form of vapour, clouds, liquid, snow and ice, as well as during phase transitions, water plays opposing roles in heating and cooling the environment. Fifty percent of cooling results from evaporation (Chahine.et.al, 1992). The evaporation process represents a major component of the energy and water balance of bare soil and green cover (i.e. forest and farm) ecosystem (Sabziparvar.et.al, 2009). Evaporation is the process whereby liquid water is converted to water vapour (vaporization) and removed from the evaporating surface (vapour removal). Water evaporates from a variety of surfaces, such as lakes, rivers, pavements, soils and wet vegetation (Allen.et.al, 1998).

Evaporation depends on the supply of heat energy and the vapour pressure gradient, which, in turn, depend on meteorological factors such as temperature, wind speed, atmospheric pressure, solar radiation, quality of water and the nature and shape of evaporation surface (e.g. Morton,1968)

(Singh.et.al, 1997).The process of evaporation is influenced by air temperature, relative humidity, wind speed and bright sunshine hours (Jhajharia.et.al, 2006).

Sri Lanka is a tropical country with surrounding small area. Inside the country orographic characters is created different climates. Sri Lankan climate is based on main zones such as Dry, Inter mediate and Wet (Fig: 01). It has been separated considering the total year rainfall. The rainfall amount more than 2500 mm is Wet zone, rainfall amount between 1750 mm and 2500 mm is Inter mediate zone and less than 1750 mm is Dry zone. Within one year there are four types of monsoon patterns also. Those are Northeast, 1st Inter, Southwest and 2nd Inter monsoons. Southwest monsoon is given about 60% of rainfall amount from the total year rainfall amount.

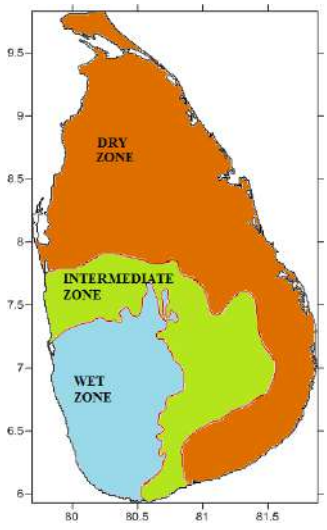

Fig: 01 Main Zones in Sri Lanka

The Evaporation is also different over the country under the different climate conditions. To investigate the distribution of the Evaporation around the country as related to the Meteorological parameters and to develop the evaporation model representing overall country, the regression method was followed.

The regression analysis was also performed to observe the combined effect of all the meteorological parameters on Pan Evaporation (Jhajharia.et.al, 2006). The linear regression method was provided to analyze combine relation with the Meteorological parameters which affect to the Evaporation. Different climates were considered to the model also. The Evaporation obtained with the regression model is compared with the observed evaporation in different climates over the country and the evaporation obtained from regression models where developed to each climates separately. All the

data values were collected from Department of Meteorology, Sri Lanka. It is connected with Meteorological observation network. Both Meteorological and Agro meteorological stations are situated around the Sri Lanka as number of 23 and 40 stations respectively.

2. Methodology

2.1 Data Collection With Respect To the Climate of Sri Lanka

The data values were collected from different areas considering main zones. All the stations were selected as Agro meteorological stations. Jaffna, Mahailluppallama, Puttlum and Vauniya stations were selected for Dry zone. Kurunegala, Kundasale and Bandarawela stations were selected for Intermediate zone. Colombo, Rathnapura and Gannoruwa stations were selected for Wet zones. These main zones are more divided into sub zones considering upper, medium and low levels also.

Climate is the study weather change parameters in a long time period. It is also given time period at a particular period. Sri Lanka is a member of WMO[1]. Then all the standard methods are followed according to the WMO standards. Climate is studied with 30 year average data values. This 30 year range is from 1961 to 1990 or from 1981 to 2010. It is given by according to the WMO standards. Then data values were collected as daily values and year range was selected from 1981 to 2010.

The daily observed pan evaporation varied from 0.1mm to 13.5mm. Maximum Temperature, Relative Humidity and Wind Speed are the Meteorological parameters were collected for the regression model.

2.2 Correlation and Regression Methods for Pan Evaporation and Meteorological Parameters

Correlation is defined as a measure of linear association[2] between two (ordered) lists. Two variables can be strongly correlated without having any casual relationship, and two variables can have a casual relationship and yet be uncorrelated (Stark, 2013).The Correlation Coefficient *r* is a measure of how nearly a scatter plot[3] falls on a straight line. The coefficient range is between +1 and -1. When the coefficient value near either +1 or -1, scatter plot falls to straight line with either acute or obtuse angles respectively (Stark, 2013).

The Linear Regression fits a line to a scatter plot in such a way as to minimize the sum of the squares of the residuals[4] (Stark, 2013).R-squared is a statistical measure of how close the data are to the fitted regression line. It is also known as coefficient of determination (Frost, 2013). Though the regression line can be created with any of data set, sometimes data set might be not fitted with the regression line. Then R-squared is used to identify the data distribution around the regression line. If R-squared is more than 70% the regression line is fitted to the data set.

[1]WMO is called as the World Meteorological Organization.
[2] Two variables are associated if some of the variability of one can be accounted for by the other (Stark, 2013).
[3] A scatter plot is a plot of pairs of measurements on a collection of "individuals" (which need not be people) (Stark, 2013).
[4] The difference between a datum and the value predicted for it by a model (Stark, 2013).

The range of pan evaporation is from 0.1mm to 13.5mm according to the selected overall data set. All the data values have been measured to the decimal point one. Therefore the every each point can have more than one set of the other Meteorological parameters. As example if considered the 0.1mm pan evaporation value, there can be sets of the other Meteorological parameter values inside the overall datasets which has measured pan evaporation as 0.1mm. Then the correlation method should apply for the all values of the pan evaporation with various data sets of other Meteorological parameters. Therefore all data the values have been consists with sets of data values which have different other Meteorological parameters for each evaporation values (Table: 01).

Table 01: Other Meteorological Parameters related to the same Evaporation point.

Evaporation (mm)	Maximum Temperature (ºC)	Relative Humidity (0830h)(%)	Relative Humidity (1530h)(%)	Wind Speed (ms^{-1})
0.1	28.2	96	79	3.0
0.1	27.6	90	96	4.2
0.1	27.8	97	87	1.9
0.1	30.2	91	67	3.4
0.1	23.7	83	76	1.4
0.1	22.8	86	95	3.0
0.1	22.9	92	78	0.0
0.1	23.2	83	91	1.4
0.1	20.0	90	97	0.0
0.1	24.9	99	98	2.7
0.1	29.4	93	97	8.7
0.1	27.1	88	93	1.3
0.1	28.7	81	93	8.7
0.1	25.0	96	91	2.6
0.1	29.0	91	85	0.7
0.1	26.2	97	97	1.2
0.1	27.0	91	97	2.1
0.1	29.0	86	75	0.2
0.1	28.2	84	75	1.2

The data values in every area are different according to the climate. Then every different area needs to have regression method to fit the data values as suitable to each area. The completed Regression equation needs to fit with them.

2.3 Main Steps to Regression Model between Pan Evaporation and Meteorological Parameters

- ✓ The lists of data sets were selected from the year of 1981 to 2010 as 30 year range according to the WMO standards.
- ✓ All the data values were collected from the different area of the Sri Lanka and the areas were selected according to the main Zones.
- ✓ The lists of overall data sets were arranged as area wise separately with fitted Regression lines using Minitab14[5] Software.
- ✓ The lists of overall data sets in the all areas were arranged in to the one file and the file data sets were sorted from small value to maximum value. Then the same pan evaporation value with the different sets of other Meteorological parameters was appeared.
- ✓ The arranged file was consisted without considering area separately and the lists of overall data sets in that file were arranged with fitted Regression line using Minitab14 Software.
- ✓ Obtained Evaporation values from the all Regression equations related to the area were compared with true Pan Evaporation values.
- ✓ Obtained Evaporation values from the Regression equation related to the overall daily data was compared with true Pan Evaporation values.
- ✓ Obtained Evaporation values from both types of equations were compared with each other.
- ✓ For the validation, true data sets were collected as the year which is not in selected range from 1981 to 2010.

3. RESULTS AND DISCUSSION

The results of the investigation on the develop an equation between Pan Evaporation and Meteorological parameters in Sri Lanka using Regression method are as follows:

The statistical values from the Table: 02are calculated by using the Regression method as related to the different places separately. It has given the percentage values of R-squared which can decided the Regression line and the data distribution on that line.

[5] Minitab14 is main software which can do the every statistical analysis using the large number of data sets.

Table 02: Statistical Values from the Regression Method

Maximum Temperature							
Zone	Height	Station	Lat	Lon	S	R-Sq	R-Sq(adj)
DRY	Low	Jaffna	9.41	80.01	1.2799	40.80%	40.70%
	Low	Mahailluppallama	8.12	80.46	1.2543	40.10%	40.10%
	Low	Puttlum	8.03	79.83	1.2248	28.10%	28.10%
	Low	Vauniya	8.75	80.50	0.8875	54.50%	54.40%
INTER MEDIATE	Upper	Bandarawela	6.83	80.98	1.3178	22.80%	22.80%
	Medium	Kundasale	7.26	80.68	1.2937	14.90%	14.90%
	Low	Kurunegala	7.47	80.35	0.8413	46.60%	46.50%
WET	Medium	Gannoruwa	7.25	80.60	1.2087	24.90%	24.80%
	Low	Colombo	6.90	79.86	0.9914	27.80%	27.80%
	Low	Ratnapura	6.68	80.40	1.0066	30.30%	30.30%

Relative Humidity (0830)							
Zone	Height	Station	Lat	Lon	S	R-Sq	R-Sq(adj)
DRY	Low	Jaffna	9.41	80.01	1.4291	26.10%	26.10%
	Low	Mahailluppallama	8.12	80.46	1.2877	36.90%	36.90%
	Low	Puttlum	8.03	79.83	1.1851	32.70%	32.70%
	Low	Vauniya	8.75	80.50	0.8488	58.40%	58.30%
INTER MEDIATE	Upper	Bandarawela	6.83	80.98	1.3085	23.90%	23.90%
	Medium	Kundasale	7.26	80.68	1.3237	10.90%	10.90%
	Low	Kurunegala	7.47	80.35	0.9894	26.10%	26.10%
WET	Medium	Gannoruwa	7.25	80.60	1.1312	34.20%	34.20%
	Low	Colombo	6.90	79.86	1.0219	23.30%	23.20%
	Low	Ratnapura	6.68	80.40	1.1481	9.30%	9.30%

Relative Humidity (1530)							
Zone	Height	Station	Lat	Lon	S	R-Sq	R-Sq(adj)
DRY	Low	Jaffna	9.41	80.01	1.5015	18.50%	18.50%
	Low	Mahailluppallama	8.12	80.46	1.3511	30.50%	30.50%
	Low	Puttlum	8.03	79.83	1.3324	14.90%	14.90%
	Low	Vauniya	8.75	80.50	0.9334	49.70%	49.60%
INTER MEDIATE	Upper	Bandarawela	6.83	80.98	1.2936	25.60%	25.60%
	Medium	Kundasale	7.26	80.68	1.3051	13.40%	13.40%
	Low	Kurunegala	7.47	80.35	0.8395	46.80%	46.80%
WET	Medium	Gannoruwa	7.25	80.60	1.0036	48.20%	48.20%
	Low	Colombo	6.90	79.86	1.0235	23.00%	23.00%
	Low	Ratnapura	6.68	80.40	0.9865	33.10%	33.00%

Wind Speed							
Zone	Height	Station	Lat	Lon	S	R-Sq	R-Sq(adj)
DRY	Low	Jaffna	9.41	80.01	1.2259	45.70%	45.60%
	Low	Mahailluppallama	8.12	80.46	1.3827	27.20%	27.20%
	Low	Puttlum	8.03	79.83	1.2461	25.60%	25.50%
	Low	Vauniya	8.75	80.50	0.9876	43.70%	43.60%
INTER MEDIATE	Upper	Bandarawela	6.83	80.98	1.4261	9.60%	9.60%
	Medium	Kundasale	7.26	80.68	1.3897	1.80%	1.80%
	Low	Kurunegala	7.47	80.35	1.1408	1.70%	1.70%
WET	Medium	Gannoruwa	7.25	80.60	1.3003	13.00%	13.00%
	Low	Colombo	6.90	79.86	1.1086	9.70%	9.70%
	Low	Ratnapura	6.68	80.40	1.1943	1.90%	1.80%

The Maximum temperature in dry zone was more affected to the Pan Evaporation. More than 50% of Evaporation amount on 80% area of the Dry Zone has given by the Maximum Temperature (Fig: 02) and It has given a positive influence for the Pan Evaporation regression model. The highest R-Squared value was represented in Vauniya. It is dry area where received the total year rainfall amount less than 1750mm amount. It has good daily sunshine and high maximum temperature values. The Intermediate and Wet zones are given less percentage for R-Squared values. Both zones have less maximum temperature than to the dry zone. Then it was affected to the pan evaporation with fewer amounts. The result shows that the maximum temperature in dry zone more affected to the pan evaporation than the other zones.

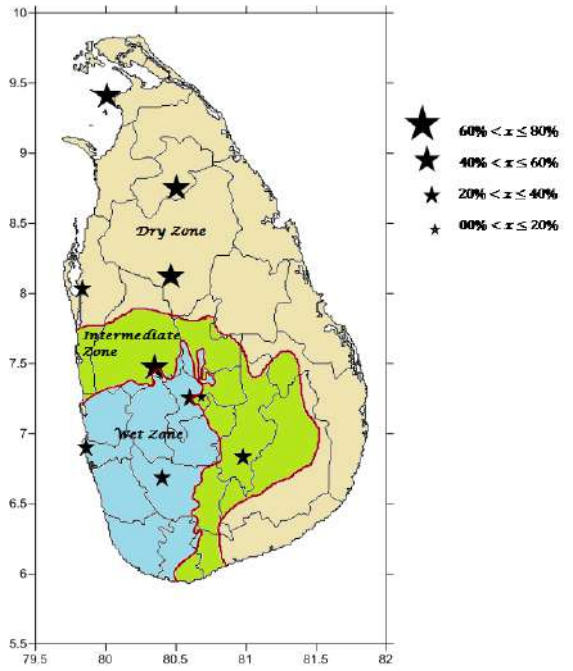

Fig 02: *R-Squared value for Maximum Temperature*

Relative Humidity describes the vapour amount around the atmosphere and less vapouring the atmosphere increase the Evaporation process. In dry area due to the high temperature values the surround atmosphere vapour content is less than the other areas. Then dry area relative humidity is less and it was affected to the pan evaporation more. The relative humidity was given negative influence with the regression model. It is because when relative humidity is high, surround vapour amount also high and it was given less affect to the pan evaporation. Therefore relative humidity is inversely proportional to the pan evaporation. Other intermediate and wet zones have much vapour content around the atmosphere. Then relative humidity high and it was less affected to the pan evaporation than the dry zone.

Relative Humidity considered as morning and afternoon values. In the morning, vapour amount of surround atmosphere is high. Morning vapour amount is decreased with the sun rise. Sunshine heat the atmosphere and vapour amount decrease. Then evaporation process needs to fill the lost vapour amount and evaporation increase. Therefore afternoon values of Relative Humidity (Fig: 03) were more affected than the morning values (Fig: 04). It's because morning relative humidity was given high values than the afternoon values. Both were given negative influence for the model of Pan Evaporation. Vauniya was represented the highest R-Squared value to the both morning and afternoon relative humidity values with regression model. Wet zone was less affected to the pan evaporation than the other zone. Then result shows the relative humidity more affected to the regression model in dry area than the other area.

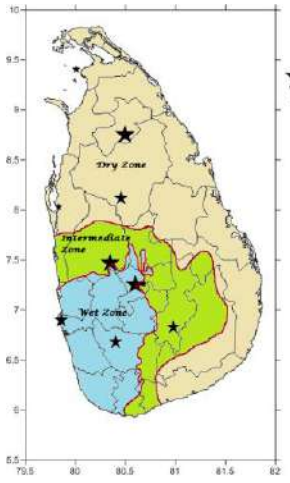

Fig03: R-Squared value for Relative Humidity (1530h)

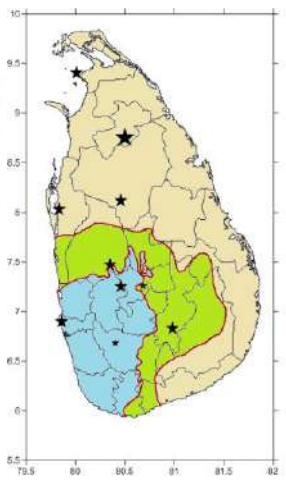

Fig04: R-Squared value for Relative Humidity (0830h)

Wind can increase the evaporation process by moving the vapour amount of above the water surface. Then more wind can affect to the pan evaporation more. Wind measured as wind speed to find the regression with the pan evaporation. Wind Speed has also given positive influence. Statistical values were given high R-Squared percentage in Dry zone. Other intermediate and wet zones were less affected to the pan evaporation due to the surround wind is less than the dry areas. Low height dry area is possible for more wind flow and wet and intermediate zone are consist with hills. Due to the orography around the Sri Lanka wind is more flows around the dry zone. Then the result shows Wind Speed most affected to the Pan Evaporation in Dry Zones than the other areas and percentage value of R-Squared was represented in Fig: 05. Jaffna was given highest percentage value and in that area wind was more influenced to the pan evaporation.

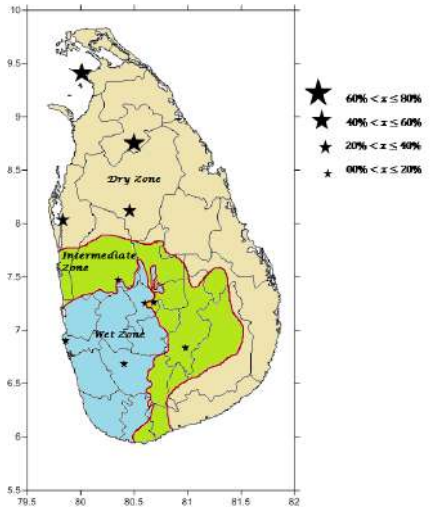

Fig05: R-Squared value for Wind Speed.

3.1 Combine Linear Regression for All Meteorological Parameters

All the considered Meteorological parameters have correlated together (Table: 03). Those parameters have given linear relation to the Pan Evaporation. The Maximum R-squared percentage value has given in Dry Zone and the considered Meteorological parameters have correlated to the Pan evaporation more than 50%area around in the Sri Lanka (Fig: 06).

Table 03: *The Combine Linear Regression for All Meteorological Parameters*

Zone	Height	Station	Lat	Lon	S	All R-Sq	R-Sq(adj)
DRY	Low	Jaffna	9.41	80.01	0.8367	74.70%	74.70%
	Low	Mahailluppallama	8.12	80.46	1.0190	60.50%	60.50%
	Low	Puttlum	8.03	79.83	0.9209	59.40%	59.30%
	Low	Vauniya	8.75	80.50	0.6051	78.90%	78.80%
INTER MEDIATE	Upper	Bandarawela	6.83	80.98	1.1889	37.20%	37.20%
	Medium	Kundasale	7.26	80.68	1.2225	24.10%	24.00%
	Low	Kurunegala	7.47	80.35	0.7433	58.30%	58.30%
WET	Medium	Gannoruwa	7.25	80.60	0.8440	63.40%	63.40%
	Low	Colombo	6.90	79.86	0.8972	40.90%	40.80%
	Low	Ratnapura	6.68	80.40	0.8951	44.90%	44.90%

The results from separated regression methods for other meteorological parameters which affected to the pan evaporation were given high percentage values for dry zone. Then high R-Squared value was also given for combine regression method in dry zone. Other areas such as intermediate and wet zones weren't given much result for other meteorological parameters related to the pan evaporation. It's because in that area evaporation is less than the dry area. In that case high evaporation values were represented the various data sets as identify the parameters specifically and in order to find the good regression model.

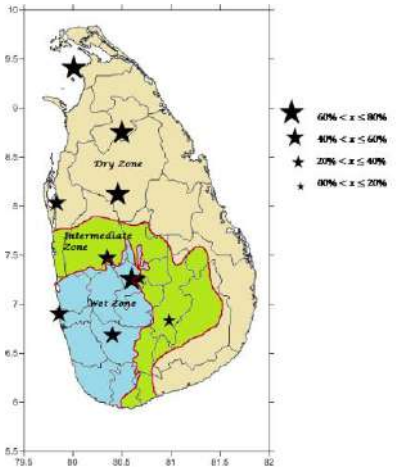

Fig***: 06***R-Squared value for the overall Meteorological Parameters

In order to observe combined effect of Meteorological parameters on the Pan Evaporation, a multiple linear regression model was developed.

The lists of overall data have taken from 1981 to 2010 as 30 year range according to the WMO standard. The Regression method was applied for all data values considering all parameters. And all the Meteorological parameters were considered separately using Regression method with the Pan Evaporation. The developed Regression model of Pan Evaporation (with R-squared 51.7% value) in overall area around Sri Lanka is, $E_{pan} = 4.10 + (0.128 \times T_{max}) - (0.0426 \times RH_{0830}) - (0.0269 \times RH_{1530}) + (0.157 \times WS)$, where T_{max} is the Maximum Temperature, RH_{0830} is Relative Humidity at 0830h, RH_{0830} is Relative Humidity at 1530h and WS is wind speed.

The Regression method was applied for all data in order to find the linear Regression models indifferent areas around the Sri Lanka (Table: 04) as area Regression models.

Table 04: The Regression Models in Different Areas

Station	Regression Model
Jaffna	Evap = - 2.04 + 0.306 Tmax - 0.0253 RH0830 - 0.0421 RH1530 + 0.202 WS
Mahailluppallama	Evap = - 2.69 + 0.281 Tmax - 0.0219 RH0830 - 0.0244 RH1530 + 0.146 WS
Puttlum	Evap = - 2.73 + 0.369 Tmax - 0.0533 RH0830 - 0.0221 RH1530 + 0.165 WS
Vauniya	Evap = - 0.787 + 0.206 Tmax - 0.0219 RH0830 - 0.0304 RH1530 + 0.236 WS
Bandarawela	Evap = 1.12 + 0.187 Tmax - 0.0200 RH0830 - 0.0264 RH1530 + 0.102 WS
Kundasale	Evap = 0.110 + 0.212 Tmax - 0.0289 RH0830 - 0.0183 RH1530 + 0.0782 WS
Kurunegala	Evap = - 0.845 + 0.230 Tmax - 0.0223 RH0830 - 0.0280 RH1530 + 0.146 WS
Gannoruwa	Evap = 2.07 + 0.211 Tmax - 0.0343 RH0830 - 0.0387 RH1530 + 0.155 WS
Colombo	Evap = - 2.18 + 0.316 Tmax - 0.0331 RH0830 - 0.0265 RH1530 + 0.112 WS
Ratnapura	Evap=- 2.52 + 0.248Tmax - 0.0143RH0830 - 0.0277RH1530 + 0.116WS

All the regression models related to the different areas were shown the positive influence of maximum temperature, wind speed and negative influence of relative humidity.

The Meteorological Data of years which are not included in selected range were validated separately considering area regression models (Table: 04). The obtained Evaporation values from those models were compared with the observed Evaporation values (Fig: 07).The linear equation (R-Squared 62.4%) was obtained during the validation is, $Y = 0.679X + 1.22$; where, Y is Evaporation obtained from the area regression models and X is observed Pan Evaporation. Also as main validation, the obtained Evaporation values from the developed regression model were compared with the observed Pan Evaporation values (Fig: 08). The linear equation (R-Squared 58.4%) was obtained during the validation is, $Y = 0.565X + 1.60$; where, Y is the Pan Evaporation obtained from the Developed Regression Model and X is observed Pan Evaporation.

Finally, both obtained data values in different methods were compared with each other in order to find the one model for every climate condition around the Sri Lanka. The R-squared value was given

as 90.2%. Then both Regression methods were closely matched with together. Therefore combined Regression model can be used to calculate the Evaporation.

Thus, the Developed Regression Model can be used to predict the Pan Evaporation in absence of Pan Evaporation around the different areas in Sri Lanka.

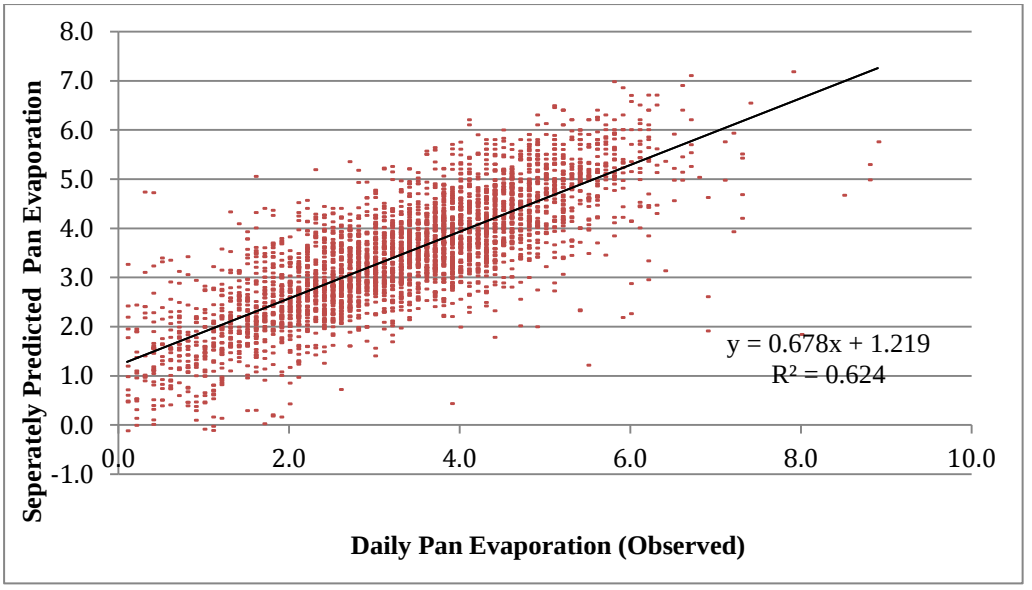

Fig 07: *Comparison between Observed (mm) and Predicted Evaporation (mm) related to the different area.*

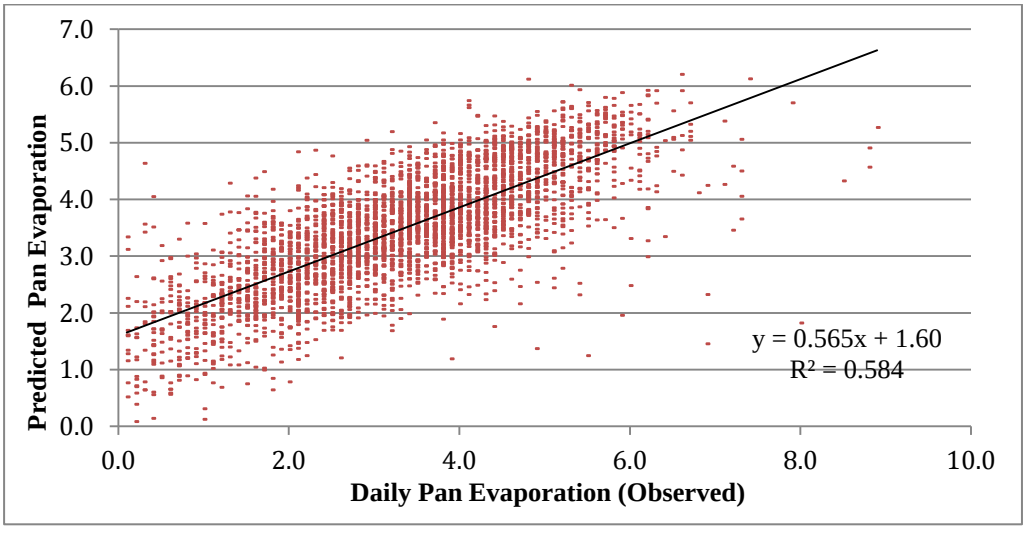

Fig 08: *Comparison between Observed (mm) and Predicted Evaporation (mm) related to the one model.*

4. Conclusions

Effect of considered Meteorological parameters on Pan Evaporation was studied according to the different area in main Zones around the Sri Lanka. The overall area around the Sri Lanka was studied in order to find the total linear regression model on Pan Evaporation. The considered Meteorological parameters were Maximum Temperature, Relative Humidity (0830h and 1530h) and Wind Speed.

The important conclusions of this study as follows;

1. The Maximum Temperature and Wind speed were given a positive influence for the Pan Evaporation. The Relative Humidity was given a negative influence for the Pan Evaporation.
2. The Pan Evaporation was mainly affected with the combine relation of Maximum Temperature, Relative Humidity and Wind speed. Then Regression model was developed with the considered Meteorological Parameters.
3. The developed Pan Evaporation model for overall area in the Sri Lanka is given as, $E_{pan} = 4.10 + (0.128 \times T_{max}) - (0.0426 \times RH_{0830}) - (0.0269 \times RH_{1530}) + (0.157 \times WS)$
4. Dry Zone Evaporation values were most closed to the linear Regression model more than the other Zone.
5. The developed Regression model's evaporation values matched very closely with the observed Pan Evaporation values around the Sri Lanka in any area of the Country.

5. Acknowledgement

Author is thankful to the Mr.Mahipala (Officer in Charge at the Agro meteorological Division of the Department of Meteorology) for his support during the research study.

REFERENCES

Allen, R.G., Pereira, L.S., Raes, D. and Smith, M., 1998. Crop evapotranspiration-Guidelines for computing crop water requirements-FAO Irrigation and drainage paper 56. *Fao, Rome*, *300*(9), p.D05109.

Chahine, M.T., 1992. The hydrological cycle and its influence on climate. *Nature*, *359*(6394), p.373.
Frost, J., 2013. Regression analysis: How do I interpret R-squared and assess the goodness-of-fit. *The Minitab Blog*, *30*.

Jhajharia, D., 2006. Correlation between pan evaporation and meteorological parameters under the climatic conditions of Jorhat (Assam). *J. Indian Water Resour. Soc. Vol*, *26*(1-2).

Stark, P.B., 2004. SticiGui: statistics tools for internet and classroom instruction with a graphic user interface. *Available at Web site: http://stat-www. berkeley. edu/users/stark/SticiGui/index. htm (8 August 2004)*.

Tabari, H., Marofi, S. and Sabziparvar, A.A., 2010. Estimation of daily pan evaporation using artificial neural network and multivariate non-linear regression. *Irrigation Science*, *28*(5), pp.399-406.

Xu, C.Y. and Singh, V.P., 1998. Dependence of evaporation on meteorological variables at different time-scales and inter-comparison of estimation methods. *Hydrological processes*, *12*(3), pp.429-442.

Two Dimensional Sea Breeze & Land Breeze Model with Application to Sri Lanka

H.A.G. Dharmappriya
Department of Meteorology
Colombo 7

ABSTRACT

Two dimensional sea breeze & land breeze model describes a combined observational and theoretical study of sea breeze & land breeze over Sri Lanka. The structure of the sea breeze circulation and its variations in time were obtained from observations. The observational data were gathered with surface stations, pilot balloons and radar radiosonde stations.

Over the land the depth of the layer of sea breeze flow is approximately 1500 m and velocity of 8 knots (4 ms^{-1}) is observed with 34 km inland penetration. Well defined sea breeze current is apparent early afternoon and dies away in the evening.

The wind model for simulating the wind flow in two dimensional spaces is described. The model predicts winds at different levels, in terrain following σ coordinate. Physical processes such as horizontal diffusion, diurnal heating and cooling are incorporated.

The empirical constants associated with the physical effect terms in the horizontal momentum equations and thermodynamic equation of the wind model is properly calibrated. Calibrated model is applied to Sri Lanka under the inter monsoon condition in order to check the performance of the model. The use of computer and the fraction of time required to run the program are the principal advantages of this model.

A two dimensional, time dependent, primitive equation model was constructed to simulate the observed sea breeze. The numerical simulation is reasonably realistic; however the sea breeze intensity and the inland penetration were under estimated.

1. Introduction

The sea breeze and land breeze are important in determining the local climatology. These affect both cloud amount and moisture evaporation in and around the island. It may be important in influencing the water circulations especially in the near sea shore water. The sea around the around exerts a strong influence on local and large scale atmospheric behavior in the island. The wind field plays a major role in weather over Sri Lanka. The steady wind flow, termed as monsoons, is characterized by southwest and northeast wind regimes in the annual march of seasons. Topography of island modifies these winds flows both in speed and direction. In complex terrain, the wind varies significantly over short distances. Therefore wind turbines are cited in the region of complex terrain. Dixit and Nicholson (1964) at Bombay (19N) did observe a reversed flow above the sea breeze. In the latter case the sea breeze return current is still clearly evident at heights exceeding 3000m. The interpretation of these results is more complicated at the above locations where local mountain wind

systems occur. In mid latitudes horizontal velocities in the sea breeze have maximum values of about $10ms^{-1}$ (17.44 knots) as observed at level below 300m (Fisher, 1960; Frizzola and Fisher 1963) and inland penetration is 30 – 50km (Fisher, 1960; Wallington, 1963, 1965).

This study describes the results of combined observational and theoretical study of land and sea breezes and related diurnal variations. These events were observed to be dominant during the inter-monsoon periods where the prevailing wind tends to be calm and having no definite direction. The model predicts the wind fields at the anemometer level along a cross section over the interested area. This type of model was previously introduced by Estoque M.A. (1972) to simulate Lake Breeze over southern Lake Ontario, Canada. Similar type of model was utilized by Dr. Basnayaka B.R.S.B (1994) to calibrate a single-level meso-scale wind model, which was applied for Sri Lanka area. Physical processes such as frictional drag, horizontal diffusion, slope wind, diurnal heating and cooling and upper air forcing were incorporated in the model.

The objective of the analysis of synoptic situation over Sri Lanka area is to determine the diurnal variations of the lower atmosphere throughout a day in an inter-monsoon season. This was done by analyzing observational data, which were gathered by a special observational network.

The objective of the theoretical part of the study is to simulate the results of the observational analysis with a numerical model. The model is a two dimensional, time dependent and primitive equation. It is hoped to calibrate the numerical model in order to use as a forecasting tool in day to-day weather forecasting.

2. Data and Methodology

a. Observational Data

The particular sea and land breeze which was studied in this project occurred during the 2^{nd} inter monsoon period [Oct-Nov) in 1999. In this study the relative humidity was also determined at the anemometer level because it was felt to determined sea breeze boundaries. Wind analysis using wind charts, convergence or divergence is well recognized. The sea and land breeze circulations and their variation with time were obtained from the observations. Observational data were used to calibrate the numerical model with observational data and again to verify with an independent set of data for improvements. More dense of observation network was chosen and more frequently (hourly) observations were taken to identify the behavior of the thermally induced phenomena such as land and sea breezes, slope winds (katabatic and anabatic winds).

The observational data program consists of meteorological and agrometeorological stations and special observational posts. Each meteorological station is occupied with the instruments for measuring pressure, wind, temperature, humidity and rainfall. Each agrometeorological stations is

occupied with the instruments for measuring wind, temperature, humidity, radiation, evaporation and rainfall; especial observation posts were occupied with anemometer and wind vane. The map of observational stations is shown in fig 2.1.

Meteorological observations are obtained from department of meteorology where routine observations are made 3 hourly. For observing the condition of the atmosphere above surface, meteorological department is released radiosonde balloons from Colombo station to measure the vertical distribution of temperature, humidity, pressure and winds and pilot balloons are done at Colombo, Puttalam, Trincomalee and Hambantota to measure the vertical distribution of wind speed and direction.

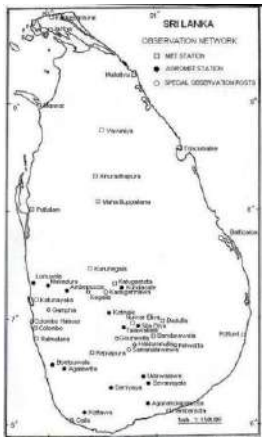

FIG 2.1 Observational stations

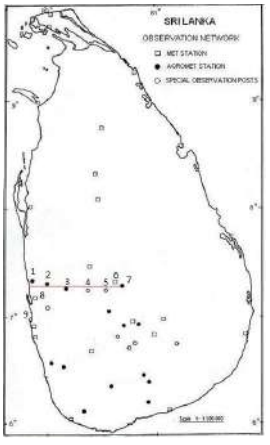

FIG 2.2 selected stations

Observational data were collected at sites between Lunuwila and Galle on the western shore of Island. The selecting of stations was done in order to get the strongest gradients and test the two dimensions of phenomena by assessing variations along a direction. It was horizontal line; parallel to earth surface. Selected stations in my study are shown in fig 2.2. It may be seen that the stations extend from shoreline to 113 km inland. The area of observations is rural in character; the countryside characterized by coconut estates, farmed and wooded sections. The terrain rise elevation as one goes inland from the shoreline. The major feature of this rise is an abrupt increasing in elevation associated with one ridge; it is located at about 60km from the coast.

Colombo and Katunayaka where hourly special observational data were taken and agro-meteorological stations, Ambepussa, Kundasale, Lunuwila and Makandura were included to enhance this project. In addition, wind data were taken from the pilot station at Colombo harbor. Wind data from special observation centers were collected in areas of Kegalle, kadugannawa, especially to study the inland penetration of sea breeze, location and magnitude of sea breeze wind maxima, magnitude of Anabatic/katabatic wind etc.

Hourly wind and temperature data for 16 days were collected during the inter monsoon periods within span of one year. Experimental period was selected as inter monsoon periods which were fallen October, November in the year 1999 and March, April and two weeks May in the year 2000.

(A) Observational data

October	1999	07th	14th	21st	28th
November	1999	04th	11th	18th	25th
March	2000	21st	27th	31st	-
April	2000	03rd	06th	25th	-
May	2000	04th	10th	-	-

Data were taken from Department of Meteorology and Dr. Senaka Basnayaka. Hourly data were collected on the above dates from 0600hrs to following day 0600 hrs. Radar and Radiosonde data for upper winds and vertical temperature of atmosphere and pilot balloon data for upper winds were obtained from Department of Meteorology.

b. Model Description

The model is a two dimensional primitive equation model which was previously described by Estoque, Gross and Lai (1976). It is a predictive model. The predictive model (surface wind model) predicts the surface winds at the anemometer level over the interested area.

2.2.1 Surface wind model

The model is used the horizontal coordinates x, y and terrain elevations indicating sigma coordinates as vertical coordinates (z).

The sigma is defined as,

$$\sigma = \frac{Z - h}{H - h}$$

Where, Z and h are the height of a point and the height of the terrain above the sea respectively while H is the height of the upper boundary of the model domain. The value of H is arbitrarily chosen to be sufficiently large so that the effects of the sea breeze are negligible.

The equations are formulated for a vertical plane along x direction (west to east direction) using a coordinate system, x, y, σ; σ varies from $\sigma = 0$ (surface) to $\sigma = 1$ (top of the model domain).

The principal dependent variables are,

u wind component along the selected line (x direction)

v wind component normal to the selected line (y direction)

θ Potential temperature

$\dot{\sigma}$ vertical velocity in the transformed coordinate

p pressure

The first three variables are predicted by means of the following equations and the horizontal momentum equations along x and y can be written as,

$$\frac{\partial u}{\partial t} = -u\frac{\partial u}{\partial x} - \dot{\sigma}\frac{\partial u}{\partial \sigma} + fv - \theta\frac{\partial \emptyset}{\partial x} - g(1-\sigma)\frac{\partial h}{\partial x} + \frac{1}{(H-h)^2}\frac{\partial}{\partial \sigma}\left(K_z\frac{\partial u}{\partial \sigma}\right)\ 8 + Kz\left[\frac{\partial^2 u}{\partial x^2} - \frac{1-\sigma}{H-h}\left(\frac{\partial^2 u}{\partial \sigma \partial x}\right) - \frac{\partial h}{\partial x}\right] \quad (4.1)$$

$$\frac{\partial v}{\partial t} = -u\frac{\partial v}{\partial x} - \dot{\sigma}\frac{\partial v}{\partial \sigma} + f(u_g - u) + \frac{1}{(H-h)^2}\frac{\partial}{\partial \sigma}\left(Kz\frac{\partial v}{\partial \sigma}\right) + Kx\left[\frac{\partial^2 v}{\partial x^2} - \frac{1-\sigma}{H-h}\left(\frac{\partial^2 v}{\partial \sigma \partial x}\right) - \frac{\partial h}{\partial x}\right] \quad (4.2)$$

Thermodynamic equation,

$$\frac{\partial \theta}{\partial t} = -u\frac{\partial \theta}{\partial x} - \dot{\sigma}\frac{\partial \theta}{\partial \sigma} + \frac{1}{(H-h)^2}\frac{\partial}{\partial \sigma}\left(Kz\frac{\partial \theta}{\partial \sigma}\right) + Kx\left[\frac{\partial^2 \theta}{\partial x^2} - \frac{1-\sigma}{H-h}\left(\frac{\partial^2 \theta}{\partial \sigma \partial x}\right) - \frac{\partial h}{\partial x}\right] + \frac{\partial \theta}{\partial t} \quad (4.4)$$

Where, f and g are Coriolis parameter and gravitational acceleration and K_x and K_Z are horizontal diffusivity along x direction and Vertical diffusivity along z direction respectively while $\emptyset$ is Exner function.

$\emptyset$ is defined as,

$$\emptyset = -c_p\left(\frac{p}{p_o}\right)^k \quad , \quad k = R/c_p$$

Where C_P and P are specific heat capacity at constant pressure and pressure at any level and P_o and R are pressure at surface and gas constant for dry air, respectively.

Hydrostatic equation is in σ coordinate system,

$$\frac{\partial \emptyset}{\partial \sigma} = -\frac{g}{\theta}(H-h) \quad (4.4)$$

The pressure is computed by integrating the hydrostatic equation along the vertical.

Here,

$$\dot{\sigma} = \frac{[w - u(\partial h/\partial x)(1-\sigma)]}{(H-h)}$$

And $\dot{\sigma}$ is a measure of vertical velocity. $\dot{\sigma}$ implies the following contribution at the lower and upper boundaries.

$$z = h \; or \; \sigma = 0 \quad \dot{\sigma} = 0 \; or \; w = u \frac{\partial h}{\partial x}$$
$$z = H \; or \; \sigma = 1 \quad \dot{\sigma} = 0 \; or \; w = 0$$

The vertical velocity σ is computed from the horizontal wind component u and the density ρ, of the standard atmosphere, by using the equation continuity,

$$\frac{\partial \rho \dot{\sigma}}{\partial \sigma} = \frac{\partial \rho u}{\partial x} \qquad (4.5)$$

3. Results and Discussion

3.1 Observed behaviors & Structure

An analysis of sea breeze flow patterns over the land is presented using data obtained on 07th October 1999.It was the most justify day for the sea breeze when the wind fields for 07th October are presented as typical of the sea breeze rather than those of other seven days.

Before presenting the results of the analysis, .first I will describe the synoptic conditions which prevailed on 7th October 1999. Maps on this day for which observations are presented are shown in fig 3.1, fig 3.2 and fig 3.3 - 3.6 for the region of interest. In both weather maps fig 3.1 low pressure area at sea level was over Arabian Sea and was weak pressure gradient result in light winds and confirms the introduction. At 1200SLST Inter Tropical Converge Zone (ITCZ) developed northern sea of Sri Lanka and southern part of India. In fig 3.2 at 1800SLST an anticyclone condition over Bay of Bengal and cyclonic condition over Arabian Sea were at 850hpa (1500m above

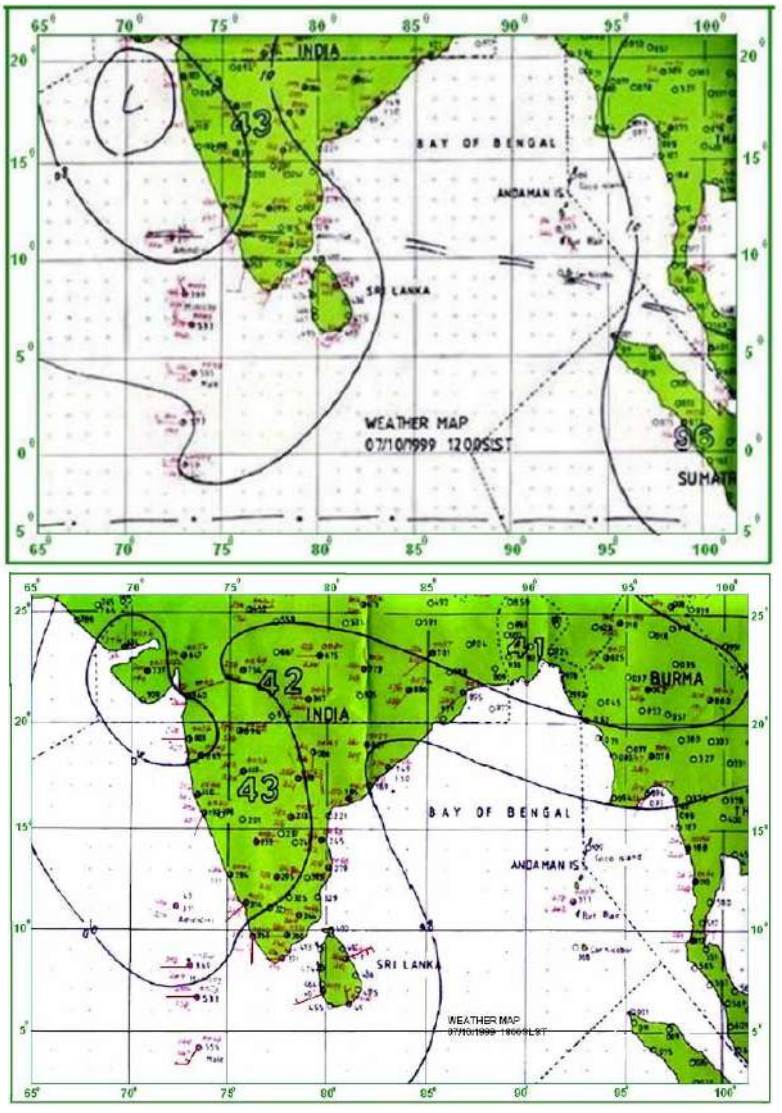

FIG 3.1 Meteorological Department Daily Weather Maps for 7 October 1999 show the sea level pressure contours at 1200 SLST and 1800 SLST

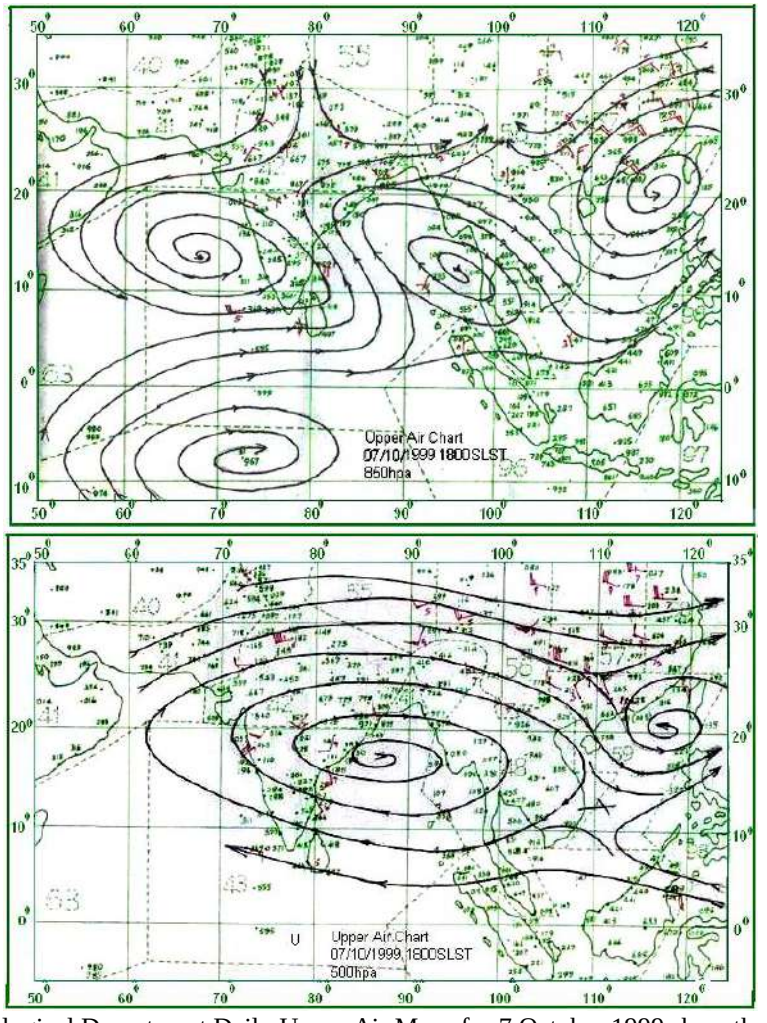

FIG 3.2 Meteorological Department Daily Upper Air Maps for 7 October 1999 show the height contours for 850hpa 500hpa at 1800 SLST

sea level) level and winds were from sea to land.Pressure gradient over the land (fig 3.3, 3.4, 3.5, 3.6) were weak. In fig 3.3 and fig 3.4 near the cost on-shore wind set at late morning and rose to maximum early afternoon then died in the evening. In fig 3.2 at high levels (500mb ≈ 5500m) winds were from land to sea. This is favorable for sea breeze occurrence, prevailed for the next few days.

In fig 3.5 thunderstorms did occur over down slope of hills in the afternoon and interaction of the sea breeze. If air over the land is moist and unstable, thunderstorms may even develop after the onset of sea breeze. Middle layer of troposphere, at 500hpa winds were light and decreasing. It was favorable for good convection.

In fig 3.7 at the different surface stations located close to the line which was selected for theoretical study at various distances inland. At Katunayaka (station No.8) 4km inland from the shore, air

temperature increased rapidly after dawn until 100hrs.Between 1000hrs and 1100hrs a sharp drop of temperature occurred as a result of onset of sea breeze. After 1100hrs the dry bulb temperature felt irregular until 1600hrs when afternoon radiation cooling results in a rapid decrease. At Makadura (station No. 2) dry bulb temperature continued to increase until onset of sea breeze between 1100hrs and 1200hrs at 15km. Thereafter, surface dry bulb temperature changed little until the effect of radiation cooling became significant. At katugastota (station No 6) 87km inland air temperature was normal diurnal variation undisturbed by sea breeze.

Both surface temperature and relative humidity for 07th October from 6.00am to following day 6.00am were plotted in fig 3.8 for several stations located from the shore line at various distances inland. The effect of the sea breeze could be seen conveniently from the different graphs by comparing each one of them with corresponding graph from station No 6. This station was unaffected by the sea breeze; therefore, the temperature and the relative humidity variation at this station represents normal diurnal variations. It is noted that the passage of the leading edge of the sea breeze (sea breeze front) is indicated by a near simulations decrease in temperature and increase in the relative humidity. The decrease in temperature is slight (a few degree) while the increase in relative humidity is relatively large.

At station No 8, about 4km from the shore, the increase in relative humidity is about 8%. It is noted in table 3.1 between 1000hrs and 1100hrs. The traces show that a distinct increase of relative humidity occurred with the sea breeze front crossed the station No 8 at about 1000SLST and at station No 2, 15km inland slight increase of relative humidity was noted between 1000hrs and 1100hrs during the period when the sea breeze front could be expected to pass this station and reached the station No 3, 34km inland at about 1200SLST. The average rate of movement corresponding to these times is about 8knots (4 ms^{-1}) that the sea breeze penetrated as far as station No 3.

Short distance from the sea shore to the inland after passage of the sea breeze front the significantly small increase of the relative humidity indicates that vertical mixing of drier air from aloft has occurred. It also suggests that moisture transport upward from the sea surface. It has been limited to shallow layer at the surface in a short trajectory of air over the water (Bellaire 1965).

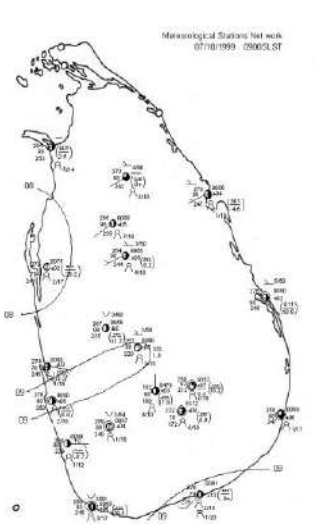

FIG 3.3

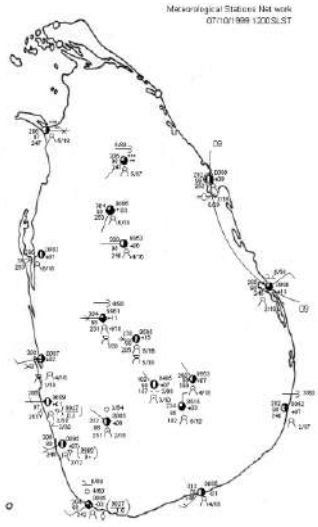

FIG 3.4

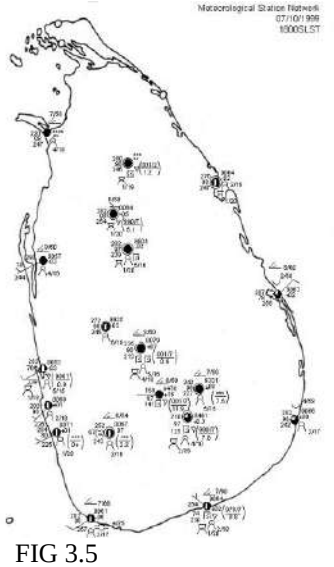

FIG 3.5

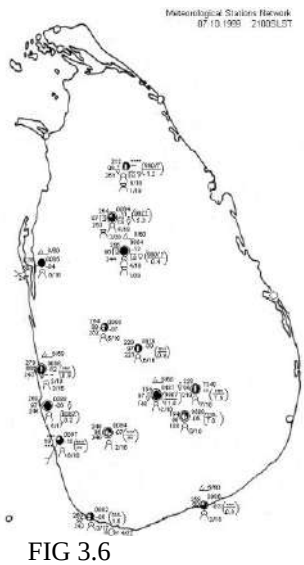

FIG 3.6

Some of the general characteristics of the sea breeze at the surface are shown n fig 3.7 and fig 3.8.

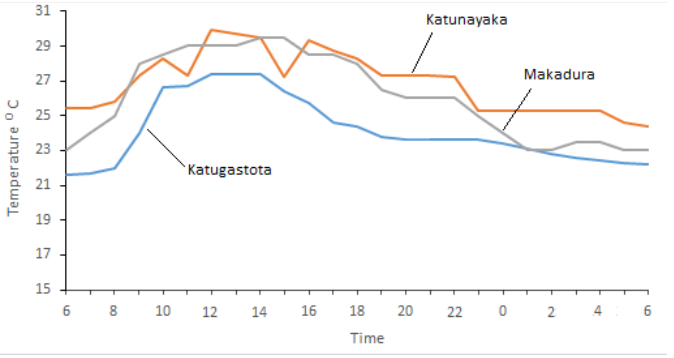

FIG 3.7 surface dry bulb temperature (^{0}C) at various distances inland from sea shore, 07 October 1999

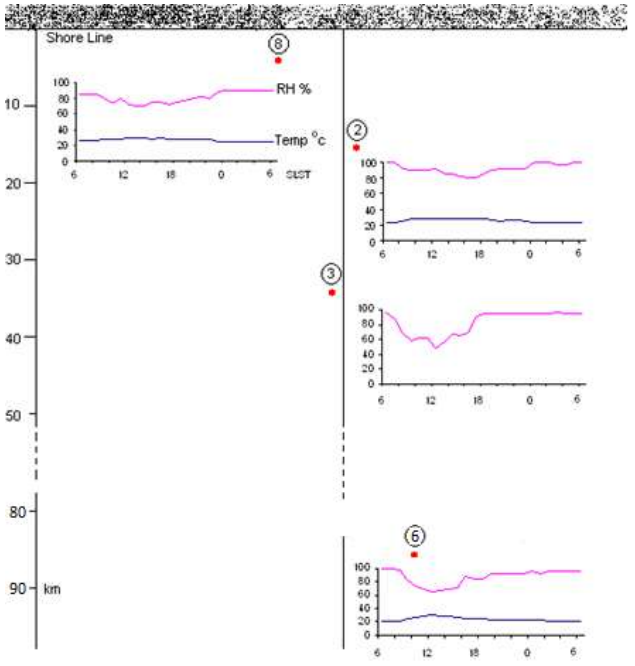

FIG 3.8 Temperature and relative humidity traces at the surface station

Table 3.1 temperature in ^{0}C and Relative Humidity in % at various distances inland from the shore line 07 October 1999.

	Katunayaka 4km inland		Makadura 15km inland		Ambepussa 34km inland	
	Temp	RH	Temp	RH	Temp	RH
6.00	25.4	87	23.0	100	-	96
7.00	25.4	87	24.0	100	-	87
8.00	25.8	85	25.0	92	-	69
9.00	27.3	80	28.0	93	-	59
10.00	28.3	74	28.5	89	-	61
11.00	27.5	82	29.0	89	-	61
12.00	29.9	73	28.1	92	-	49
13.00	29.7	71	29.0	86	-	57
14.00	29.5	71	29.5	86	-	67
15.00	27.2	77	29.5	82	-	66
16.00	29.3	75	28.5	79	-	70
17.00	28.7	73	28.5	79	-	91
18.00	28.3	76	28.0	85	-	94
19.00	27.3	78	26.5	89	-	95
20.00	27.3	82	26.0	92	-	95
21.00	27.3	83	26.0	92	-	95
22.00	27.2	81	26.0	92	-	96
23.00	25.3	89	25.0	92	-	95
0.00	25.3	91	24.0	100	-	95
1.00	25.3	91	23.0	100	-	95
2.00	25.3	91	23.0	100	-	95
3.00	25.3	91	23.5	96	-	96
4.00	25.3	91	23.5	96	-	95
5.00	24.6	91	23.0	100	-	94
6.00	24.4	91	22.0	100	-	93

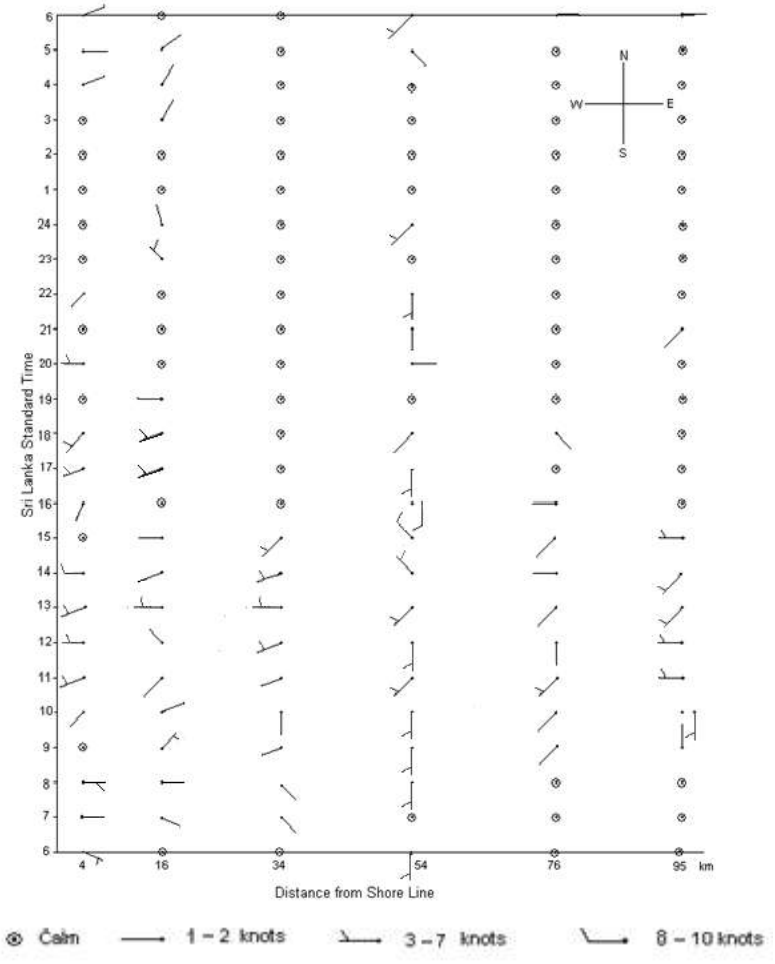

FIG 3.9 the horizontal – time cross section wind

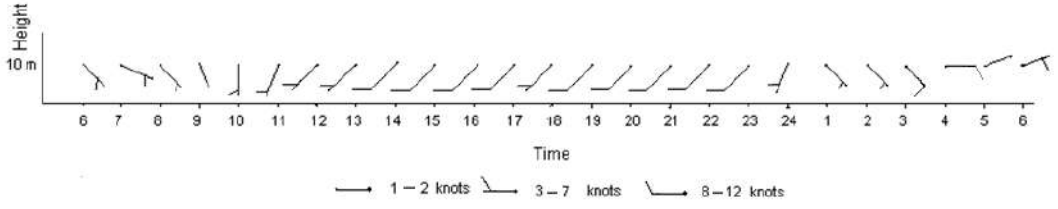

FIG 3.10 surface wind at Colombo pilot station on 07.10.1999

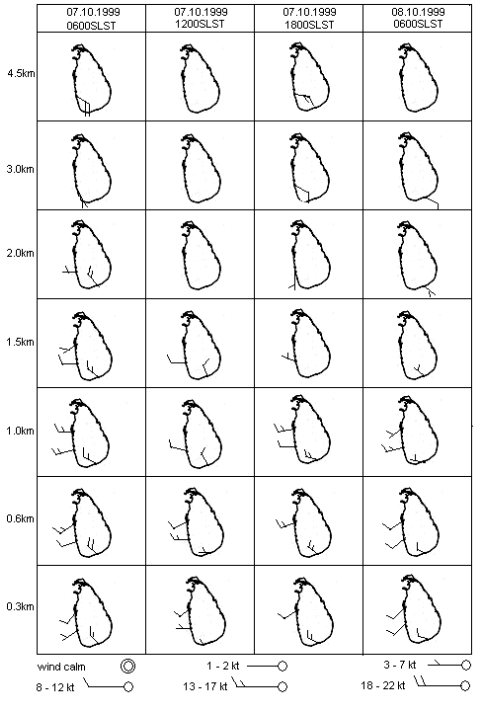

FIG 3.11 Upper winds over Sri Lanka

The surface winds diagram fig 3.9, over the station 1, 4km from the shore the wind direction was shifted from easterly to southwesterly. At Katunayaka 4km, and Ratmalana 6km from the shore line the wind direction was easterly and Colombo 7km wind was calm (see fig 3.3). The maximum sea breeze occurred over the station 1, with maximum speed of 10knots at about 1400 SLST. The wind confirm the temperature and humidity indications mentioned above that the sea breeze penetrated, at about 34km inland, on set at about 1100 SLST. At the next station farther inland (54km inland) the wind changed from southerly to very weak southwesterly at about 1100 and 1300 SLST, it is minute indication. But these wind changes are not conclusive indications of a sea breeze front passage. The sea breeze appears to persist up to about 2200 SLST over station No 1. At this time, the wind gradually veers by little with time becoming southwesterly. The wind at 76km and 95km were very light and almost calm.

At Colombo pilot station (station No 9) near the shore line the surface winds are shown in fig 3.10. Flows were towards the water till 0900SLST. The sea breeze was first observed near the sea shore between 1000SLST and 1100SLST at anemometer level and between 1200hrs and 1300hrs the sea breeze circulation did not change significantly. From fig 3.1 to 3.6 the surface winds was weak and from the west over Colombo. Upper winds are shown in fig 3.11. The wind veered with height becoming westerly at about 1km with a speed of 10-15knots. Sea breeze was clearly apparent over

Colombo between the surface and 2000m. Its maximum velocity 15knots occurs at 1000m. Horizontal convergence occurs at lower levels near the sea breeze frontal surface.

At 1400hrs wind field (fig 3.10) shows that the sea breeze has intensified up to 2300hrs but it has not progressed significantly further inland. Flow is still appearing at the sea shore and convergence remains at the sea breeze front. The sea breeze return current has emerged as the dominant feature above onshore flow.

By 1800hrs (fig3.11) change in the dimension and intensity of the sea breeze onshore flow has occurred. Onshore flow has decreased to 10knots at 1000m. The return current aloft which is from the southeast/south of southeast. The return is clearly shown in the observations.

By 2400hrs (fig 3.10) sea breeze had begun to decrease in intensity over the shore. The most interesting feature of the wind field is the changed in the wind direction from southwesterly to southeasterly between 2300 and 0100 SLST. This change had begun at about 2300 SLST.

The depth of the sea breeze (approximately 1500m) is indicated by the upper wind observations (pilot and radar) from Colombo station (fig 3.11). Aloft the velocity increases upward and southerly component becomes more and more at higher levels. Above 3km flow pattern is turning towards the water and southerly component is decreasing rapidly. Fig 3.11 shows sea breeze circulation clearly.

3.2 Numerical Integration

The model was applied to simulate the wind over Sri Lanka. The *x* coordinate was chosen parallel to the west – east line andσcoordinate along vertically for the model.

The model equations were integrated over the rectangular domain (590 x 5km) shown schematically in fig 5.1. The diagram also indicates the height of the terrain. There 38 and 17 grid points along the x and σ coordinate respectively. The grid distance is 10km at interior points. The mesh size was made variable in order to achieve high resolution near the ground. The grid size increased outward from the 3rd and 34th grid points at the boundary by a factor of two. The coordinates of the grid points are given in tables 5.1 and 5.2.

	0	1	2	3	4	5	6	7	8	9	10	11	12
X (km)	-110	-30	10	30	40	50	60	70	80	90	100	110	120
I	13	14	15	16	17	18	19	20	21	22	23	24	25
X (km)	130	140	150	160	170	180	190	200	210	220	230	240	250
I	26	27	28	29	30	31	32	33	34	35	36	37	
X (km)	260	270	280	290	300	310	320	330	340	360	400	480	

Table 5.1 coordinates of grid points along the horizontal. The land starts at $I = 7$

J	0	1	2	3	4	5	6
Z (m)	0	10	50	100	200	300	500
σ	0	0.002	0.010	0.20	0.040	0.060	0.100
p (g)	100870	100770	100370	99870	98870	97870	95370
J	7	8	9	10	11	12	13
Z (m)	800	1100	1500	1900	2400	2900	3000
p (g)	92080	88130	84930	80940	76400	71830	70830
J	14	15	16				
Z (m)	3500	4200	5000				
p (g)	67700	66840	55240				

Table 5.2 coordinates of grid points along the vertical. The values of *Z* refers to points over the sea

The so called finite difference scheme is used in numerically integrating the equations in the wind model. In the time dependent terms forward difference scheme was used. Centered difference scheme was used for other space derivatives.

The initial wind components are based on the morning Radiosonde sounding at Colombo. The actual value of the components (u= 1.5ms^{-1}, v= 1.3ms^{-1}) at the anemometer level, 10m. Corresponding initial value of temperature is also based on same sounding. The model integration started at 0800 SLST, when the sea surface temperature was slightly higher than land surface temperature.

The model integration was tuned with real observed data. The observational study was done to understand the structure of sea breeze circulation and its variation in time. Calibration of the predictive wind model is an important object of this study using observational data network. Selected cross section of Sri Lanka is used to calibrate the wind model with terrain. The model was run and tuned by adjusting coefficients until the wind flow at the anemometer level were more realistic. After adjustments, that the model is suitable for application

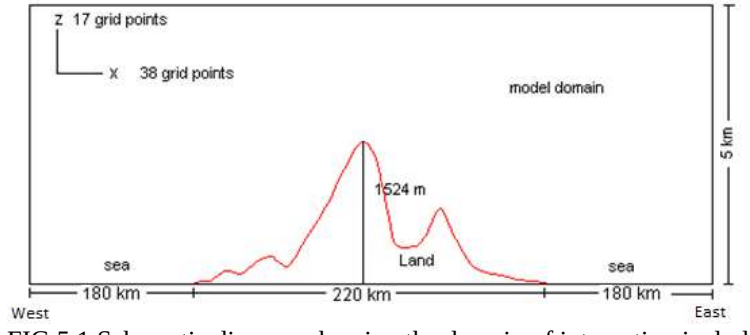

FIG 5.1 Schematic diagram showing the domain of integration including the height (h) variation of the domain

Model was run in smaller grid distances near the shore line and larger grid distances away from the shore line over sea. Positive distances are chosen towards the land from the shore line while negative distances are chosen towards the sea from the shore line. The high resolution near the ground is used

to observe the location of the maximum velocity and penetration that is useful for accurate calibration of the wind model.

3.3 Conclusion

In general the observed behavior and structure conforms to those of previous studies. Horizontal temperature contrast between air over the land and air over the water are pronounced near the sea shore. Sea breeze penetration is appeared to be about 35km from the shoreline and depth of the sea breeze was about 1500km. The return flow has about twice the depth of the layer of on shore flow.

In the numerical simulation, the sea breeze intensity and inland penetration are under estimated with the observational values. It was reasonably realistic, and reproduced satisfactorily the time of onset and the variation in the wind. The return flow increases probably with the combination of sea breeze and slope wind effect. The return flow aloft is clearly shown in the theoretical model. Convergence at the sea breeze front occurs in both model and observations. Maximum velocity of on shore flow shifts inland with time. This feature is not as pronounced in the actual flow system.

The model could be further improved to simulate slope winds over the complex terrain. After improvement of the model, in general the model would be applicable for the prediction of the sea breeze over an interested area.

REFERENCES

Atkinson, B.W., 1981: Meso-scale atmospheric circulation, Academic press.

Basnayake B.R.S.B., 1994: A hybrid meso-scale wind model and application to Sri Lanka. Ph.D Dissertation, Dept of Met and Ocean., University of the Philippines.

Bellaire, F. R., 1965: The modification of warm air moving over cold water. Proc. 8th Conf. Great Lakes Res. Inst., University of Michigan, Ann Arbor, 249-256.

Dixit, C. M., and J. R. Nicholson, 1964: The sea breeze at and near Bombay. Indian J. Meteor. Geophys., 15, 603- 608.

Estoque, M. A., 1962: The sea breeze as a function of the prevailing synoptic situation. J. Atmos. Sci., 19, 244-250

_____ , M. A., C. M. Bhumralkar, 1969: Flow over a localized heat source. Mon. Wea. Rev., 97,850-859.

_____ , M. A., J. Gross and H.W. Lai, 1976: A lake breeze over southern lake Ontario Mon. Wea. Rev., 104, 386-396.

Fisher, E. L., 1960: An observational study of the sea breeze. J. Meteor., 17, 645-648.

Fizzola, J. A., and E. L. Fisher, 1963: A series of sea breeze observations in the New York City area. J. App. Meteor., 2, 722-729

SRI LANKA JOURNAL OF METEOROLOGY

Contents

Vol. 3, September 2018

Articles:

Comparison of NEX NASA Statistical Downscaling Data and CORDEX Dynamical Downscaling Data For Sri Lanka
..... H.M.R.C. Herath, I. M. S. P. Jayawardene pp 3 - 18

Multi Model Ensemble Climate Change Projections for Annual and Seasonal Rainfall in Sri Lanka
..... D. W. T. T. Darshika, I. M. S. P. Jayawardane, D. M. S. C. Dissanayake pp 19 - 27

Modulation of Monthly Rainfall in Sri Lanka by ENSO and ENSO Modoki Extremes
..... H. A. S. U. Hapuarachchi, I. M. S. P. Jayawardene pp 28 - 42

Influence of ENSO to the Following Year Southwest Monsoon Dry/Wet Conditions in Sri Lanka
..... A. M. A. H. D. Alagiyawanna, I. M. S. P. Jayawardene, D. M. S. C. Dissanayake pp 43 - 52

Assessment of the Behaviour of K-Index, Lifted Index and Convective Availability Potential Energy (CAPE) in Development of Thunderstorms in Sri Lanka
..... M. Fernando and M. Millangoda, K. H. M. S. Premalal pp 53 - 63

Investigation of Combine Effects of El Nino, Positive IOD and MJO on Second Inter-Monsoon Rainfall 2015 in Sri Lanka
..... K. A. K. T. W. Weerasinghe and I. M. S. P. Jayawardena, P. A. A. Priyantha pp 64 - 85

Develop an Equation Between Pan Evaporation and Meteorological Parameters in Sri Lanka Using Regression Method
..... M. R. C. Silva, K. H. M. S. Premalal pp 86 - 99

Two Dimensional Sea Breeze & Land Breeze Model with Application to Sri Lanka
..... H. A. G. Dharmappriya pp 100 - 116

ISSN 2478-057X